139

CRYOGENICS

An International Journal of Low Temperature Engineering and Research

VOL. 1 NO. 1 SEPTEMBER 1960

Editorial

With the rapid expansion of science and technology, rational economy in the means of communication and information becomes of prime importance. Any addition to the great number of technical journals already in existence can only be justified when, apart from providing a forum for its subject matter, it will also save time and labour of those working in the field. The editors and publishers of CRYOGENICS believe that this justification exists in the realm of low temperature engineering and research, and they would like to take this opportunity of thanking their colleagues who have encouraged them in this venture.

Until fairly recently cryogenic technology was mainly confined to the large-scale liquefaction and separation of gases and no other serious engineering problems had arisen at the temperatures of liquid air or below. Since the war, however, the use of cryogenic propellants has greatly extended this field and has created an entirely new set of problems involving the handling, storage, and transport of conventional cryogenic substances as well as the use of new ones. Liquid hydrogen has important prospects not only as a propellant but also for low temperature deuterium separation and it is already being used in considerable quantities in bubble chambers. Here its use will be shared by liquid helium and both substances may be employed in cooling magnet coils for thermonuclear reactors.

Apart from the much enlarged use of liquefied gases, a host of other applications of low and very low temperatures to a wide variety of problems has arisen. In some cases these applications, such as the superconductive computer elements, are beginning to reach the engineering stage, while in others, as for instance the work on free radicals, the exploratory phase has still to be passed.

The different trends of low temperature research and development are not only intensified, they are also divergent. However, all share the same cryogenic methods and techniques and all must rely on the same basic research and engineering data. The relevant information on these subjects is at present scattered over a wide variety of journals and we feel confident that concentration of these papers in one journal will be found convenient and helpful. We are therefore providing, in addition to the subject matter, a summary of titles of cryogenic work published elsewhere.

The purpose of CRYOGENICS is to publish original papers on all aspects of low temperature engineering and research and to feature in each issue one invited survey article, written by an authority on the subject. For rapid publication of important results, the editors will accept short letters up to six weeks before the publication of each quarterly issue.

K. Mendelssohn

Cooling by Adiabatic Demagnetization of Nuclear Spins

N. Kurti Clarendon Laboratory, Oxford

Received 24 May 1960

THE exploration of low temperatures down to about 1 °K was made possible by the use of liquefied gases. The object of this article is to review briefly and in general terms the technique used to cover the temperature range down to about 10^{-3} °K and to describe some recent work which shows the way the temperature range down to 10^{-6} °K may be similarly opened up.

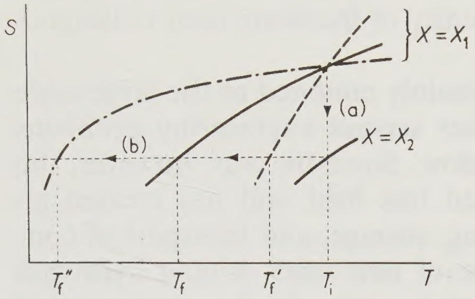

Figure 1. The cooling process in the entropy–temperature diagram: (a) Isothermal $X_1 \longrightarrow X_2$; (b) Isentropic $X_2 \longrightarrow X_1$

The basic principle of generating low temperatures is best explained with the help of an entropy diagram. In Figure 1, the full line represents the entropy of a system for a constant value $X = X_1$ of some external intensive parameter (e.g. pressure, magnetic field, etc.) as a function of the temperature. A brief portion of the entropy for $X = X_2$ is also indicated. The principle of the generation of low temperatures becomes clear from this diagram. At the initial temperature T_i, the entropy is reduced by an isothermal change of X from X_1 to X_2. The system is then thermally isolated from its surroundings and the subsequent adiabatic-reversible, and therefore isentropic, change of X_2 in the opposite direction results in cooling. If X_2 is brought back to its original value X_1, the final temperature T_f is given by the intersection of the horizontal isentropic line with the entropy curve for $X = X_1$.

As may be seen from this representation, two conditions have to be satisfied for appreciable coolings to result. First, the system must, in its initial state, possess a finite entropy, and this must be capable of an appreciable reduction by the alteration of an external parameter. Second, the degree of cooling one can obtain with a given initial isothermal entropy reduction ΔS depends on the shape of the entropy curve for $X = X_1$. If this curve is steep (dotted line in Figure 1), the final temperature T_f' will be considerably higher than T_f'', which would be obtained with a flat entropy curve (dash–dot). Remembering that the specific heat is given by $T(\mathrm{d}S/\mathrm{d}T)$, we can say that in order to reach low temperatures the heat capacity of the system for the final value (X_1) of the external parameter must be low. We can express this in another form by stating that the fractional cooling is given by

$$\frac{\Delta T}{\bar{T}} = \frac{\Delta S}{\bar{C}}$$

where $\bar{T}$ and $\bar{C}$ are appropriate mean values of the temperature and of the heat capacity.

To summarize, the two essential conditions for the production of low temperatures are:

(1) Finite entropy, entropy reduction possible;
(2) Flat S/T curve, i.e. small specific heat for $X = X_1$ in a wide temperature range.

The first of these conditions is reasonably well satisfied in the case of a gas, as it is easy to produce sizeable entropy reduction by compression. The second condition is satisfied as long as one only considers the gas itself, but is no longer so when the additional heat capacity of the container is taken into account. In this case, one finds that the single process results in small temperature reduction, so that progressive cooling involving heat exchangers has to be employed. Only when the starting temperature T_i is low enough for lattice specific heats to become small can single or batch processes be used for gas cooling and gas liquefaction. This is, for instance, the case of the Simon expansion method for the liquefaction of helium.

The temperature of a liquefied gas can be further reduced by pumping off the vapour, but a practical limit is set by the rapidly decreasing vapour pressures. To achieve a predetermined rate of cooling $\mathrm{d}T/\mathrm{d}t$ of the liquid or to absorb a given amount of heat influx $\dot{Q}$, the rate of evaporation has to be maintained at a definite value given by

$$\frac{C}{\lambda} \cdot \frac{\mathrm{d}T}{\mathrm{d}t}$$

or

$$\frac{\dot{Q}}{\lambda}$$

respectively, where λ is the heat of evaporation and C the heat capacity to be cooled down. The lower the vapour pressure the more difficult it is to maintain this rate of evaporation since the required pumping speed has to be increased proportionally to the reciprocal of the pressure. Let us consider, for instance, helium-3 which is the liquid with the lowest boiling point or highest vapour pressures, and thus the most suitable cryogenic liquid for reaching low temperatures. We find, assuming a pumping speed of 100 l./sec at the surface of the liquid, that the rate of heat absorption at 0·3 °K (a vapour pressure of $1{\cdot}5 \times 10^{-3}$ mm Hg) is 2×10^{-4} W. At 0·2 °K this is reduced to 2×10^{-6} W and at 0·15 °K to 10^{-8} W. Alternatively, we find that at 0·2 °K the rate of cooling for 1 cm³ of liquid helium-3 is about 3×10^{-5} deg.K/sec; in other words, it would take about 1 hr to lower the temperature by 0·01 °K.

It is clear from these considerations that even with liquid helium-3 the lowest practical limit is about 0·3 °K. Fortunately, just where liquefied gases lose their usefulness for producing very low temperatures, another group of substances, namely the ideal paramagnetic salts, which satisfy both essential conditions stated above, come into their own. In an ideal paramagnetic substance, the interaction energy of the elementary magnets is by definition vanishingly small. Therefore, in the absence of an external magnetic field the $2J+1$ possible orientations of the elementary magnet (J being the angular momentum) are energetically equivalent and such a system has an entropy of

$$R \times \ln (2J+1)$$

Moreover, this entropy can be appreciably reduced by means of modest magnetic fields. In a magnetic field H, the $(2J+1)$-fold degenerate level is split into $2J+1$ equidistant levels of separation $g\beta H$, where g is the spectroscopic splitting factor and β is the Bohr magneton for the electron. For a field of 10 kgauss this energy difference is approximately $k \times 1$ °K. Therefore, at 1 °K and 10 kgauss there will be a markedly preferential population of the lower energy levels according to the Boltzmann distribution law and, correspondingly, a decrease in entropy.

Our second condition is also satisfied by such a substance. The entropy of the elementary magnets in zero field is, at least in the first approximation, temperature independent and the corresponding specific heat is zero. On the other hand, the entropy and specific heat associated with the lattice vibrations are negligibly small compared to the possible entropy reductions. It was the realization of the fact that both these conditions are satisfied by a large group of paramagnetic salts that led Debye[1] and, independently, Giauque[2] to propose producing very low temperatures by isentropic demagnetization of paramagnetic salts. If one knows the entropy in zero magnetic field as a function of temperature and the entropy of magnetization at the starting temperature, the method outlined in Figure 1 enables one to predict the final temperatures attainable.

The temperature changes obtainable by isentropic reduction of a magnetic field can be calculated either by a thermodynamical or by a statistical argument—just as for an ideal gas—and one obtains for a strictly ideal paramagnetic salt with negligible specific heat the simple relation

$$T_{\mathrm{f}} = H_{\mathrm{f}} \frac{T_{\mathrm{i}}}{H_{\mathrm{i}}} \qquad \ldots(1)$$

where the indices i and f refer to the initial and final state. A simple way of correcting for the departure from ideal behaviour is to characterize the interaction energies by an internal field h. Equation (1) then becomes

$$T_{\mathrm{f}} = \sqrt{(H_{\mathrm{f}}^2 + h^2)} \frac{T_{\mathrm{i}}}{H} \qquad \ldots(2)$$

(This is an approximate formula and is only valid for temperatures at which the deviation from ideal behaviour is small, in other words, when the entropy in zero field does not differ markedly from the ideal value $R \times \ln (2J+1)$. In this case we can write

$$S_{\mathrm{i}} = R \ln (2J+1) - \frac{a}{2} \cdot \frac{1}{T_{\mathrm{i}}^2} - \frac{\lambda}{2} \left(\frac{H_{\mathrm{i}}}{T_{\mathrm{i}}} \right)^2$$

$$S_{\mathrm{f}} = R \ln (2J+1) - \frac{a}{2} \cdot \frac{1}{T_{\mathrm{f}}^2} - \frac{\lambda}{2} \left(\frac{H_{\mathrm{f}}}{T_{\mathrm{f}}} \right)^2$$

λ being the Curie constant. Now $S_{\mathrm{i}} = S_{\mathrm{f}}$ and hence

$$T_{\mathrm{f}} = \frac{\sqrt{(a/\lambda + H_{\mathrm{f}}^2)}}{\sqrt{(a/\lambda + H_{\mathrm{i}}^2)}} T_{\mathrm{i}} = \sqrt{(h^2 + H_{\mathrm{f}}^2)} \frac{T_{\mathrm{i}}}{H_{\mathrm{i}}}$$

since in most cases of practical interest $h \ll H_{\mathrm{i}}$. A more rigorous derivation of this relation has been given by Abragam and Proctor.[3])

For the case of demagnetization to zero field ($H_{\mathrm{f}} = 0$), equation (2) becomes

$$T_{\mathrm{f}} = h \frac{T_{\mathrm{i}}}{H_{\mathrm{i}}} \qquad \ldots(3)$$

We see that the final temperature depends in a simple fashion on the initial temperature, the initial field, and h. That is, it depends on the interaction energies.

Thanks to suitable paramagnetic salts with small values of h, temperatures down to nearly 10^{-3} °K are becoming common in many cryogenic laboratories. This is not the place to describe in detail the various experimental techniques that have been developed for working in this range; there are quite a few informative and up-to-date survey articles on the subject.[4–8] It seems, however, worth while to point out one fundamental difference between such a system of elementary magnets or spins and the other more common cryogenic systems. One is accustomed to dealing with systems whose energy spectrum has no upper limit. Such systems have the well-known property that at high enough temperatures where quantum effects become negligible the law of equipartition of energy holds, the energy of the system becomes infinite with temperature. In a system of spins, the energy spectrum has an upper bound and the law of equipartition of energy does not apply; in fact the specific heat of such a system tends to zero as temperature approaches infinity. This has an interesting consequence; a finite amount of energy is sufficient to bring the system to an infinitely high temperature characterized by an equal distribution of the particles among all the energy levels. If, then, the system is made to absorb an amount of energy which is more than necessary to bring it to infinitely high temperatures, one gets a preferential population of the upper energy levels, a state that can be described by a negative absolute temperature. Such negative temperatures, corresponding to true equilibrium states, have been realized with nuclear spins[9] which, because of the very weak coupling with their environment, can be regarded as forming a system with a bounded energy spectrum. In describing the production of negative temperatures by the absorption of a surplus of energy, one brings out clearly the essential feature of these temperatures: they are reached by passing through infinitely high temperatures and not through absolute zero, which remains an unattainable singularity of the temperature scale.

Fundamentals and practical requirements of nuclear cooling

Equation (3) shows the importance of having low interaction energies if very low temperatures are to be reached, without, however, telling the whole story. There is one unavoidable interaction, namely that between spins, and this produces a co-operative self-ordering of the spins when $\mu h \simeq kT$, μ being the elementary magnetic moment. This is accompanied by a steep drop of entropy (high specific heat), which sets a limit to the cooling by demagnetization, given by

$$T_{\text{lim}} = \frac{\mu h}{k}$$

If the interaction is dipolar,

$$h \simeq \frac{\mu}{r^3}$$

where r is the distance between two adjacent dipoles and we have

$$T_{\text{lim}} = \frac{\mu^2}{kr^3}$$

One way to reduce T_{lim} is by increasing r, e.g. by replacing the paramagnetic ions with isomorphous diamagnetic ions. But to achieve a thousand-fold reduction of T_{lim} would require a thousand-fold magnetic dilution and the maximum possible entropy change. ΔS for a given volume would be reduced in the same ratio. Since the cooling capacity of such a system, i.e. the quantity of heat it can absorb after demagnetization, is roughly $T_f \Delta S$, one should try to keep ΔS as large as possible.

For this reason it is preferable to reduce μ. This can be done by using a 'nuclear' paramagnetic substance in which the magnetization is due to the nuclear magnetic moments,[10, 11] which are about 1,000 times smaller than the electronic magnetic moments of ordinary paramagnetics. However, the smallness of the nuclear magnetic moment raises one difficulty; to satisfy the condition $g\beta_n H \simeq kT$ (where β_n is the nuclear Bohr magneton), one needs values of H_i/T_i a thousand times larger than for 'electron' paramagnetic substances. Even at 0·01°K, fields of the order of 50 kgauss would be required to achieve an entropy decrease of a few per cent of the full nuclear entropy, $R\ln(2I+1)$, where I is the nuclear spin. Thus the starting temperature has to be about 0·01 °K and the nuclear demagnetization temperature has to be preceded by a conventional cooling step.

A general review of the conditions to be fulfilled for successful nuclear cooling has been given by Simon.[12] The present account, without repeating his arguments, gives in a more detailed fashion the design of the actual experiments performed in the last few years at the Clarendon Laboratory.[13, 14]

The most important requirement is to be able to transfer reasonably quickly the heat of magnetization of the nuclear spins to the heat sink at 0·01°K formed by a paramagnetic salt cooled by adiabatic demagnetization. The two principal resistances in this energy transfer are between the nuclear spin system and its own crystal lattice and between this crystal lattice and the paramagnetic salt. As to the first of these, it is well known that in dielectric crystals the nuclear spin–lattice relaxation time becomes very long at low temperatures, and at 10^{-2}°K may reach days or weeks. On the other hand, in a metal the nuclear spins can transfer their energy relatively rapidly to the conduction electrons, which in turn can communicate it to the lattice. The energy transfer is accomplished by a process[15] in which a change of orientation of the nuclear spin is accompanied by an equal and opposite change of orientation of the spin of a conduction electron at the top of the Fermi distribution. Angular momentum is conserved in this process while the small magnetic energy change $g\beta_n H$ of the nuclear spin can be converted into kinetic energy of the conduction electron since the states near the Fermi level are not fully occupied. The number of these unpaired conduction electrons is proportional to T; the transition probability for a nuclear spin flip has the same temperature dependence and the relaxation time is thus inversely proportional to T. These relaxation times are of the order of [16] a second at 1 °K and thus, even at 0·01°K, the time for nuclear magnetization as far as this process is concerned is of the order of minutes.

Much work has been done on the establishment of thermal contact between a metal and a paramagnetic salt at very low temperatures.[13, 17, 18] The method which seemed to be particularly suitable for this work uses a low temperature glass as bonding agent. The paramagnetic salt specimen consists of a viscous slurry made up of powdered chrome potassium alum suspended in a mixture of about equal volumes of a saturated aqueous solution of the same salt and glycerol. The metallic link between this 'paramagnetic' stage and the nuclear stage—they have to be 15–20 cm apart so that the stray field during the nuclear magnetization does not affect the paramagnetic stage—is embedded into this mixture. On cooling, this slurry turns into a glass without any sudden volume changes, and experiments both in Leiden and Oxford have shown that reasonably good thermal contact can be maintained in this way down to 0·01°K. For calculating the rate of heat transfer between this thermal link and the paramagnetic salt, the empirical formula

$$Q = 10^3 A(T_1^3 - T_2^3) \quad \text{ergs/sec} \qquad \ldots(4)$$

(where T_1 and T_2 are the temperatures of the two boundary surfaces and A is the macroscopic contact area in square centimetres) has been found useful. No great accuracy is claimed for this equation but it gives at least the right order of magnitude within a factor of 2 or 3. Using this formula we can calculate the contact area needed to remove the heat of nuclear magnetization in a reasonable time, say 1 hr for the highest field used. Let us assume $T_i = 0{\cdot}012$ °K (temperature of the co-operative anomaly of chrome potassium alum) and $H_i = 30$ kgauss and take 20 g ($\frac{1}{3}$ g.atom) of metallic copper as the nuclear stage. The heat of magnetization is

$$Q_m = T_i \Delta S = \tfrac{1}{3} T_i \frac{\lambda}{2}\left(\frac{H_i}{T_i}\right)^2$$

where $\lambda = 3{\cdot}2 \times 10^{-7}$ is the nuclear Curie constant per gram-atom. With the given numerical data we find $Q_m = 4{,}000$ ergs. Equation (4) then gives for the area of contact about 1,000 cm², which can be obtained with a bundle of 2,000 copper wires of 0·1 mm diameter and embedded over a length of 15 cm in the paramagnetic stage. The lower end of this thermal link serves as the nuclear stage. Such a divided specimen has the further advantage that heat evolution due to eddy currents is greatly reduced.

As shown earlier, effective cooling requires an entropy vs temperature curve which for $H = 0$ is flat over a wide temperature range. Figure 2 shows the two chief components of the entropy of a metal with nuclear spins. We see that the nuclear entropy with the constant value of $R \ln(2I+1)$ at high temperatures (in practice above 10^{-4} °K) satisfies this condition. Superimposed on it is the entropy of the conduction electrons which increases linearly with temperature. The Figure is not drawn to scale and it is only intended to illustrate the argument. As to the lattice entropy, it is altogether negligible compared with that of the conduction electrons at temperatures below 1°K.

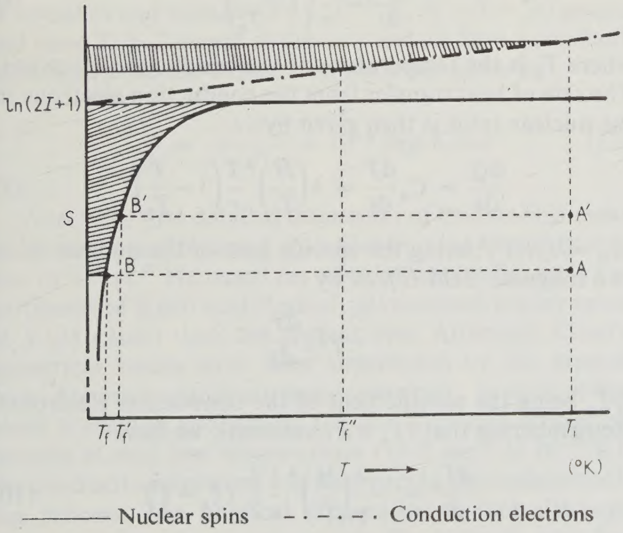

Figure 2. The relative importance of nuclear spins and conduction electrons in nuclear cooling

We must distinguish between two cases, according to whether there is thermal equilibrium or not between the nuclear spins and the conduction electrons during demagnetization. We shall compare the temperatures reached in these two cases with the temperature T_f which would be attained (isentropic line AB) if one had the nuclear spin system by itself. Let us first consider the case where there is equilibrium (reversible and hence isentropic process). Our starting point is now given by A′, the distance AA′ being equal to the conduction electron entropy at T_i. Since the process is isentropic, the final temperature T_f' is again given by the intersection of the appropriate horizontal line (A′B′) with the entropy curve for $H = 0$.

The position is different in the second case where during demagnetization there is no temperature equilibrium between the nuclear spins and the conduction electrons. Let us take the extreme case in which the coupling between these two systems is so weak that during demagnetization the temperature of the conduction electrons does not alter at all, so that the nuclear spins reach T_f. Now, as time goes on, there will be energy exchange between the two systems and equilibrium will be reached at a temperature at which the total heat Q gained by the nuclear spin system equals that lost by the conduction electrons. Remembering that

$$Q = \int T \, dS$$

we find that the final temperature T_f'' reached in this process is given by the condition that the two differently shaded areas are equal. Clearly, the irreversible process gives much poorer results than the reversible process.

We can calculate for each of these two cases the conditions under which the presence of the conduction electrons has only a small influence on the final temperature reached in nuclear cooling. For the reversible case we have $S_i = S_f$, with

$$S_i = R \ln(2I+1) - \frac{\lambda}{2}\left(\frac{H_i}{T_i}\right)^2 + \gamma T_i$$

and

$$S_f = R \ln(2I+1) - \frac{\lambda}{2}\left(\frac{h}{T_f'}\right)^2$$

(where λ is the nuclear Curie constant, γT_i the electronic specific heat, and h the local internal field), since in all cases of practical interest $T_f' \ll T_i$ and $h < H_i$. Remembering that T_f, the temperature that would be reached by the nuclear spin system alone, is given by

$$T_f = \frac{h T_i}{H_i}$$

we find

$$1 - \frac{T_f^2}{T_f'^2} = 2 \frac{\gamma}{\lambda} \frac{T_i^3}{H_i^2} \qquad \ldots(5)$$

or, substituting numerical values for copper ($\gamma = 7{\cdot}5 \times 10^3$ erg (deg.K)$^{-2}$ (g.atom)$^{-1}$ and $\lambda = 3{\cdot}2 \times 10^{-7}$ (g.atom)$^{-1}$),

$$1-\frac{T_f^2}{T_f'^2} = 4{\cdot}7\times 10^7\frac{T_i^3}{H_i^2} \qquad \ldots(5a)$$

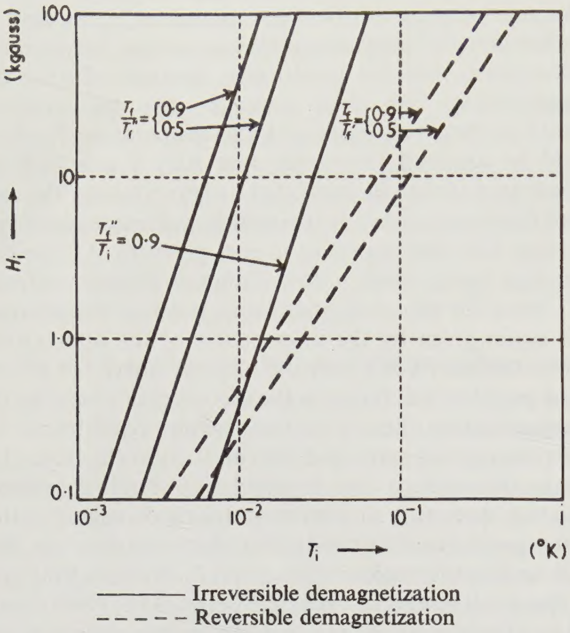

Figure 3. The effect of the conduction electrons on the final temperatures reached in the nuclear demagnetization of copper. The lines indicate limiting values of H_i and T_i for stated deviations of the actual final temperatures (T_f' and T_f'') from those that would be reached in the absence of conduction electrons

Equation (5) defines pairs of values T_i, H_i, leading to T_f' not exceeding T_f by more than a given factor. Figure 3 shows two T_i, H_i lines corresponding to $T_f/T_f' = 0{\cdot}9$ and $T_f/T_f' = 0{\cdot}5$; only T_i, H_i values lying under these lines satisfy the respective conditions. We see that in this reversible case nuclear demagnetizations can be carried out from a wide range of initial conditions without the results being appreciably influenced by the conduction electrons.

Let us next consider the irreversible case. T_f'' is now given by the condition

$$\int_T^{T_f''} C_n \, dT = \int_{T_f''}^{T_i} C_e \, dT$$

where
$$C_n = \lambda\frac{h^2}{T^2}$$

and $C_e = \gamma T$. Making the same simplifying assumptions as before we have

$$1-\frac{T_f}{T_f''} = \frac{\gamma}{2\lambda h}\frac{T_i^3}{H_i} = 3{\cdot}9\times 10^9\frac{T_i^3}{H_i} \qquad \ldots(6)$$

(with $h = 3$ gauss, the value found for copper[14]).

As may be seen from Figure 3, the conduction electrons have a great effect in this case; the lines for $T_f/T_f'' = 0{\cdot}9$ and $T_f/T_f'' = 0{\cdot}5$ leave only a small range of permissible T_i, H_i values. The third line for the irreversible case refers to $T_f''/T_i = 0{\cdot}9$ and defines the limits of the nuclear cooling experiments with copper under conditions of poor energy exchange between nuclear spins and conduction electrons.

The foregoing calculations show that the effect of the heat capacity of the conduction electrons is negligible in the reversible case but not if the process is irreversible. We shall next discuss whether under actual experimental conditions there is equilibrium between the nuclear spin system and the conduction electrons during demagnetization. For the simplest case of $I = \frac{1}{2}$ (two nuclear spin orientations of energy difference u, to be denoted by '+' and '−'), the approach to equilibrium between the nuclear spins and their surroundings is given by

$$\frac{dn}{dt} = \frac{1}{\tau}(n-n_0) \qquad \ldots(7)$$

where $n = N_+ - N_-$ is the population difference between the two states and n_0 is the distribution corresponding to temperature equilibrium with the 'temperature bath', i.e. the conduction electrons at T_0. The relation between the relaxation time τ and the transition probability for a nuclear spin flip is given by

$$\frac{1}{\tau} = 2w\cosh\frac{u}{kT_0}$$

with
$$w_+ = w\exp(-u/kT_0)$$
and
$$w_- = w\exp(u/kT_0)$$

being the probabilities for the (+ −) and (− +) transitions, respectively. In most cases of practical interest $u/kT_0 \ll 1$ and τ is independent of the level separation; it depends, however, as mentioned earlier, on the temperature of the conduction electrons. We can define by means of n a nuclear spin temperature T,[20] and as long as $u/kT \ll 1$ we have $n \propto 1/T$ and equation (7) may be written

$$\frac{dT}{dt} = \frac{T}{\tau}\left(1-\frac{T}{T_e}\right) \qquad \ldots(8)$$

where T_e is the temperature of the conduction electrons. The rate of heat transfer from the conduction electrons to the nuclear spins is then given by

$$\frac{dQ}{dt} = C_n\frac{dT}{dt} = \lambda\left(\frac{H}{T}\right)^2\frac{T}{\tau}\left(1-\frac{T}{T_e}\right) \qquad \ldots(9)$$

($C_n = \lambda(H/T)^2$ being the specific heat of the nuclear spins in a magnetic field H), or by

$$-\gamma T_e\frac{dT_e}{dt}$$

(γT_e being the specific heat of the conduction electrons). Remembering that $\tau T_e = \alpha$ (constant), we have

$$\frac{dT_e}{dt} = -\frac{\lambda}{\gamma}\left(\frac{H}{T}\right)^2\frac{1}{\alpha}\frac{T}{T_e}(T_e-T) \qquad \ldots(10)$$

We must now calculate the value of $(T/T_e)(T_e-T)$ which makes the cooling rate dT_e/dt of the conduction electrons about equal to the cooling rate of the nuclear spins due to demagnetization. Let us assume that the field is reduced at a constant rate, $\mathrm{d}H/\mathrm{d}t = -\beta$, then for the nuclear spin system alone

$$\frac{T}{H} = \frac{T_\mathrm{i}}{H_\mathrm{i}}$$

and hence
$$\frac{\mathrm{d}T}{\mathrm{d}t} = -\frac{T_\mathrm{i}}{H_\mathrm{i}}\beta$$

equating this with the right-hand side of equation (8), we find

$$\frac{T}{T_\mathrm{e}}(T_\mathrm{e}-T) = \frac{\gamma}{\lambda}\alpha\beta\left(\frac{T}{H}\right)^2\frac{T_\mathrm{i}}{H_\mathrm{i}} \simeq \frac{\gamma}{\lambda}\alpha\beta\left(\frac{T_\mathrm{i}}{H_\mathrm{i}}\right)^3 \quad \ldots(11)$$

Substituting numerical values ($\alpha = 1$ sec/deg.K, $\beta = 10^3$ gauss/sec), we find with $T_\mathrm{i} = 1{\cdot}2\times10^{-2}$°K and $H_\mathrm{i} = 10^4$ gauss

$$(T_\mathrm{e}-T) = 4\times10^{-5}\,°\mathrm{K}$$

In other words, not till a temperature of about 4×10^{-4}°K is reached does the temperature difference between conduction electrons and nuclear spins exceed 10 per cent. We were thus justified in regarding T/H as constant during most of the demagnetization. It is true that while in the final stage the temperature of the nuclear spins drops from 4×10^{-4} °K to

$$T_\mathrm{f} = h\frac{T_\mathrm{i}}{H_\mathrm{i}} = 3\times\frac{1{\cdot}2\times10^{-2}}{10^4} = 3{\cdot}6\times10^{-6}\,°\mathrm{K}$$

the conduction electrons will lag behind. But, as may be seen from Figure 3, at these temperatures even irreversible cooling of the conduction electrons will have only a negligible effect.

It can also be shown that at the end of demagnetization the time-lag is only of the order of seconds. In equation (8), T the temperature of the nuclear spins may now be taken as constant and equal to $3{\cdot}6\times10^{-6}$°K, $H = h = 3{\cdot}0$ gauss, and since $T_\mathrm{e} \gg T$ except at the very end we have a constant cooling rate for the conduction electrons given by

$$\frac{\mathrm{d}T_\mathrm{e}}{\mathrm{d}t} = -\frac{\lambda h^2}{\gamma T}\frac{1}{\alpha} = 10^{-4}\ \mathrm{deg.K/sec} \quad \ldots(12)$$

(*Note:* The first detailed discussion of the establishment of thermal equilibrium in a nuclear cooling experiment is due to Kittel.[21] He based his calculations on the early experiments of Kurti et al.[13] which gave a much higher value of h (25 gauss) than the present one. Although Kittel's numerical values have been superseded by the present ones, his main argument remains correct; in spite of the small transition probability for the Korringa relaxation process at very low temperatures (10^{-6} sec^{-1} at 10^{-6}°K), the conduction electrons can take part in the nuclear cooling process. The physical explanation is that although the probability for a nuclear spin flip is small, very few such flips are necessary to cool the conduction electrons.)

We have assumed all along that immediately before demagnetization the thermal contact with the electronic stage is broken so that the nuclear stage as a whole—i.e. nuclear spins, conduction electrons, and lattice—is thermally insulated. While this should be possible with a superconducting heat-switch, various experimental difficulties have prevented the use of such a device and so far all experiments have been carried out *without* a heat-switch. This may seem to make nonsense of these nuclear cooling experiments, but the presence of the two thermal resistances, nuclear spin–conduction electron relaxation and heat transfer from copper to paramagnetic salt, justified the expectation of an observable cooling effect.

As mentioned above a typical specimen used in the nuclear cooling experiments consists of a bundle of insulated copper wires, about 35 cm long, whose lower end constitutes the nuclear stage and whose upper end is embedded into the electronic stage of chrome potassium alum. This specimen is suspended in a jacket whose walls are at a low enough temperature (< 0·35°K) for heat influx due to gas to be negligible. Mutual inductance coils surrounding the electronic stage and the nuclear stage permit the measurement of their respective susceptibilities and hence their temperatures.

The apparatus used in the first experiments[13] had two main shortcomings. The nuclear susceptibility was measured by a ballistic method; thus no continuous record of the rather rapid warming-up of the nuclear stage could be obtained, and this made the analysis of the results difficult. The second difficulty was caused by the manganous ammonium sulphate cylinder used to cool the shield surrounding the nuclear stage to about 0·1°K. Since this

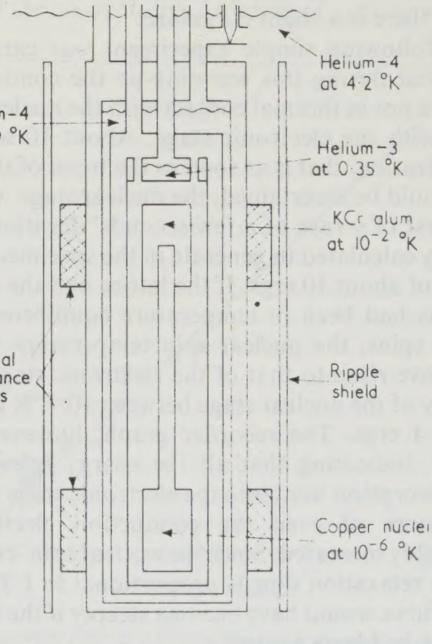

Figure 4. Schematic view of the cryostat for nuclear demagnetization

cylinder was at the height of and concentric with the electronic stage, it was impossible to determine with any accuracy the temperature of the latter and hence T_i.

To remedy these drawbacks, a new apparatus was constructed[22] which uses a shield cooled by liquid helium-3 and an a.c. mutual inductance bridge permitting continuous measurement of the nuclear susceptibility starting about 2 sec after demagnetization. The apparatus is shown diagrammatically in Figure 4. Figure 5 is a photograph of the cryostat, with the magnetizing solenoid.

Results and discussion

We shall now briefly describe some of the results obtained with the new apparatus. First a series of demagnetizations were carried out, all starting from the same initial temperature, $T_i = 0{\cdot}012$°K, and from fields between 3 kgauss and 30 kgauss. Figure 6 shows the recorder graph of the nuclear susceptibility after a typical demagnetization. The mutual inductance was balanced at the starting temperature and the amplifier sensitivity so adjusted that the lowest temperature (highest susceptibility) gave approximately full deflection. Immediately after the nuclear stage had warmed up to the starting temperature—this usually took about 90 sec—the instrument was calibrated by altering the compensating mutual inductance in known steps. The times corresponding to integer values of the mutual inductance were then read off these warming-up curves and plotted logarithmically, as shown in Figure 7. Since the mutual inductance is proportional to the nuclear susceptibility, these plots in effect give $n = N_+ - N_-$ or $1/T$ as a function of time. If the warming-up is governed by a relaxation process between nuclear spins and conduction electrons, the latter being at a constant temperature given by the electronic stage ($T_e \gg T$), one would expect, according to equation (8), straight lines, all parallel to each other. We see that the lines are indeed nearly parallel, though there is a slight curvature.

The following simple experiment was carried out to prove that during this warming-up the conduction electrons are not in thermal contact with the nuclear spins but rather with the electronic stage. About 10 sec after demagnetization, that is as soon as the trend of the warming curve could be ascertained, the nuclear stage was exposed to a burst of γ-rays of a few seconds' duration and of an intensity calculated to generate in the specimen a quantity of heat of about 10 ergs. If the lattice and the conduction electrons had been in temperature equilibrium with the nuclear spins, the nuclear spin temperature would suddenly have risen to that of the electronic stage, since the enthalpy of the nuclear stage between 10^{-6}°K and 10^{-2}°K is only 4 ergs. The recorder graph, however, was unaffected, indicating that all the energy released by the γ-ray absorption went into the electronic stage without the temperature of even the conduction electrons being appreciably increased. Since the nuclear spin–conductance electron relaxation time is proportional to $1/T$ the warming-up curve would have become steeper if the conduction electrons had been heated.

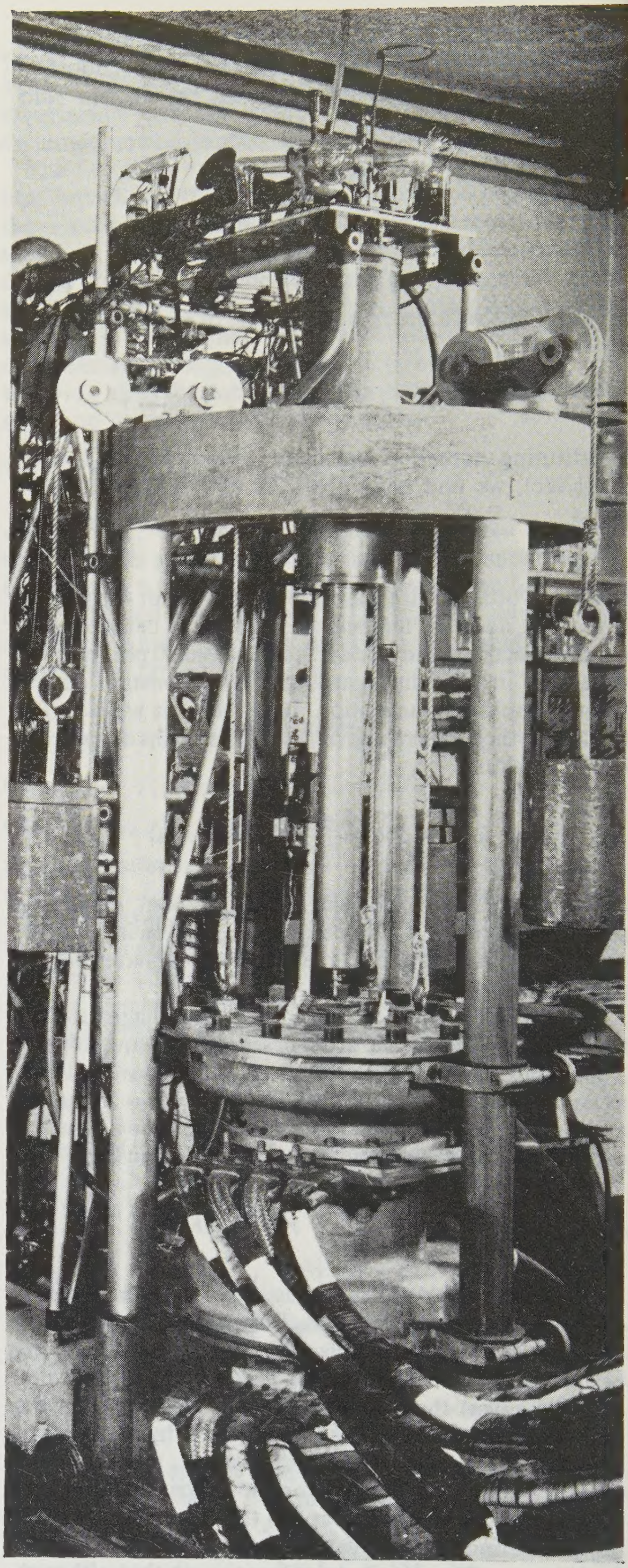

Figure 5. View of the nuclear cooling apparatus. Underneath the metal Dewar, enclosing the actual cryostat, is the water-cooled high powered solenoid

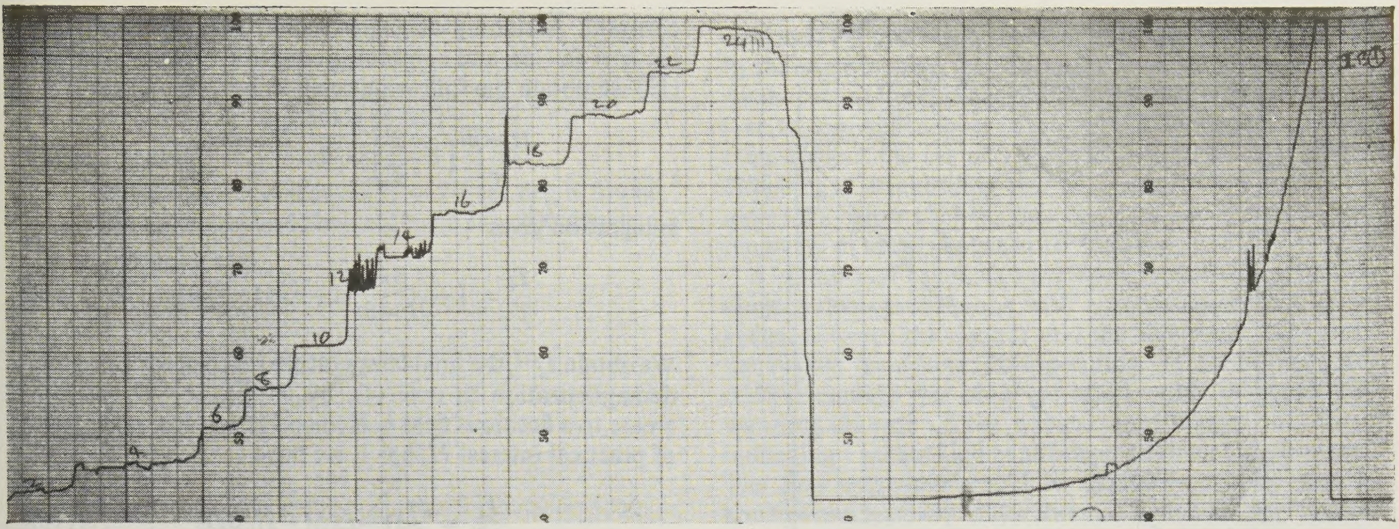

Figure 6. Recorder graph of the magnetic thermometer. Right: nuclear susceptibility after demagnetization; Left: calibration of the bridge with a variable mutual inductance. Each small division represents 5 sec

A number of nuclear demagnetizations were carried out with the electronic stage, and hence the conduction electrons, at higher temperatures, and these experiments served to determine the temperature dependence of the relaxation time. The results are given in Figure 8 which shows that the temperature dependence is not far off the predicted one. The straight line gives $\tau T = 0{\cdot}4$ sec.deg.K, which agrees reasonably well with the value of $\tau T = 0{\cdot}45$ sec.deg.K found by Anderson and Redfield[16] in the liquid helium temperature range and in small fields. It should be emphasized that, as shown by these authors, the relaxation time increases about 2·5 times between 1 and 100 gauss, and reaches at higher fields the value of $\tau T = 1{\cdot}1$ sec.deg.K.

Figure 9 gives the final temperature reached by demagnetization from 0·012 °K and from various fields. The results obey equation (3) and from the slope of the line we obtain $h = 3{\cdot}1$ gauss, in good agreement with the predictions of various theories of interaction between nuclear spins in metals, and with the results from nuclear resonance experiments. Clearly, nuclear cooling is a rather cumbersome method for obtaining h; but when it becomes possible to use 3 or 4 times larger values of H_i/T_i than has been done hitherto one would probably get below the critical temperature of the co-operative ordering of nuclear spins and

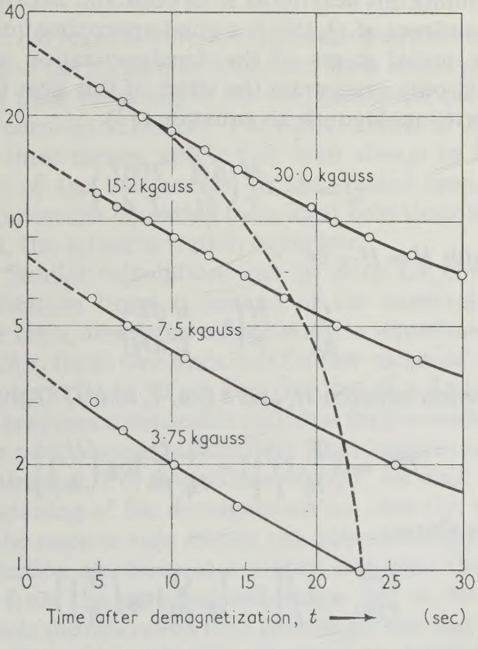

Figure 7. Nuclear susceptibility (in arbitrary units) as a function of time after demagnetizations from 0·012°K and the stated fields. The broken line (– – – –) indicates the trend one would expect if the warming-up were governed by the heat resistance between the paramagnetic salt and the copper specimen

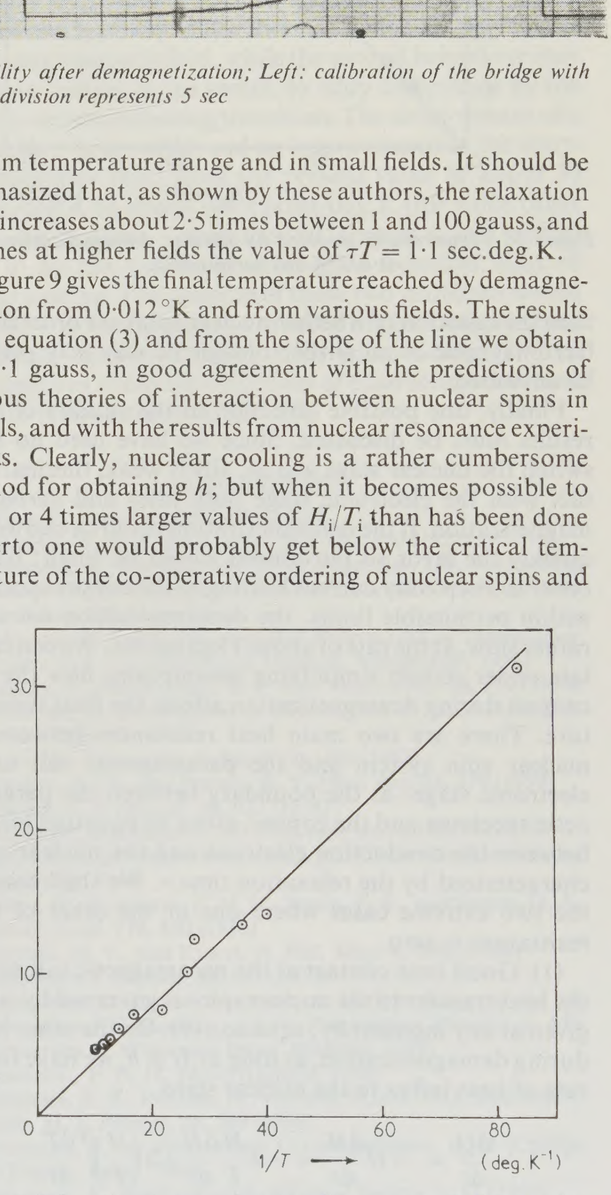

Figure 8. Relaxation time as a function of the reciprocal of the conduction electron temperature

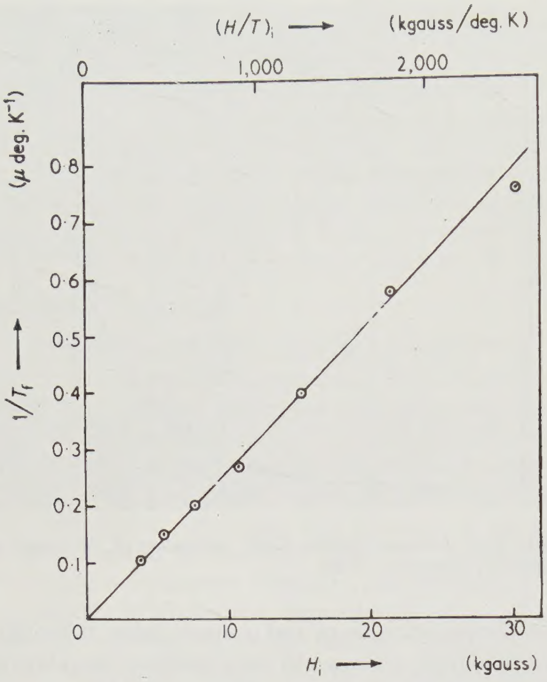

Figure 9. Temperatures attained by nuclear demagnetization from 0·012°K and various fields

then the question of whether nuclear spins are ordered in a ferromagnetic or an antiferromagnetic way may perhaps be answered.

Finally, one possible objection to the validity of these results must be discussed. Since we have used no heat-switch the nuclear stage was in, albeit weak, thermal contact with the electronic stage both after and *during* demagnetization. If the demagnetization could be carried out quickly the error so introduced would be small; but, in order to keep eddy current heating in the copper specimen within permissible limits, the demagnetization has to be rather slow, at the rate of about 1 kgauss/sec. We can calculate under certain simplifying assumptions how the heat contact during demagnetization affects the final temperature. There are two main heat resistances between the nuclear spin system and the paramagnetic salt of the electronic stage: at the boundary between the paramagnetic specimen and the copper, given by equation (4), and between the conduction electrons and the nuclear spins, characterized by the relaxation time τ. We shall consider the two extreme cases where one or the other of these resistances is zero.

(1) Good heat contact at the paramagnetic salt so that the heat transfer to the nuclear spins is governed by, and is given at any moment by, equation (9). On the other hand, during demagnetization, as long as $H \gg h$, we have for the rate of heat influx to the nuclear spins

$$\frac{\mathrm{d}Q}{\mathrm{d}t} = -H\frac{\mathrm{d}H}{\mathrm{d}t} = -\lambda\frac{H}{T}\frac{\mathrm{d}H}{\mathrm{d}t}+\lambda\left(\frac{H}{T}\right)^2\frac{\mathrm{d}T}{\mathrm{d}t} \qquad \ldots(13)$$

since the internal energy of a system of ideal spins is constant. Assuming demagnetization at a constant rate, i.e. $H = H_i - \beta t$, and combining equation (9) and equation (13) we obtain the following relation between T and H

$$\frac{H_i-\beta t}{\tau}\left(1-\frac{T}{T_i}\right) = \beta+\frac{H_i-\beta t}{\tau}\frac{\mathrm{d}T}{\mathrm{d}t} \qquad \ldots(14)$$

Integration gives

$$\frac{T_i}{T} = 1+\frac{\beta\tau}{H_i-\beta t}[1-\exp(-t/\tau)] \qquad \ldots(15)$$

We obtain $T_f^{(1)}$, the final temperature reached for complete demagnetization in case (1), by letting $H = H_i - \beta t$ decrease to a fictitious field h. Remembering that in all cases of practical interest $H_i/h \gg 1$, we have

$$\frac{T_i}{T_f^{(1)}} = \frac{\beta\tau}{h}[1-\exp(-H_i/\beta\tau)] \qquad \ldots(16)$$

Since in the ideal adiabatic-reversible case

$$\frac{T_i}{T_f^{(\mathrm{id})}} = \frac{H_i}{h}$$

we obtain for the ratio of final temperatures

$$\frac{T_f^{(1)}}{T_f^{(\mathrm{id})}} = \frac{H_i}{\beta\tau[1-\exp(-H_i/\beta\tau)]} \qquad \ldots(17)$$

(2) Short relaxation time; heat leak to the nuclear spins governed by the heat influx $\dot{Q}$ at the electronic stage. This is given by equation (4) and we can simplify the calculations by assuming this heat influx to be constant. Because of the T^3 dependence of $\dot{Q}$, this is a good approximation except for the initial stages of the demagnetization and will, anyway, only exaggerate the effect of this heat leak. We now have, analogously to equation (13)

$$\dot{Q} = -\lambda\frac{H}{T}\left(\frac{\mathrm{d}H}{\mathrm{d}t}-\frac{H}{T}\frac{\mathrm{d}T}{\mathrm{d}t}\right) \qquad \ldots(18)$$

and, with $H = H_i - \beta t$

$$\frac{\dot{Q}}{\beta\lambda} = \frac{H}{T}\left(1-\frac{H}{T}\frac{\mathrm{d}T}{\mathrm{d}H}\right) \qquad \ldots(19)$$

Integration between H_i and h (i.e. T_i and $T_f^{(2)}$) gives

$$T_f^{(2)} = h\frac{T_i}{H_i}1\Big/\left[1-\frac{T_i}{H_i}\cdot\frac{\dot{Q}}{\beta\lambda}\log\left(\frac{H_i}{h}\right)\right] \qquad \ldots(20)$$

and, as above,

$$\frac{T_f^{(2)}}{T_f^{(\mathrm{id})}} = 1\Big/\left[1-\frac{T_i}{H_i}\cdot\frac{\dot{Q}}{\beta\lambda}\log\left(\frac{H_i}{h}\right)\right] \qquad \ldots(21)$$

We can now calculate the effect of non-adiabatic conditions in these two extreme cases by substituting into equations (17) and (21) the following numerical values appropriate to our experiments:

$T_i = 1{\cdot}2 \times 10^{-2}\,°\mathrm{K}$
$h = 3{\cdot}1$ gauss
$\lambda = 1{\cdot}1 \times 10^{-7}$ (for $\frac{1}{3}$ g.atom of Cu)
$\dot{Q} = 1$ erg/sec
$\tau = 90$ sec (corresponding to $\tau T = 1{\cdot}1$ sec.deg.K found by Anderson and Redfield[16] for $H > 100$ gauss)
$\beta = 10^3$ gauss/sec.

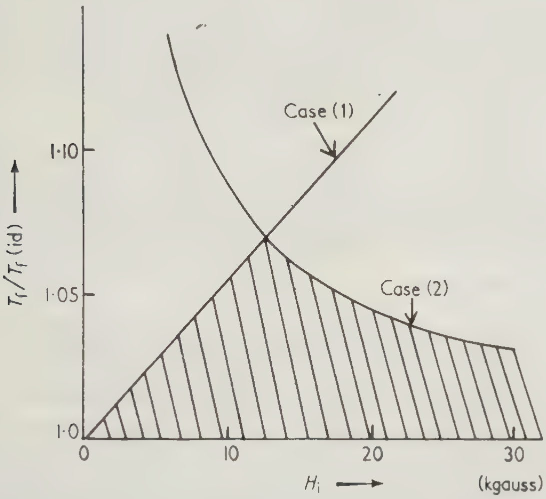

Figure 10. The effect of non-adiabatic conditions during demagnetization on the final temperatures. Case (1): Good heat contact at the paramagnetic salt, heat influx governed by the relaxation time; Case (2): Short relaxation time, heat influx governed by the thermal resistance at the paramagnetic salt

The two curves of Figure 10 representing equations (17) and (21) give the maximum deviations from ideality, since in each of these cases one of the energy transfer mechanisms was considered perfect. The actual values of $T_f/T_f^{(id)}$ lie below these curves, and in fact must always lie below the lower of the two curves, in the shaded area. The maximum possible deviation from ideal behaviour is thus 8 per cent, the actual deviation being less.

(*Note:* Similar calculations can be done for constant demagnetization times t_d instead of for constant field reduction rates, simply by substituting in equations (17) and (21) H_i/t_d for β. One finds that for low values of H_i the deviation may rise to 20 per cent, but for $H_i > 15$ kgauss the effect becomes comparable with that for $\beta =$ constant.)

We can now discuss qualitatively what happens during demagnetization. For low values of H_i/T_i we shall have, at the beginning of the demagnetization, case (2); this is because the nuclear spin system can absorb energy from the conduction electrons at a higher rate than the heat influx $\dot{Q}$ from the paramagnetic stage. But as the bulk copper cools the relaxation time gets longer and finally the nuclear spins and conduction electrons 'separate' (this occurs at a few thousandths of a degree according to the conditions), the latter warming to T_i and the former continuing to cool to T_f. This discussion shows that, while in the present experimental arrangement the conduction electrons do not reach the lowest temperatures attained by the nuclear spins, they do, under favourable conditions, participate in the cooling process. It seems feasible, therefore, to cool bulk copper below 10^{-2} °K by nuclear cooling even without the use of a thermal switch. In view of the difficulty of establishing thermal contact with paramagnetic salts below 10^{-2} °K, this may be a useful method for the study of metals between 10^{-3} °K and 10^{-2} °K.

A number of attempts have been made[22] to carry out nuclear demagnetizations with a superconducting heat-switch between the nuclear and the electronic stage, but the results have been disappointing. In some cases no nuclear cooling was observed at all, while in others the warming-up rate of the nuclear spin system was fast, indicating a rather high conduction electron temperature. The first behaviour could be explained by too low a thermal conductivity of the thermal switch at 0·01 °K and in a strong magnetic field, while the second behaviour may be due to heating in the switch by eddy currents or by the normal–superconducting transition. The development of a satisfactory heat-switch and an improvement in the starting conditions H_i/T_i from the present value of about 30 kgauss/deg.K to about 100 kgauss/deg.K (for some other nuclei, e.g. protons, a more modest increase would suffice) seem to be the two main short-term technical aims of nuclear cooling. The solution of these two problems would open the way to the study of ordered nuclear spin systems in thermal equilibrium with their surroundings and to investigations about the behaviour of conduction electrons down to temperatures of 10^{-7} °K.

REFERENCES

1. Debye, P. *Ann. Phys.* **81,** 1154 (1926)
2. Giauque, W. F. *J. Amer. chem. Soc.* **49,** 1870 (1927)
3. Abragam, A., and Proctor, N. G. *Phys. Rev.* **109,** 1441 (1958)
4. Garrett, C. G. B. *Magnetic Cooling* (Harvard University Press, Cambridge, Mass., 1954)
5. de Klerk, D., and Steenland, H. J. *Progress in Low Temperature Physics*, Vol. 1, p. 224 (North Holland, Amsterdam, 1955)
6. Ambler, E., and Hudson, R. P. *Rep. Progr. Phys.* **18,** 251 (1955)
7. de Klerk, D. *Encyclopedia of Physics*, Vol. 15, p. 38 (Springer, Berlin, 1956)
8. Kurti, N. *Nuovo Cim.* **6,** Suppl. 3, 1101 (1957)
9. Purcell, E. M., and Pound, R. V. *Phys. Rev.* **81,** 279 (1959)
10. Gorter, C. J. *Phys. Z.* **35,** 923 (1934)
11. Kurti, N., and Simon, F. E. *Proc. roy. Soc.* **A149,** 152 (1935)
12. Simon, F. E. *Le Magnetisme*, Vol. 3, p. 1 (Collection Scientifique, Strasbourg, 1940)
13. Kurti, N., Robinson, F. N. H., Simon, F. E., and Spohr, D. A. *Nature, Lond.* **178,** 450 (1956)
14. Hobden, M. V., and Kurti, N. *Phil. Mag.* **4,** 1092 (1959)
15. Korringa, J. *Physica,* **16,** 601 (1950)
16. Anderson, A. G., and Redfield, A. G. *Proceedings of the 5th International Conference on Low Temperature Physics*, p. 616 (University of Wisconsin Press, Madison, 1958)
17. Robinson, F. N. H. *Thesis* (Oxford, 1954)
18. Miedema, A. R., Postma, H., van der Vlugt, N. J., and Steenland, M. J. *Physica,* **25,** 509 (1959)
19. Mendoza, E. *Les Phénomènes Cryomagnétiques*, p. 48 (Collège de France, Paris, 1948)
20. Abragam, A. *Yearbook of the Physical Society*, p. 61 (1958)
21. Kittel, C. *Phys. Rev.* **104,** 1807 (1956)
22. Hobden, M. V. *Thesis* (Oxford, 1960)

Abstracts

A JOULE–THOMSON HELIUM LIQUEFIER AND SOME PROBLEMS IN ITS DESIGN

D. H. PARKINSON

THIS paper gives the construction and layout of a Joule–Thomson helium liquefier which yields 8 l./hr with a consumption of 1·3 l. of liquid hydrogen for each litre of liquid helium produced. Attention is given only to certain unusual aspects of design such as the use of Collins and space-wound cross-flow exchangers above the liquid nitrogen and liquid hydrogen bath. The choice of heat exchangers and problems of 'splash' and heat transfer in the liquid hydrogen bath are discussed. Methods of dealing with 'splash' and of obtaining more effective pre-cooling have been tried out.

RECENT IMPROVEMENTS IN INSULANTS

A. H. COCKETT W. MOLNAR

A THEORETICAL examination of the modes of heat transfer through evacuated insulants has been made and applied to experimentally determined thermal conductivities to separate the heat transferred by conduction from that transferred by radiation. The contribution due to radiation for a powder like Santocel is a high proportion of the total and the admixture of particles of high emissivity effects an appreciable reduction. A multiple screen insulant incorporating aluminium foils with net separators is also shown to have low thermal conductivity.

METALLOGRAPHY AT LIQUID HELIUM TEMPERATURES

D. HULL H. M. ROSENBERG

AN apparatus has been designed for the microscopic examination of metals at liquid helium temperatures and it has been used to study the martensitic transformations which occur in lithium and sodium. At 20° K between 40 and 50 per cent of the large grained specimens of sodium were transformed to the new phase and no further change was observed on cooling to 6° K. For small grained specimens the amount of transformation was much less. For lithium nearly the whole of the specimen had transformed to the new phase at 20° K. Transformation started at 31° K for sodium and at approximately 76° K for lithium.

A CRYOSTAT FOR STUDYING TRANSURANIC SUBSTANCES

G. T. MEADEN J. A. LEE

A CRYOSTAT used in conjunction with a glove-box is described. Such an apparatus is suitable for measuring the electrical resistivity and Hall effect of strongly alpha-active metals and alloys over the temperature range 1·4–300° K.

ON THE PROPERTIES OF THE VAPOUR PRESSURE CURVE

E. H. BROWN

SOME general mathematical properties of the vapour pressure as a function of temperature are investigated by rigorous methods. In particular, the limiting shape of the vapour pressure curve is shown to be determined by the vanishing of the limits of the derivatives of all orders in the neighbourhood of absolute zero. Some comments on the inapplicability of the Third Law of Thermodynamics to the sublimation curve are included.

ON THE SPECIFIC HEAT OF LIQUID HELIUM IN BRENIG'S THEORY

W. E. PARRY D. TER HAAR

THE specific heat of a system of non-interacting bosons is calculated assuming an energy spectrum of the Brenig type. Such a spectrum consists of a linear phonon branch which is cut off at a certain wave number k_0 and a quadratic quasi-particle branch which starts at k_0 and which is characterized by an effective mass m. The specific heat c_V shows a discontinuity at a transition temperature T_c. The dependence of T_c, the height of the c_V curve, and the magnitude of the jump in c_V at $T=T_c$ on k_0 and m are investigated.

A CRYOGENIC DEVICE FOR IRRADIATION IN LIQUID NITROGEN

L. BOCHIROL J. DOULAT L. WEIL

A BRIEF review of existing types of liquid nitrogen loops followed by a description of a loop operating according to a new principle, for irradiation in a permanent liquid nitrogen bath. This extra-pure nitrogen contained in a small vessel is recondensed in ordinary liquid nitrogen at a certain distance from the core in a zone where the flux is weak, so as to eliminate any explosion hazards, and flows back into the bath under the action of gravity. The design of the apparatus is extremely simple and it is reliable in operation owing to the absence of mechanical circulating equipment. The consumption of nitrogen is quite small. The apparatus enables the samples to be taken out in a cold condition. It has operated satisfactorily for several continuous one-week periods.

THE EFFECT OF RADIATION DAMAGE ON THE THERMAL CONDUCTIVITY OF SUPERCONDUCTORS

K. D. CHAUDHURI K. MENDELSSOHN
M. W. THOMPSON

THE effect of neutron irradiation at 30° C on the thermal conductivity of niobium and vanadium single crystals has been investigated at low temperature. Measurements were carried out in both superconducting and normal states where conduction is due predominantly to phonons and electrons, respectively. The observed effect on the phonon conductivity indicates an increase in the dislocation density whereas changes in electron conduction revealed the presence of vacancies.

CRYOSTATS FOR OPTICAL INVESTIGATIONS

P. PESTEIL R. PHILIP

THREE types of cryostat for optical investigations are described: for visible, ultra-violet, and infra-red light. They are of simple design, have a very small consumption of liquid coolant, and take up little space. These instruments can be used for the examination of absorption spectra and luminescence or for the cooling of photomultipliers.

Résumés

APPAREIL JOULE–THOMSON DE LIQUEFACTION DE L'HELIUM ET CERTAINS PROBLEMES DE SA CONSTRUCTION

D. H. PARKINSON

Cet article décrit la construction et le schéma de montage d'un appareil Joule–Thomson de liquéfaction de l'hélium qui produit 8 l./h. avec une consommation de 1,3 l. d'hydrogène liquide, pour chaque litre d'hélium liquide produit. On explique seulement certains aspects peu communs de la construction, tels que l'emploi d'échangeurs Collins et d'échangeurs à circulation transversale et serpentins à intervalles au-dessus du bain à azote liquide et à hydrogène liquide. Le choix des échangeurs de chaleur et les problèmes 'd'éclaboussage' et de transmission de chaleur dans le bain d'hydrogène liquide y sont discutés. Des méthodes ont été essayées pour parer à 'l'éclaboussage' et pour obtenir un refroidissement préalable plus effectif.

RECENTS PROGRES EN ISOLANTS

A. H. COCKETT W. MOLNAR

Une étude théorique des modes de transmission de la chaleur à travers les isolants évacués a été faite et appliquée pour déterminer expérimentalement les conductibilités thermiques, pour séparer la chaleur transmise par conductivité de celle transmise par rayonnement. La contribution due au rayonnement pour une poudre telle que Santocel, représente une proportion élevée du total et le mélange de particules à forte émission produit une réduction appréciable. On démontre également un isolant à écrans multiples incorporant des clinquants en aluminium avec séparateurs en filet ayant une basse conductibilité thermique.

METALLOGRAPHIE AUX TEMPERATURES DE L'HELIUM LIQUIDE

D. HULL H. M. ROSENBERG

Un appareil a été construit pour l'examen microscopique des métaux aux températures de l'hélium liquide, et il a été utilisé pour étudier les transformations martensiques qui se produisent dans le lithium et le sodium. A 20° K entre 40 et 50 pour cent des spécimens de sodium à gros grains furent transformés à la nouvelle phase, et aucune autre transformation ne fut observée en refroidissant à 6° K. Pour des spécimens à petits grains la valeur de la transformation fut beaucoup plus basse. Pour le lithium presque tous les spécimens furent transformés à la nouvelle phase à 20° K. La transformation commença à 31° K pour le sodium et approximativement à 76° K pour le lithium.

CRYOSTAT POUR L'ETUDE DES SUBSTANCES TRANSURANIQUES

G. T. MEADEN J. A. LEE

Un cryostat utilisé en conjunction avec une boîte à gants est décrit. Cet appareil est utile pour mesurer la résistance électrique et de l'effet Hall de métaux et alliages fortement alpha-actifs, sur une gamme de température de 1,4 à 300° K.

SUR LES PROPRIETES DE LA COURBE DE PRESSION DE VAPEUR

E. H. BROWN

Certaines propriétés mathématiques générales de la pression de vapeur comme fonction de la température sont examinées par des méthodes rigoureuses. En particulier, on démontre que limite de forme de la courbe de pression de vapeur est déterminée par la disparition des limites des dérivés de tous ordres dans le voisinage du zéro absolu. Cet article comprend quelques commentaires sur l'impossibilité d'application de la Troisième Loi de la Thermodynamique à la courbe de sublimation.

SUR LA CHALEUR SPECIFIQUE DE L'HELIUM LIQUIDE DANS LA THEORIE DE BRENIG

W. E. PARRY D. TER HAAR

La chaleur spécifique d'un système de bosons non-conjugués est calculée en présumant un spectre d'énergie du type Brenig. Un tel spectre consiste en une branche linéaire de phonons qui est coupée à un certain nombre d'onde k_0 et en une branche quasi-particule quadratique qui commence à k_0 et est caractérisée par une masse effective m. La chaleur spécifique c_v montre une discontinuité à une température de transition T_c. L'on recherche la dépendance de T_c, la hauteur de la courbe c_v et la magnitude du saut dans c_v à $T = T_c$ sur k_0 et m.

DISPOSITIF CRYOGENIQUE POUR IRRADIATION DANS L'AZOTE LIQUIDE

L. BOCHIROL J. DOULAT L. WEIL

Aprés une brève revue des boucles à azote liquide construites jusqu'ici, on décrit une boucle fonctionnant sur un principe nouveau et permettant l'irradiation dans un bain permanent d'azote liquide. Cet azote extra-pur, confiné dans un volume réduit, est recondensé par de l'azote liquide ordinaire, à une certaine distance du cœur, dans une région où le flux est atténué—ce qui élimine tout risque d'explosion—et regagne le bain par gravité. L'absence de tout appareil mécanique de circulation rend la construction très simple et le fonctionnement sûr. La consommation est réduite. Le dispositif permet la récupération des échantillons froids. Il a fonctionné de façon satisfaisante pendant plusieurs périodes continues d'une semaine.

L'EFFET DE L'ENDOMMAGEMENT PAR RADIATION SUR LA CONDUCTIBILITE THERMIQUE DES SUPERCONDUCTEURS

K. D. CHAUDHURI K. MENDELSSOHN
M. W. THOMPSON

L'effet de l'irradiation par les neutrons à 30° C sur la conductibilité thermique des cristaux simples de niobium et de vanadium a été étudié à basse température. Les mesures ont été prises tant à

l'état supraconducteur qu'à l'état normal, lorsque la conductibilité est surtout due aux phonons et aux électrons respectivement. L'effet observé sur la conductibilité des phonons indique une augmentation de la densité de dislocation alors que les changements dans la conductibilité des électrons révèlent la présence de vacances.

CRYOSTATS POUR ETUDES OPTIQUES

P. PESTEIL R. PHILIP

On décrit trois types de cryostats destinés aux études d'optique en lumière visible, ultra-violette ou infra-rouge. Leur construction est simple, leur consommation en liquide réfrigérant minime et leur encombrement faible. Utilisation possible de ces appareils pour l'étude des spectres d'absorption et de luminescence et pour le refroidissement de photomultiplicateurs.

Auszüge

EIN JOULE–THOMSON HELIUMVERFLÜSSIGER UND EINIGE DAMIT VERBUNDENE KONSTRUKTIONSPROBLEME

D. H. PARKINSON

Die Konstruktion und Anordnung eines Joule–Thomson Heliumverflüssigers, der 8 Liter pro Stunde liefert, bei einem Verbrauch von 1,3 Liter flüssigen Wasserstoffs pro Liter flüssigen Heliums wird beschrieben. Einige aussergewöhnliche Konstruktionsprobleme, wie z.B. die Benutzung von Collins- und Kreuzstromwärmeaustauschern mit Windungen über dem flüssigen Stickstoff und flüssigem Wasserstoff werden hervorgehoben. Die Wahl der Wärmeaustauscher und die Probleme des Spritzens und des Wärmeaustausches in flüssigem Wasserstoff werden untersucht. Verfahren zur Vermeidung des Spritzens und um eine wirkungsvollere Vorkühlung zu erreichen werden untersucht.

NEUERE ENTWICKLUNGEN AUF DEM GEBIETE DER ISOLIERSTOFFE

A. H. COCKETT W. MOLNAR

Eine theoretische Untersuchung der Wärmeübertragung durch Isolierstoffe in Vacuum wurde ausgeführt und die Resultate wurden mit durch Experiment bestimmten Wärmeleitfähigkeiten verarbeitet, um die Wärmeübertragung durch Leitung von der durch Strahlung zu trennen. Die Wärmeübertragung durch Strahlung macht bei Pulver, wie z.B. Santocel, einen grossen Prozentsatz der gesamten Wärmeübertragung aus, wird aber durch Beimischung von Teilchen mit einer hohen Emission erheblich reduziert. Ein aus mehreren Lagen bestehender Schirm mit Aluminiumfolie und netzartigen Abstandschichten hat ebenfalls eine niedrige Leitfähigkeit.

METALLOGRAPHIE BEI DER TEMPERATUR DES FLÜSSIGEN HELIUMS

D. HULL H. M. ROSENBERG

Beschreibung eines Geräts für die mikroskopische Untersuchung von Metallen bei der Temperatur des flüssigen Heliums. Dieses Gerät wurde zur Untersuchung der martensitischen Umwandlungen in Lithium und Natrium benutzt. Zwischen 40–50% eine Probe grobkristallinen Natriums wurden bei 20° K in die neue Phase übergeführt, und beim Kühlen auf 6° K wurden keine weiteren Änderungen bemerkt. Für feinkristalline Proben ist der umgewandelte Prozentsatz viel kleiner. Bei Lithium wurde beinahe die ganze Probe bei 20° K in die neue Phase umgewandelt. Die Umwandlung begann bei 31° K bei Natrium und ungefähr 76° K bei Lithium.

EIN KRYOSTAT FÜR DIE UNTERSUCHUNG TRANSURANISCHER SUBSTANZEN

G. T. MEADEN J. A. LEE

Beschreibung eines Kryostaten in Verbindung mit einem strahlungsgeschützten Abzug. Ein solches Gerät eignet sich zum Messen des spezifischen elektrischen Widerstandes und des Halleffektes starker alpha-aktiver Metalle und Legierungen im Temperaturbereich von 1,4–300° K.

ZU DEN EIGENSCHAFTEN DER DAMPFDRUCKKURVE

E. H. BROWN

Einige allgemeine mathematische Eigenschaften der Dampfdruckkurve (als Funktion der Temperatur) werden genauer untersucht. Insbesondere wird gezeigt, dass die Grenzform der Dampfdruckkurve dadurch gegeben wird, dass die Grenzwerte der Differenzialkoeffizienten aller Ordnungen in der Nähe des Nullpunktes unendlich klein werden. Einige Bemerkungen werden auch zur Unmöglichkeit der Anwendung des dritten Hauptsatzes der Thermodynamik auf die Sublimationskurve gemacht.

ÜBER DIE SPEZIFISCHE WÄRME FLÜSSIGEN HELIUMS IN DER THEORIE VON BRENIG

W. E. PARRY D. TER HAAR

Die spezifische Wärme eines Systems von nicht einander beeinflussenden Bosonen wird mit Annahme eines Energiespektrums nach Brenig berechnet. Ein solches Spektrum besteht aus einem linearen Phononzweig, der bei einer bestimmten Wellenzahl k_0 abgeschnitten wird, und einem quadratischen Quasiteilchenzweig, der bei k_0 anfängt und durch eine effektive Masse m gekennzeichnet wird. Die spezifische Wärme c_v weist bei der Übergangstemperatur T_c einen Sprung auf. Die Beziehungen zwischen T_c, der Höhe der c_v-Kurve und der Grösse des Sprunges bei c_v bei $T=T_c$ auf k_0 und m werden untersucht.

AUSZÜGE

EIN TIEFTEMPERATURGERÄT FÜR BESTRAHLUNG IN FLÜSSIGEM STICKSTOFF

L. BOCHIROL J. DOULAT L. WEIL

Eine kurze Übersicht über die bereits bestehenden Stickstoffschleifen, mit Beschreibung einer nach einem neuartigen Prinzip arbeitenden Schleife für Bestrahlung in einem Stickstoffbad. Besonders gereinigter Stickstoff befindet sich in einem kleinen Behälter; der Dampf wird von gewöhnlichem flüssigem Stickstoff in einiger Entfernung vom Kern in einer Zone mit niedrigen Neutronenfluss kondensiert, um Explosionen zu vermeiden. Das Kondensat fliesst dann unter seinem eigenen Gewicht ins Bad zurück. Die Konstruktion dieses Geräts ist äusserst einfach und es ist im Betrieb sehr zuverlässig, da es keine mechanische Umlaufapparatur enthält. Der Stickstoffverbrauch ist sehr gering. Es ist möglich, die Proben im kalten Zustand herauszunehmen. Das Gerät ist während mehrere kontinuierlicher Perioden von je einer Woche erfolgreich in Betrieb gewesen.

WIRKUNG VON STRAHLUNGSBESCHÄDIGUNG AUF DIE WÄRMELEITFÄHIGKEIT VON SUPRALEITERN

K. D. CHAUDHURI K. MENDELSSOHN
M. W. THOMPSON

Die Wirkung von Neutronenbestrahlung bei 30° C auf die Wärmeleitfähigkeit von Niobium- und Vanadiumeinkristallen wurde bei niedrigen Temperaturen untersucht. Messungen wurden im supraleitfähigem Zustand, sowie im Normalzustand, wo die Leitfähigkeit überwiegend auf Phononen bezw. Elektronen beruht, ausgeführt. Die beobachtete Wirkung auf Phononenleitfähigkeit zeigt ein Anwachsen der Versetzungsdichte an, während Änderung der Elektronenleitfähigkeit die Gegenwart von Löchern anzeigt.

KRYOSTATE FÜR OPTISCHE UNTERSUCHUNGEN

P. PESTEIL R. PHILIP

Drei Kryostate für optische Untersuchungen im sichtbaren, ultravioletten und infraroten Gebiet werden beschrieben. Sie sind einfach gebaut, haben einen geringen Kühlmittelverbrauch und beanspruchen wenig Platz. Diese Geräte eignen sich zur Untersuchung von Absorptionsspektren und Lumineszenz, und zum Kühlen von Photoverstärkern.

Резюме

ДЖОУЛЬ ТОМСОНА РАЗЖИЖИТЕЛЬ ГЕЛИЯ И НЕКОТОРЫЕ ПРОБЛЕМЫ ЕГО КОНСТРУКЦИИ

D. H. PARKINSON

Этот доклад дает конструкцию и схему Джоуль Томсона разжижителя гелия с выходом 8 л/час, потребляя 1,3 л/час жидкого водорода на каждый литр произведенного жидкого гелия. Внимание обращено только на некоторые необыкновенные виды конструкции, как, например, употребление над ваннами азота и жидкого водорода Коллинса и перекрестного тока теплообменников. Дискутируется выбор теплообменников и проблемы «брызгивания» и передачи тепла в ванну жидкого водорода. Были испытаны методы по «брызгиванию» и получению более эффективного предварительного охлаждения.

НОВЫЕ ДОСТИЖЕНИЯ В ИЗОЛИРОВОЧНЫХ МАТЕРИАЛАХ

A. H. COCKETT W. MOLNAR

Было проведено исследование форм передачи тепла через эвакуированные изолировочные материалы и применено к экспериментально определенным удельным теплопроводностям, чтобы отделить теплоту переданную проводимостью от теплоты переданной излучением.

Часть переданная радиацией для порошка как Сантосел составляет большую пропорцию целого, и добавление частичек высокой лучеиспускательности вызывает значительное уменьшение. Многоэкранный изолировочный материал, включающий алюминиевую фольгу с сетчатыми сепараторами, тоже, как доказано, дает низкую удельную теплопроводность.

МЕТАЛЛОГРАФИЯ ПРИ ТЕМПЕРАТУРАХ ЖИДКОГО-ГЕЛИЯ

D. HULL H. M. ROSENBERG

Конструктирован аппарат для микроскопического исследования металлов при температурах жидкого-гелия и применялось к изучению мартенситских трансформаций, имеющих место в литие и натрие. При 20° К между 40–50% крупнозернистых образцов натрия были превращены в новую фазу и при охлаждении до 6° К не наблюдалось никакой дальнейшей перемены. Для малозернистых образцов количество трансформации было гораздо меньше. Для лития почти весь образец был превращен в новую фазу при 20° К. Трансформация началась для натрия при 31° К и для лития при приблизительно 76° К.

КРИОСТАТ ДЛЯ ИЗУЧЕНИЯ ТРАНСУРАНОВЫХ ВЕЩЕСТВ

G. T. MEADEN J. A. LEE

Описывается употребленный криостат в соединении с перчаточной коробкой. Такой аппарат пригоден для измерения электрического сопротивления и эффекта Холла сильно альфа-активных металлов и сплавов в пределах температур 1,4–300° К.

Реэюме

О СВОЙСТВАХ КРИВОЙ ПАРОВОГО ДАВЛЕНИЯ

E. H. BROWN

Исследованы строгими методами общие математические свойства давления пара как функция температуры. В частности, показано, что ограниченная форма кривой давления пара определяется исчезновением пределов производних всех порядков в зоне абсолютного нуля.

Включены некоторые комментарии о неприменимости Третьяго Закона Термодинамики к кривой сублимации.

ОБ УДЕЛЬНОЙ ТЕПЛОТЕ ЖИДКОГО ГЕЛИЯ В ТЕОРИИ БРЕНИГА

W. E. PARRY D. TER HAAR

Вычисляется удельная теплота системы не взаимо-действующих бозонов, допуская спектр энергии типа Бренига. Такой спектр состоит из линейного фононной ветви которое обрывается при известном волновом числе k_0 и квадратного ветви квази-частиц, начинающегося при k_0 и характеризующегося эффективной массой m. Удельная теплота c_v показывает обрыв при переходной температуре T_c. Исследуются зависимость T_c, высота кривой c_v и величина подъема в c_v при $T = T_c$ на k_0 и m.

КРАЙОГЕНИЧЕСКОЕ ПРИСПОСОБЛЕНИЕ ДЛЯ ОБЛУЧЕНИЯ В ЖИДКОМ АЗОТЕ

L. BOCHIROL J. DOULAT L. WEIL

После краткого обзора существующих типов петель жидкого азота следует описание петли, оперирующей согласно новому принципу, для облучения в постоянной ванне жидкого азота. Этот специально чистый азот находящийся в маленьком сосуде, во избежание взрыва, реконденсируется в обыкновенном жидком азоте на известном расстоянии от центра, приблизительно до трех футов, в зоне где излучение слабое и обратно течет в ванну под действием силы тяжести. Конструкция аппарата чрезвычайно проста и надежна в работе, благодаря отсутствии механического циркулирующего оборудования. Потребление азота довольно небольшое. Аппарат позволяет вынимание образцов в холодном состоянии. Оперирование производилось удовлетворительно в течение нескольких безпрерывных периодов одной недели.

ВЛИЯНИЕ ПОВРЕЖДЕНИЯ ИЗЛУЧЕНИЙ НА ТЕПЛОПРОВОДНОСТЬ СВЕРХПРОВОДНИКОВ.

K. D. CHAUDHURI K. MENDELSSOHN
M. W. THOMPSON

Было исследовано влияние облучения нейтронами при 30° Цельсия на теплопроводность ниобия и ванадия монокристаллов при низких температурах. Были сделаны измерения как в сверхпроводимом так и нормальном условиях где проводимость, главным образом, является следствием присуствия фононов и электронов, последовательно. Наблюдаемое влияние на фононную проводимость показывает увеличение плотности дислокаций в то время как изменения в электронной проводимости обнаружило присуствие вакансий.

КРИОСТАТЫ ДЛЯ ОПТИЧЕСКИХ ИССЛЕДОВАНИЙ

P. PESTEIL R. PHILIP

Описываются три типа криостатов для оптических исследований: для видимого, ультрафиолетового и инфра красного света. Они простой конструкции, малого потребления жидкого охладителя и малого объема.

Эти инструменты могут быть употребляемы для исследования спектров поглощения или для охлаждения фотоумножителей.

A Joule–Thomson Helium Liquefier and Some Problems in its Design

D. H. Parkinson *Royal Radar Establishment, Malvern, Worcs*

Received 10 February 1960

THE liquefier described here has a number of novel features and has been used to study various problems connected with liquefier design besides supplying laboratory requirements for liquid helium. In its normal condition it has a production rate of about 8·0 l./hr and consumes 1·3 l. of hydrogen per litre of helium produced. The liquefaction coefficient is entirely dependent on the hydrogen bath conditions which are discussed later.

The liquefier is split into three sections. Collins-type exchangers are used in the first section which is cooled with liquid nitrogen. In the second there are space-wound multi-tube cross-current exchangers over a single precooling bath into which liquid hydrogen is siphoned directly and pumped to 14° K. Liquid helium is produced and collected in the third section. In the original design using all-metal Dewars everywhere, the second and third stages were combined, but it was found that the level of hydrogen boiling rapidly in a closed metal vessel could not be estimated reliably. The system was split, therefore, into the three units and a glass Dewar with a sighting slit used for the liquid hydrogen. In this respect the liquefier resembles that at the Clarendon Laboratory, Oxford;[1] however, the heat exchange system is very different.

In the following sections the layout and operation of the liquefier are described, but those parts which follow well-known designs are dismissed as 'conventional' or not mentioned. Some aspects of liquefier design and operation are discussed, as are heat exchangers, hydrogen bath conditions, and collection and handling of helium.

The liquefier

Figure 1 shows a 'circuit diagram' of the liquefier. In section A, liquid nitrogen, which is blown in periodically using compressed air, boils at atmospheric pressure in an all-metal Dewar, i.d. 16 cm, length 75 cm, which completely encloses the unit.

Exchangers A_1 and A_2 are of the Collins[2] construction and are built from $\frac{1}{8}$ in. Yorkshire copper tube with copper fins, o.d. 0·9 cm, thickness 0·2 mm, and spacing 10 per centimetre. A_1 nests inside A_2 and its outer and inner

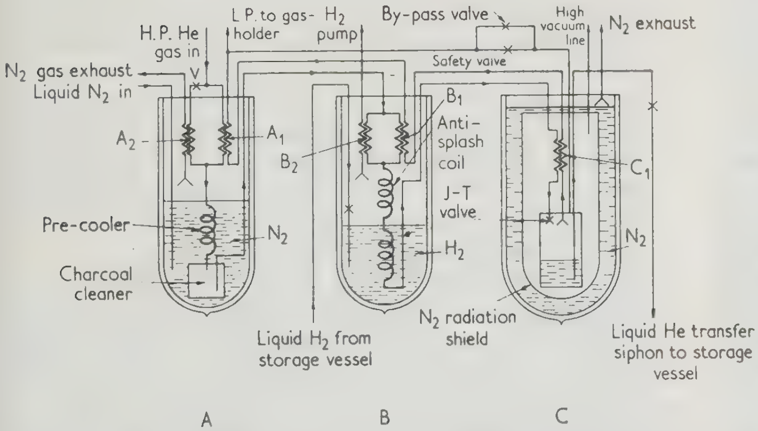

Figure 1 (above). Joule–Thomson helium liquefier. Section A: Liquid nitrogen stage, 77°K; Section B: Liquid hydrogen stage pumped to 14° K; Section C: Helium stage, 4·2°K

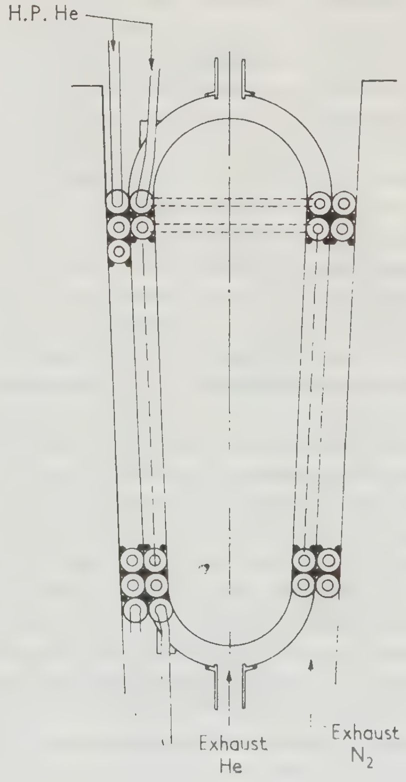

Figure 2 (right). Collins-type exchangers in unit construction envelopes are closed by domes as in Figure 2. Such a construction lends itself to the production of these exchangers as self-contained units. The split in the high pressure gas between A_1 and A_2 is governed by a pre-set valve V at the head of section A. The pre-cooler consists of two 4 m lengths of $\frac{1}{8}$ in. Yorkshire copper tubing in parallel which lead to a charcoal cleaner of approximately 2·5 l. capacity.

Section B (Figure 1) is of greater interest. Liquid hydrogen is siphoned from a 50 l. storage vessel into a glass Dewar, i.d. 13·5 cm, length 85 cm, which completely encloses the whole exchanger system and projects above it by about 10 cm, the whole being enclosed in a metal case in a conventional way. Sighting slits are provided for visual observation of the hydrogen level, normal filling 3 l., but illumination from a built-in electric lamp behind the Dewar is necessary. The inlet valve for liquid hydrogen is orthodox except that it has a finely cut needle (s.v. angle 20 degrees) with a fine control screw thread, so that the hydrogen filling rate can be adjusted to balance the rate of hydrogen evaporation. Filling need not then disturb the pressure over the liquid bath. A liquid–gas separator is arranged so that incoming liquid hydrogen swirls round the inside wall of the Dewar above the liquid and washes the sighting slit clean.

Heat exchangers B_1 and B_2 are of similar construction, space-wound cross-flow, and consist respectively of 14 and 4 cupro-nickel 80/20 tubes, 1·3 mm o.d. and 1·0 i.d.; in B_1 they are approximately 16·8 m long and in B_2 approximately 20·8 m. The distribution of high pressure gas between these two exchangers is governed entirely by the number and lengths of tube in each and is about 3:1.

In both B_1 and B_2 the tube windings are arranged in sections 5 cm long and there are eight sections in each. In A_1 there are five layers and beginning from the inside there are 2, 2, 3, 3, and 4 tubes in successive layers. At the end of each 5 cm section the four tubes from the outer layer change places with the four from the two inner layers and the three tubes in each of the remaining two layers also change places; in this way the high pressure gas is distributed fairly evenly over the annular space of the exchanger. Spacers 1 mm thick are placed between each layer and also prevent the outer and inner layers from touching the envelopes of the exchanger. The separation between turns is about 0·4 mm in all layers. With exchanger B_2 there are four layers each containing one tube. The outer and inner tubes change places at the end of each 5 cm section as do the remaining two tubes, 1 mm spacers are again used, and the separation between turns is about 2·3 mm. B_2 fits inside B_1 so that the inner sheath of B_1 forms the outer sheath of B_2. The annular section of B_2 is 2·5 cm i.d. × 5·0 cm. o.d., while that of B_1 is 5·1 cm i.d. × 7·5 cm o.d. A sheath of Tufnol tube around the sections of B_2 is used to take up about 0·2 cm of dead space outside the windings.

The pre-cooling and anti-splash coils are also space-wound and made in a similar way. The anti-splash coil, the function of which is discussed later, has fourteen tubes in parallel, 4 m long, wound with a separation of 1·3 mm. In the pre-cooling coil there are ten tubes, each 2 m long.

In section C, the helium vessel, which can hold 8 l. of liquid, is protected by a liquid-nitrogen-cooled continuously pumped vacuum jacket. The whole of this section is enveloped by a large stainless-steel Dewar, of which the outer skin is strengthened and which clips directly on to the head of C. The bottom of the outer skin is re-entrant so that the whole Dewar stands freely on its own when removed from C. This construction is standard in this laboratory. The final heat exchanger lies in the vacuum space of C and consists of seven $\frac{1}{8}$ in. Yorkshire copper tubes soft-soldered side-by-side down their length (Figure 3). High pressure gas passes down the middle tube and low pressure gas passes up the six outer tubes.

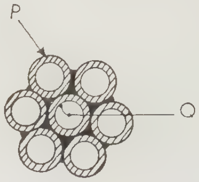

Figure 3. Bundle type of exchanger

The Joule–Thomson valve is conventional, the stem and needle do not rotate and are on the low pressure side of the valve seating. Special attention has been paid to achieving a fine control, 0·2 mm movement per turn of the Joule–Thomson valve control knob, and by using a system of spring-loaded threads backlash has been removed. These features are necessary to obtain smooth running with the minimum of adjustment. After each adjustment of the J–T valve some 2–3 min elapse before the equilibrium low pressure is established. Consequently, to assist in making adjustments, the position of the J–T control can be read on a scale enabling it to be pre-set or moved by a definite amount. A liquid–gas separator is fitted to the J–T valve exit (see later). The normal working pressure in the helium vessel is about 0·25 atm.

The remaining features of the liquefier are quite 'orthodox': a by-pass valve for running-up; complete gauging on high and low pressure sides; gas thermometer attached to the helium vessel; safety valves; etc. The inter-stage helium connections are made by removable high and low pressure siphons each individually pumped and sealed. High pressure gas is supplied by two Bristol Pneumatic B.M.3 compressors which were specially prepared to be gas-tight for this purpose. A pressure controller is fitted at the liquefier limiting the maximum supply pressure to 480 lb/in^2, the normal supply being 380 lb/in^2.

As far as the operation of the liquefier is concerned the running-up drill is quite conventional, including pre-cooling with liquid nitrogen in all stages before liquid hydrogen is introduced into B. It takes 50 min from commencing the running-up drill to the point at which helium is being collected. During this time 5·3 l. of hydrogen are required of which 2 l. remain in the bath B. In 'steady-state' running the liquefier operator is occupied principally in controlling the conditions in the hydrogen bath. It is intended at a later stage to install automatic pressure regulation on this bath.

Heat exchangers

Heat exchangers for liquefiers must have high efficiencies and at the same time low resistance to gas flow. These two requirements are difficult to reconcile with each other within the limits of the geometry and small mass desirable in a liquefier. It is a great advantage to have an overall low resistance to flow, particularly for the exhaust gases, for then the pressure over the helium is low, pressure fluctuations are small, and boiling-off with accompanying splashing on transfer is much reduced. The chief sources of resistance to flow for the exhaust gases lie in sections A and B of the liquefier. The final exchanger C_1 (Figure 1) working between 14° K and 4·2° K does not present much of a problem, for the gas is very dense at these temperatures and has a low viscosity. Hence the resistance to its flow is small.

With the construction used here (Figure 3) for C_1, the chief snag is to ensure good thermal conduction from points such as P on the low pressure tubes to the high pressure gas at Q. This can be achieved with copper tubes whereas cupro-nickel with its poor conduction is somewhat unsuitable for this construction. Conduction down the length (4·5 m) of a copper exchanger such as this is not obnoxious, calculation and measurement agree in giving an efficiency of approximately 95 per cent for C_1. The chief practical difficulties in construction are to ensure that the spaces between the tubes are filled with solder and that the tubes are pulled tightly together to reduce the solder to a minimum.

Exchangers B_1 and B_2 are concerned only with hydrogen conservation but, as such, are vital to the economics of the liquefier. The choice of a single pumped bath of liquid hydrogen makes for a simple layout and comparatively easy operation, but on the other hand it imposes such a severe restriction on the tolerable resistance to hydrogen gas flow in B_2 that the simple Linde tubular exchangers are unsuitable; with B_1 similar arguments apply but with less force.

A number of different exchanger constructions are suitable for B_1 and B_2, of these the Collins[2] or exchangers based on Still[3] tubes have the greatest appeal. With them the resistance to exhaust gas flow is small and the 'wetted perimeter' S_o on the low pressure side can be six to ten times greater than that, S_i, on the high pressure side. In consequence, in the expression for the thermal resistance between high and low pressure gas streams, i.e. $(1/H_i S_i)+$ resistance of walls$+(1/H_o S_o)$, the term $1/H_o S_o$ can be made approximately equal to $1/H_i S_i$. H_o and H_i are the thermal exchange coefficients on the low and high pressure sides. Space-wound exchangers occupying the same space are less efficient but considerably easier to build than the Collins type. For this particular liquefier the choice was governed primarily by the availability of tubing. It would have been some advantage to have used dimensions of, say, 2 mm × 1 mm for B_1 and B_2 for then $S_o = 2S_i$. The performance of B_1 and B_2 can be calculated using the data of Norris and Spofford[4] to deduce H_o. Both are approximately 92 per cent efficient. No attempt to conserve 'cold' in the exhaust from B_2 has been made. This is warmed to room temperature by a water-heated internally finned section of pumping line.

The Collins exchangers of section A have an efficiency of approximately 92 per cent and are concerned only with conservation of liquid nitrogen in section A.

Liquid hydrogen pre-cooling bath conditions

There are a number of interesting points concerned with the hydrogen bath which do not seem to have been recorded previously. First, with the vigorous boiling in the hydrogen bath, to bring the liquid to approximately 14° K the pressure near the entrance to B_2 was less than 5·5 cm (triple point pressure of hydrogen). In consequence an objectionable crust of solid hydrogen formed around the entrance of this exchanger and also around the walls of the Dewar above the liquid. Visual observation showed that this crust was caused by a fine spray or 'Scotch mist' of hydrogen liquid droplets above the liquid. This spray was also being drawn into B_2 where it 'short circuited' the lower part of the exchanger leading to high total evaporation rates. These conditions are alleviated by the 'anti-splash' coil which is arranged to cover completely the entrance to B_2. There is a baffle across the free end of the coil so that the gas–droplet mixture is drawn into the coil radially from the outside and leaves it longitudinally going into B_2. As shown in Figure 1, all the high pressure helium gas from B_1 and B_2 goes through this coil and then passes to the pre-cooling coil. The temperature of the high pressure helium in the 'anti-splash' coil is then some 8–10° K above that of the hydrogen 'Scotch mist' according to the performance of B_1 and B_2 and the liquefaction coefficient. Even if B_1 and B_2 were 100 per cent efficient there will always be a considerable temperature difference provided helium is being liquefied at a reasonable rate. As arranged (Figure 1), an anti-splash coil is very effective indeed and with the coil described earlier the full efficiency of B_2 can be realized. However, the anti-splash coil occupies the region of lowest temperature in the hydrogen bath, as can be demonstrated by the solid hydrogen crust formation and by direct measurement with a gas thermometer. The anti-splash coil could then be equally well connected into the helium circuit after the pre-cooling coil as a means of bringing the high pressure helium to as near 14° K as possible before going to the last exchanger. This arrangement has also been tried successfully but now the temperature difference across the walls of the anti-splash coil is much smaller, depending on the actual temperature of the pre-cooling bath and how effective the pre-cooling coil is. Used this way in the present geometry the anti-splash coil evaporates only about half of the hydrogen carried as droplets in the gas stream. The ideal arrangement which should permit the maximum heat dissipation in the hydrogen bath while maintaining effective cooling to 14° K seems to be to use anti-splash coils both before and after the pre-cooling coil. This has not yet been tried owing to production demands on this machine.

The conditions described here are of course peculiar to the geometry of the hydrogen bath used. If space permitted it would be advantageous to use a bath with a much larger hydrogen liquid surface area. With the present Dewar, at a normal 8·0 l./hr production rate, about 10 l. of hydrogen are evaporated per hour which corresponds, allowing for temperature and pressure, to evaporating approximately 10 cm^3 of gas per second per square centimetre of free hydrogen surface. However, about half of the present evaporation occurs in the anti-splash coil from droplets carried in the gas stream.

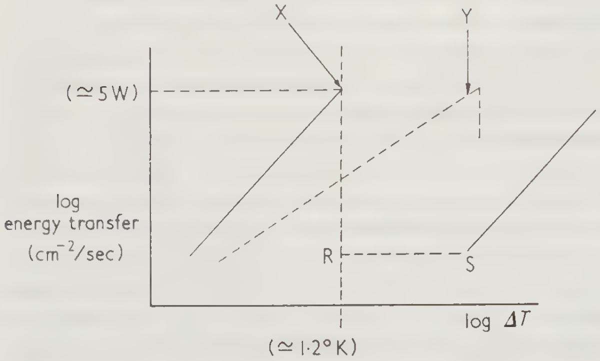

Figure 4. Energy transfer from metal surface to liquid hydrogen

A second problem occurs with the pre-cooling coil itself; it has been shown that the heat transfer between a metal surface and hydrogen liquid follows a curve as shown in Figure 4.[5] This is similar to well known curves for other liquids and for similar reasons. However, the point at which the maximum heat transfer occurs corresponds to a temperature difference between the metal surface and liquid of only about 1·2° K. With the exchanger layout in normal liquefiers the helium inevitably enters the hydrogen bath some 10° K above the hydrogen liquid temperature and with an anti-splash coil as in this liquefier at about 4° K above the liquid temperature. The first part of the pre-cooling coil must therefore work in the temperature range where the thermal transfer is heavily impaired by a gas film (R–S in Figure 4). This situation can be improved upon by coating the first half of the pre-cooling coils with Araldite thermosetting varnish, which substitutes the thermal resistance of a layer of varnish instead of gas between the liquid and metal wall. The equivalent thermal transfer curve for such a treated surface should then be such as Y in Figure 4. In this way, more effective and compact coils should be possible. This has been tried with some success marred by the varnish cracking away from the metal surface, consequently no quantitative results are yet available.

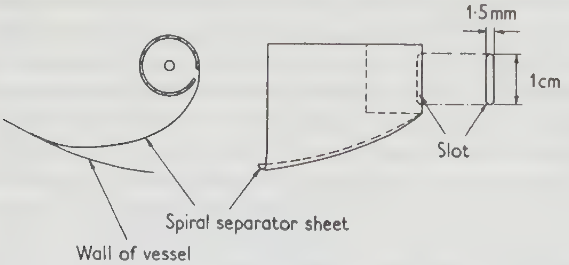

Figure 5. Liquid–gas separator for helium at s.t. value. Also for hydrogen in stage B

When this problem has been solved it should be possible to enhance the helium gas handling capacity of this machine considerably and hence its overall production rate. At present, with a normal pre-cooling coil and a circulation rate of 570 l. of free gas per minute, ϵ is approximately 0·18, yielding 8 l./hr.

Collection and handling of helium

It has been remarked already that liquid–gas separators are fitted to the hydrogen inlet valve in B and to the Joule–Thomson valve in C. In both instances these are extremely simple and the construction is shown in Figure 5. The exhausting gas–liquid mixture is forced against the spiral metal sheet from whence it runs smoothly down and round the vessel wall. With the helium vessel the liquid level can rise to within 0·5 l. of the top, at which point the separator is impaired by beginning to be covered and the liquefier must be emptied. The importance of effective separation of the helium liquid and of keeping it under a steady pressure with the minimum of disturbance must be well stressed. An otherwise efficient design can be severely impaired by lack of attention to these points.

As a monitor of the performance of the liquefier, the heights of the associated gas-holders are automatically and continuously recorded during a run. This enables the operator to make immediate estimates of the performance at a glance besides enabling a detailed study of production conditions to be made easily. It has also been invaluable in estimating the skill of the operators, particularly in transferring helium liquid with little loss. The handling of the gaseous helium, bringing it into the circuit and returning it to the high pressure reservoirs is carried out automatically by a control system working from gas-holder heights. This will be described in due course.

The author wishes to thank Mr. J. Oliver for his work in installing the liquefier and unflagging aid in testing and collecting data; he also wishes to thank those members of the workshop staff, particularly Mr. R. Cullen, who constructed it and installed the ancillary apparatus.

This paper is published by permission of the Controller of H.M. Stationery Office.

REFERENCES

1. Croft, A. J. *Progress in Cryogenics 3* (Heywood, London, 1961). To be published
2. Collins, S. C. *Rev. sci. Instrum.* **18,** 157 (1947)
3. Still, E. W. *Proc. Instn mech. Engrs, Lond.* **134,** 363 (1936)
4. Norris, R. H., and Spofford, W. A. *Trans. Amer. Soc. mech. Engrs* **64,** 489 (1942)
5. Mulford, R. N., and Nigon, J. P. *Los Alamos Rep.* No. 1416

Recent Improvements in Insulants

A. H. Cockett and W. Molnar *British Oxygen Research and Development Ltd, London*

Received 12 February 1960

WHEN liquefied atmospheric gases became readily available, the need to store them for reasonable periods of time posed new problems in thermal insulation. The first satisfactory solution was that of Dewar[1] who developed the vacuum insulated container. In this a vessel containing the liquid is surrounded by a similar, more or less concentric, vessel, and the space between the two is evacuated. By this means heat inleak due to conduction and convection through the gas is eliminated, and the heat flow down the neck of the inner vessel may be reduced by heat exchange with emerging vapour. The major heat influx is by radiation and this can be appreciably reduced by giving the surfaces facing the vacuum space a low emissivity. If the container is made of glass the whole of the surface in the vacuum space is silvered, while for larger vessels, normally made of copper and holding a few gallons, the surfaces facing the vacuum space are highly polished. Small stainless-steel vessels made for special purposes have these surfaces copper-plated and electro-polished. Some further reduction can be effected by interposing one or more metal screens of low emissivity between the surfaces bounding the vacuum space. For example, Croft and Jones[2] described a vacuum insulated tank for liquid oxygen incorporating four such screens. It is, however, mechanically difficult to support the screens unless the vessel is of some simple geometrical shape such as a right circular cylinder.

These techniques still suffice for small vessels, but with the growth of cryogenic engineering, new methods are constantly being sought, particularly for fairly large containers. The chief disadvantage of high vacuum insulation, requiring pressures below 0·001 mm Hg, for large vessels is associated with the difficulty of maintaining such a high vacuum. The heat transfer across the 'vacuum' space increases rapidly if, because of leaks, the increasing gas pressure reaches the point where the mean free path is reduced to a figure less than the distance between the bounding surfaces. The upper pressure limit for a vessel with vacuum space 10 cm thick is thus about 0·5 microns (0·0005 mm Hg).

As Dewar pointed out, if the annular space between the two vessels is filled with a powder before evacuation, a much higher gas pressure can be tolerated. The maximum allowable pressure will be between 20 and 100 microns Hg depending upon the powder, although one would expect that for an interparticle distance of 10 microns, it might be as great as 500 microns Hg. The limit is, however, set by the fact that gas conduction is a linear function of pressure in conditions where the mean free path is greater than the confining space. Above about 50 microns Hg, this contributes an increasing proportion to the overall heat transfer. Kistler,[3] measuring the variation with pressure of the thermal conductivity of Santocel, quotes the relation:

$$k_g = 0{\cdot}058\sqrt{\left(\frac{M}{T}\right)}\,C_v\,l_0\,\frac{L}{L+(2-a)/a.(l_0/P)}$$

where k_g is gas conductivity, M is molecular weight of the gas, C_v is specific heat at constant volume, l_0 is normal mean free path of the gas at the given temperature and a pressure of 1 mm Hg, L is mean free path of the gas within the powder at low pressure, and a is accommodation coefficient.

There will be some heat conduction through the powder itself but the thermal resistance at the contacts between particles is high and is the governing factor. The effect of pressure on this is due to the presence of adsorbed gases, and an increase in pressure will decrease the thermal resistance.

Radiation, although decreased considerably by the powder due to scattering and absorption, will still be the main mode of heat transfer. For example, silica aerogel, which is one of the powders commonly used, consists of very small fibre-like particles and therefore has low thermal conductivity, but like many of the others, it is relatively transparent to the far infra-red, which is the important region of the spectrum. (A source at about 300° K radiates practically all of its energy in wavelengths greater than 2 microns and the majority in wavelengths above 4 microns.)

Kropschott and others[4] have shown that the thermal conductivity of powder insulants such as Santocel can be reduced by admixing powdered aluminium or copper, and have thus produced insulants of much lower thermal conductivity than that of the separate powders.

Petersen[5] showed that a multiplicity of radiation screens with suitable separators substantially reduced the heat transfer across an evacuated space, and Riede and others[6-10] have also developed this form of insulant.

One objective of the present work has been to separate the overall heat transfer through a number of insulants into two components, radiation and conduction, to show what incentive, if any, there is for an attempt to develop less transparent materials. Both powder insulants and multiple radiation screens have been studied.

Theoretical

The following simple theoretical background has guided the approach. Consider first an evacuated space bounded by two infinite parallel plane walls at different temperatures T_1 and T_2 ($T_1 > T_2$) with emissivities ϵ_1 and ϵ_2. Some of the energy emitted from one surface will be absorbed by the other and the remainder reflected back to the source. Some of this will be re-radiated and so, by multiple reflection and absorption, the energy will be attenuated until all is absorbed. It can be shown[11] that the energy transferred per unit area from the warm surface to the cooler one is given by

$$\frac{Q}{A} = \frac{\sigma}{(1/\epsilon_1)+[(1/\epsilon_2)-1]}(T_1^4-T_2^4) \qquad \ldots(1)$$

Here Q is the total energy exchanged between equal areas, A, of the surfaces, and σ is Stefan's constant.

The radiation between two concentric spheres of radii r_1 and r_2 can be calculated in the same way. The radiation emitted by the inner sphere all falls on the outer, but only part of that which is reflected falls again on the inner one. If the analysis is continued as before, the energy exchanged is found to be

$$Q = \frac{\sigma A_2}{(1/\epsilon_1)+(A_2/A_1).[(1/\epsilon_2)-1]}(T_1^4-T_2^4) \quad \ldots(2)$$

where A_1, A_2 are the surface areas, so that $A_1/A_2 = r_1^2/r_2^2$.

Similar arguments can be used for the heat transfer between infinite concentric cylinders, in which case, in equation (2), $A_1/A_2 = r_1/r_2$.

When the evacuated space contains powder or a number of radiation screens with spacers there are two modes of heat transfer, conduction and radiation. A convenient method of analysing the heat flow is to consider a system of parallel reflecting screens separated by a perfectly transparent medium of thermal conductivity k. To simplify the analysis it will be assumed that each screen is extremely thin and a perfect conductor so that both surfaces are at the same temperature. It is further assumed that all the surfaces have the same emissivity ϵ and that both this emissivity and the thermal conductivity k of the medium are independent of temperature.

Consider a space, bounded by infinite plane parallel surfaces unit distance apart, in which there are $(N-1)$ equidistant plane parallel screens, the resulting N spaces being filled with the transparent conducting medium. The heat transferred from screen r to screen $(r+1)$ is conveyed partly by conduction and partly by radiation. If L is the distance between adjacent screens we can write

$$Q = \frac{kA}{L}(T_r-T_{r+1})+\frac{\sigma A}{(2/\epsilon)-1}(T_r^4-T_{r+1}^4) \quad \ldots(3)$$

Since there are N spaces between the bounding surfaces, $L = 1/N$ and equation (3) may be written

$$\begin{aligned} Q &= NkA(T_r-T_{r+1})+\frac{\sigma A}{(2/\epsilon)-1}(T_r^4-T_{r+1}^4) \\ &= NkA(T_r-T_{r+1})+RA(T_r^4-T_{r+1}^4) \qquad \ldots(4) \end{aligned}$$

where $R = \dfrac{\sigma}{(2/\epsilon)-1}$

When the system is in equilibrium the heat carried from one screen to the next is constant from one bounding surface to the other and thus, summing over the whole system of N spaces and $(N+1)$ surfaces, we obtain

$$NQ = NkA(T_1-T_2)+RA(T_1^4-T_2^4)$$

or

$$\frac{Q}{A} = k(T_1-T_2)+\frac{R}{N}(T_1^4-T_2^4) \qquad \ldots(5)$$

If we divide Q/A by (T_1-T_2) we obtain an effective thermal conductivity K_{12} which is a function of the wall temperatures T_1 and T_2, the emissivity ϵ, and the number of screens $(N-1)$, and is given by

$$K_{12} = \frac{Q}{A(T_1-T_2)} = k+\frac{R}{N}(T_1+T_2)(T_1^2+T_2^2) \ldots(6)$$

Similar equations can be developed for the heat transfer across spaces bounded by concentric spherical or cylindrical surfaces.

Inspection of equation (6) shows that a measurement of Q, and hence of K_{12}, with different wall temperatures enables us to determine the contribution to heat transfer due to conduction and that due to radiation over the temperature range T_1-T_2. Equation (6) can also be applied formally to a vacuum insulated metal Dewar. In this case, the first term on the right-hand side is proportional to the heat conducted down the neck, and $N = 1$.

Experimental—Apparatus

The present work formed part of a study of potential insulants for containers designed to hold liquid oxygen or nitrogen and, consequently, the main interest lay in determining a value for the effective thermal conductivity K_{12} averaged over the temperature range from about 77° K to ambient. It was therefore unnecessary to attempt to measure the thermal conductivity at any particular temperature and the heat transfer was measured by observing the rate of evaporation of liquid nitrogen in a container surrounded by the insulant under test.

Two separate containers for the liquid were used, shown in Figures 1 and 2. The first was a modified commercial 5 l. copper Dewar of spherical shape. An aperture for insertion of powder was cut at the bottom of the outer vessel to which a flange was soldered. The hole was closed when necessary by means of a cover plate screwed to the flange and sealed with an indium gasket. To the upper part of the outer vessel a copper tube was soldered through which the insulating space could be evacuated. The surfaces facing the vacuum were initially highly polished as would have been the case with an unmodified vessel. It was difficult, however, to maintain this degree of polish on successive exposure to the atmosphere and, as changes in the emissivity of these surfaces might have affected the results, most of the experiments on powders were carried out in a glass container. This was not silvered and therefore the surfaces had a constant high emissivity.

The second vessel was cylindrical in shape (Figure 2). The inner vessel had a volume of 990 cm³ and the volume

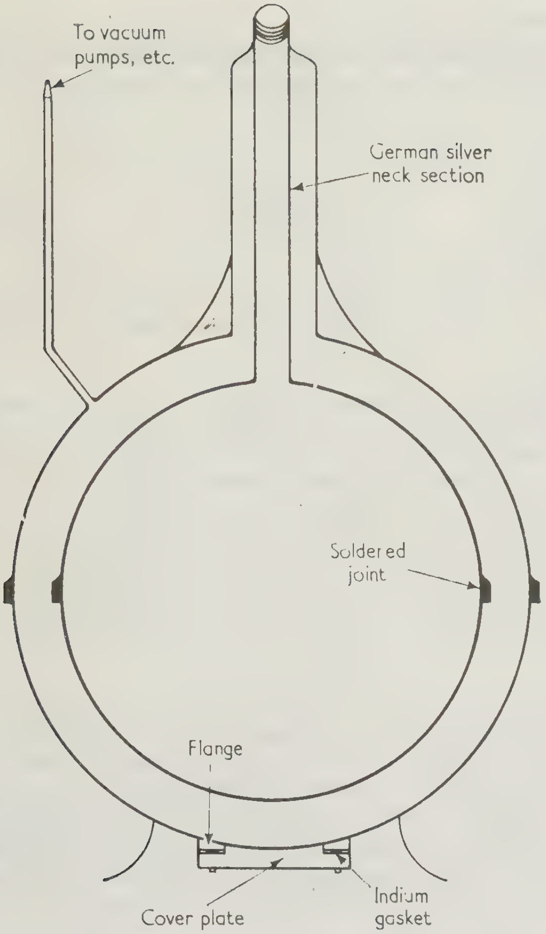

Figure 1. 5 l. copper Dewar

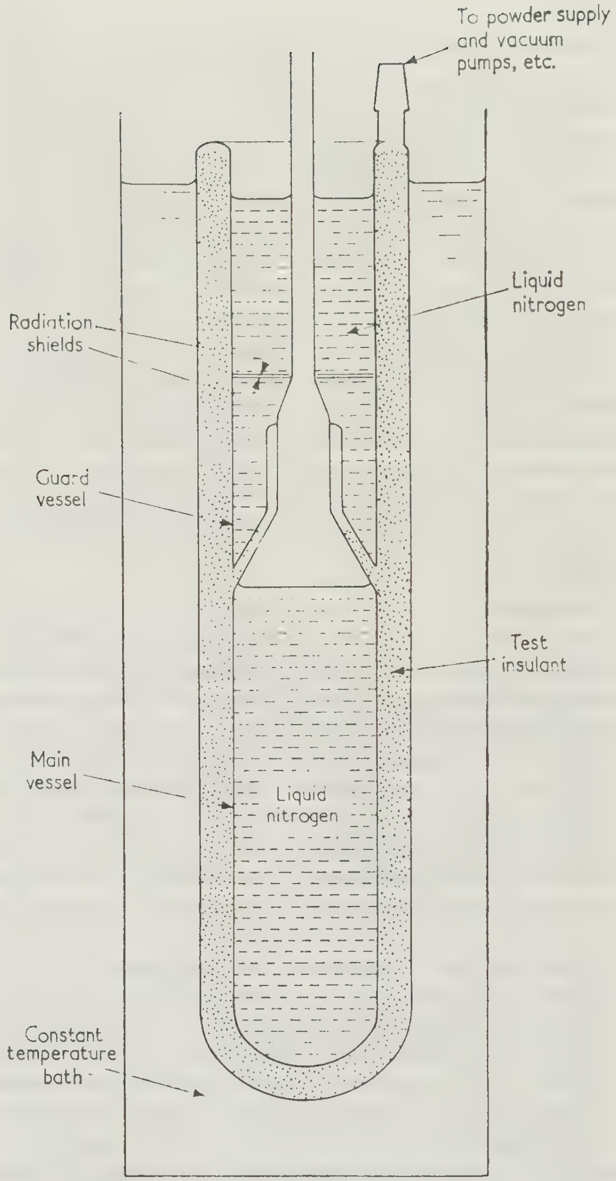

Figure 2. Glass vessel

of the insulant space was 2·2 l., the thickness of the insulant being 1·75 cm. Above the main vessel a conical shell was fitted which was partly filled with the insulant. This shell formed the lower wall of an upper vessel which was filled with liquid nitrogen and thus acted as a guard chamber ensuring that all the heat inleak to the main vessel was through the cylindrical walls and the hemispherical base. Two aluminium radiation shields were also added to the guard vessel to prevent radiation passing vertically downwards through the liquid in the upper vessel.

In order to apply equation (6) to the results, the rate of evaporation of liquid nitrogen from the inner vessel was measured while the vessels were immersed in constant temperature baths at a number of temperatures, usually −78·4° C (the sublimation point of solid carbon dioxide), 0° C, 30° C (representing a close approach to normal ambient temperatures), and 90–100° C. The volume of the evaporated gas was measured by means of a water-sealed positive displacement gas meter. The gas was therefore passed through a tower containing wet porous ceramic chips to saturate it and bring it to ambient temperature before it entered the gas meter. The arrangement used is illustrated in Figure 3.

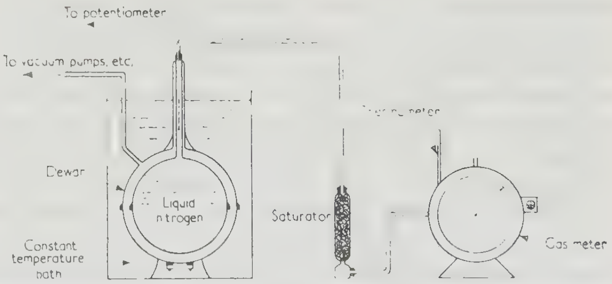

Figure 3. Experimental arrangement

Insulants

The first exploratory experiments were carried out on the copper Dewar vessel (Figure 1), followed by a study of a silica aerogel, Santocel A, in the vacuum space of the glass vessel. A number of other commercially available powders, of which a synthetic calcium silicate, Microcel E, was typical, were then examined. This was followed by studies of mixtures of these more or less transparent powders with a very fine powder of high reflectivity, metallic aluminium, in varying proportions, and also of an insulant composed of sheets of aluminium foil separated by fabric nets.

The silica aerogel, Santocel A, is composed of aggregates of fibre-like particles. After sieving, these aggregates are smaller than 120 microns but the ultimate particle size is approximately 0·05 microns. The synthetic calcium silicate is a powder of average particle size 0·05 microns. The aluminium powder was a superfine lining powder used mainly as a pigment, most of the particles being smaller than 20 microns.

Procedure

The powder mixtures were prepared by pre-mixing weighed quantities of the constituents and forcing these through a 40 mesh sieve. The powders were then mixed and sieved twice again to ensure intimate mixing. To ensure complete homogeneity of the powder it was sealed into a cylindrical jar containing two loose strips of wood, and then rotated with its axis horizontal for about 8 hr.

The powder was transferred into the vacuum space through a wide funnel inserted in the filling port. When the space was filled it was roughly evacuated and then carefully opened up to atmospheric pressure in order to compress the powder, but avoiding excessive compression. The resulting empty space was topped-up and the cycle of evacuation and topping-up repeated three or four times until very little contraction occurred when the vacuum was broken. This procedure ensured that in the final evacuation the powder did not contract. The vessel was then placed in the constant temperature bath and connected to a pumping system comprising the usual rotary and diffusion pumps, a cold trap, and pressure gauges. Evacuation was carried out slowly to avoid carrying powder into the vacuum system. Finally the vessel was wrapped with a heating tape and the temperature raised in stages to 100° C to de-gas the powder.

When the pressure in the insulating space had been reduced to less than 1 micron the vessel was allowed to cool. Then the inner vessel was filled with liquid nitrogen, and the bath brought to the required temperature. The vessel was kept topped-up with liquid nitrogen, at least overnight, to ensure equilibrium, then the evaporation of liquid nitrogen was measured at 30 min intervals over a period of approximately 8 hr. The resulting evaporation rates were then plotted and extrapolated to zero time to obtain the evaporation rate when the vessel was full. A preliminary experiment in which the evaporation rate was measured on successive days showed that equilibrium was attained within the first sixteen hours.

Results

The observed values of the effective conductivity K_{12} for the insulants studied are given in Table 1 and Figure 4. For the copper Dewar the figures given are the values of $Q/[A_2(T_1-T_2)]$ where A_2 is the surface area of the inner vessel. From Figure 4, the conductivity k can be obtained as the intercept and hence the proportion of heat transferred by radiation can be calculated for any wall temperature. The results for a warm wall temperature of 30° C are given in Table 2.

Table 1. Heat Transfer Through the Insulants

Warm wall temperature (°C)	*Effective conductivity K_{12} (cal/sec deg.C cm)*				*$\frac{Q}{A_2(T_1-T_2)}$ (cal/sec deg.C cm²)*
	Santocel	*40/60 (w/w) Aluminium Santocel*	*Microcel E*	*Foil-net insulant*	*Copper Dewar*
−78·4	1·39	0·498	1·142	—	0·82
−70·1	—	—	—	0·261	—
−18·2	1·96	—	—	—	—
0	2·66	0·674	1·605	0·366	1·16
22·4	—	—	—	0·440	—
30	3·89	0·838	1·965	—	1·49
53·8	—	—	—	0·498	—
59·8	5·42	—	2·447	—	—
85	7·15	—	—	—	—
90	—	1·138	—	—	—
98	—	—	—	—	2·36

Table 2. Conduction and Radiation Through the Insulants

Insulant	*Effective conductivity K_{12} (cal/sec deg.C cm)*	*Conduction k (cal/sec deg.C cm)*	*Radiation*	
			(cal/sec deg.C cm)	*(per cent of K_{12})*
Santocel A	$3{\cdot}90 \times 10^{-6}$	$0{\cdot}15 \times 10^{-6}$	$3{\cdot}75 \times 10^{-6}$	96
40/60 (w/w) Aluminium Santocel	0·80	0·32	0·48	60
Microcel E	1·98	0·84	1·14	58
Foil-net	0·44	0·16	0·28	64
Copper Dewar	1·48	0·40	1·08	73

Wall temperatures: $T_1 = +30°\text{C}$, $T_2 = -196°\text{C}$.

Discussion

Figure 4 and Table 2 show that 96 per cent of the heat transferred through Santocel is by radiation, giving considerable hope of reducing the overall conductivity K_{12} by the addition of a reflecting powder such as aluminium. This has been realized in the mixture containing 40 per cent (w/w) aluminium and 60 per cent Santocel for which only 60 per cent of the much smaller overall heat transfer is by radiation. Conductivity through the solid, k, has been increased by about 100 per cent over that of Santocel, but

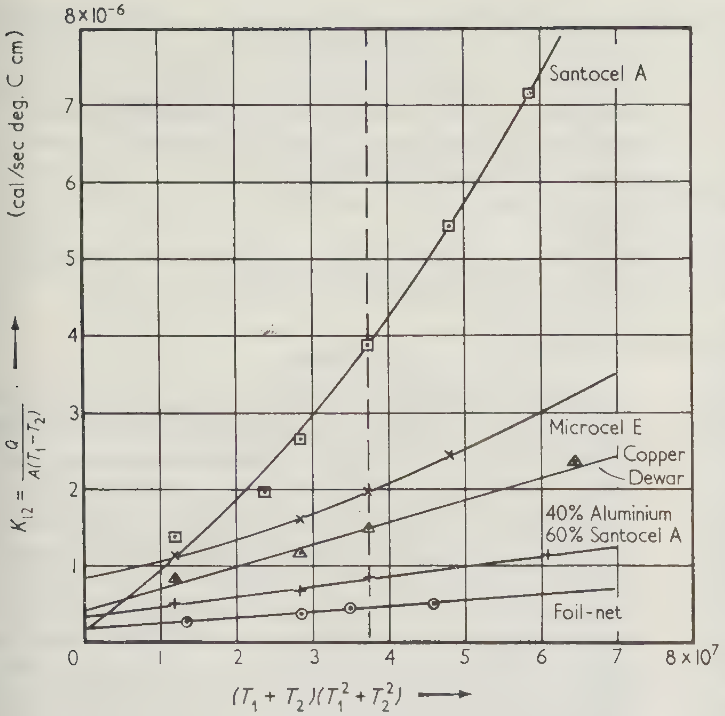

Figure 4. Effect of wall temperature on effective thermal conductivity. Wall temperatures: $T_1 = 303°K$; $T_2 = 77°K$

the figure is still quite small and radiation has been decreased almost by a factor of 8 so that the effective conductivity K_{12} has been diminished by a factor of 5. The effect on K_{12} for a warm wall temperature of 30° C of varying the proportion of aluminium in the mixture is shown in Figure 5. At low concentrations the conductivity K_{12} is high because the aluminium is present in insufficient quantity to eliminate radiation, while at high concentrations the high thermal conductivity of the metal increases the conduction through the solid; the 40/60 mixture already mentioned is near the optimum concentration. These results are similar to those that have been obtained by other workers[12] using slightly different grades of Santocel and aluminium.

The calcium silicate Microcel E has a lower overall conductivity than Santocel but from Figure 4 it is apparent that it has high conductivity k but passes little radiation, so that no great improvement can be expected from the addition of aluminium; this was confirmed by a subsidiary experiment.

The insulant composed of layers of aluminium foil and fabric net has the lowest overall conductivity K_{12} of any of the materials quoted here. Conduction through the solid is the same as for Santocel but the contribution due to radiation is very small, although equivalent to 64 per cent of the total heat transfer. The emissivity of the aluminium used as determined from these figures is 0·062.

The figures obtained with the copper Dewar indicate an unexpectedly high conduction through the solid which must have been due to the metallic neck supporting the inner vessel. Even so radiation contributes 73 per cent of the total heat flux.

According to equation (6) for any insulant having emissivity ϵ and conductivity k independent of temperature, the effective thermal conductivity K_{12} should be a linear function of $(T_1+T_2)(T_1^2+T_2^2)$. Figure 4 shows that this is a close approximation for many of the insulants studied. For some, such as Santocel A and Microcel E, appreciable departures from linearity are observed, and for these it is probable that the emissivity varies with wavelength, i.e. with the temperature of the warm surface. The value of K_{12} for Santocel A determined with wall temperatures of −196° C and −78° C, corresponding to

$$(T_1+T_2)(T_1^2+T_2^2) \simeq 1\times10^7$$

departs from a smooth curve through the other points by an amount several times the experimental error, suggesting a transmission band at the corresponding wavelength (maximum energy at 8 microns). This is also suggested by the results of other workers[13] who find that the effective conductivity K_{12} increases with increasing thickness of the insulating space. However, as indicated in Figure 4, conduction through the solid, k, must be less for Santocel A than for the 40/60 aluminium–Santocel mixture.

However, the application of equation (6) to measurements of the effective conductivity K_{12} obtained by the method described here makes it possible to distinguish the

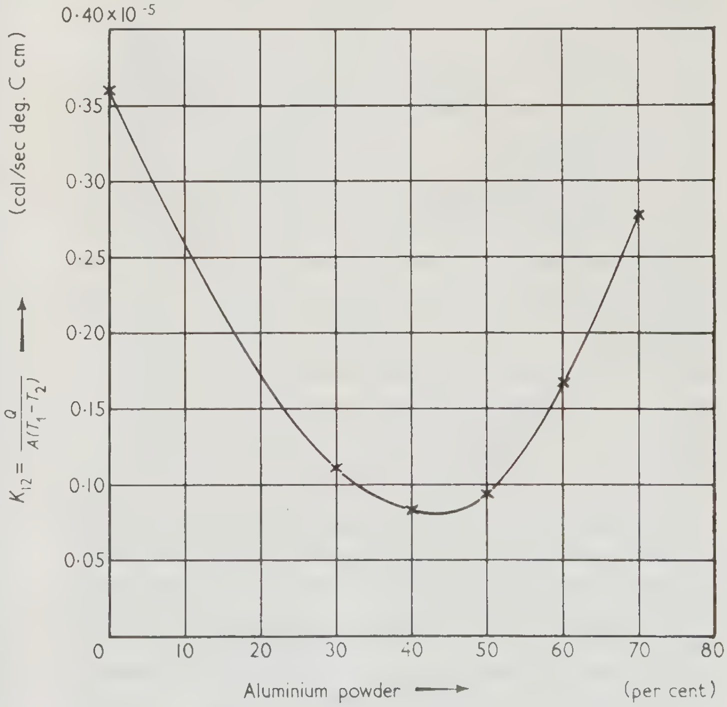

Figure 5. Effective thermal conductivity K_{12} of mixtures of aluminium powders and Santocel A. Wall temperatures: $T_1 = 303°K$; $T_2 = 77°K$

heat transferred through the insulant by radiation from that transferred by conduction. Table 2 shows that, for some insulating powders such as Santocel A, the effective conductivity can be appreciably reduced by admixing a powder with low emissivity, but that for others such as Microcel E, there is little scope for such reduction on account of the high solid conduction k. The method could be applied to other insulants and over other temperature ranges.

The insulants that have been developed as the result of this work, and similar ones developed elsewhere (see references 4–10, 12, 13), have much lower effective thermal conductivities than any previously available. With wall temperatures of 303° K and 77° K respectively, a layer 1 in. thick is a better insulant than an evacuated space between highly polished surfaces. The effective thermal conductivities are only one-fifth that of Santocel A and two orders of magnitude less than those of conventional insulants such as slag wool, expanded perlite, or basic magnesium carbonate in air at 1 atm. New developments in the design of tanks for liquid oxygen or nitrogen therefore become possible, resulting, for example, in an appreciable reduction in the rate of loss by evaporation from a container of given capacity with a given thickness of insulation. Alternatively, designs can be modified so that a given volume of liquid can be stored in a vessel of smaller overall size, or a given space can contain a greater volume of liquid. Further, it becomes practicable to construct smaller tanks with reasonable evaporation rates and these may be competitive with cylinders as a means of distributing gaseous oxygen or nitrogen. Perhaps, however, the outstanding developments will be in the construction of containers for liquid hydrogen and helium since it should be possible to dispense with liquid nitrogen shielding, and build a simpler and lighter container more convenient to handle than previous designs.

This article is published by permission of the Directors of British Oxygen Research and Development Ltd.

REFERENCES

1. Dewar, J. *Proc. roy. Inst.* **15,** 824 (1898)
2. Croft, A. J., and Jones, G. O. *Brit. J. appl. Phys.* **1,** 137 (1950)
3. Kistler, S. S. *J. phys. Chem.* **39,** 79 (1935)
4. Kropschott, R. H., Hunter, B. J., and Fulk, M. M. Paper C3, *Proc. 1959 Cryogenic Engng Conf.*
5. Petersen, P. *T. V. F.* (*Sweden*) **29,** 151 (1958)
6. Riede, P. M. Paper D5, *Proc. 1959 Cryogenic Engng Conf.*
7. Christianson, R. M. Paper C6, *Proc. 1959 Cryogenic Engng Conf.*
8. Glaser, P. E. Paper D1, *Proc. 1959 Cryogenic Engng Conf.*
9. Kropschott, R. H., Schrodt, J. E., and Fulk, M. M. Paper D2, *Proc. 1959 Cryogenic Engng Conf.*
10. Hnilika, M. P. Paper D3, *Proc. 1959 Cryogenic Engng Conf.*
11. Kern, D. Q. *Process Heat Transfer*, p. 75 (McGraw-Hill, New York, 1950)
12. Fulk, M. M., Devereux, R. J., and Schrodt, J. E. *Proc. 1956 Cryogenic Engng Conf.*, p. 163
13. Reynolds, M. M., Brown, J. D., Fulk, M. M., Park, O. E., and Curtis, G. W. *Proc. 1954 Cryogenic Engng Conf.*, p. 142

Metallography at Liquid Helium Temperatures

D. Hull *Atomic Energy Research Establishment, Harwell*
H. M. Rosenberg *Clarendon Laboratory, Oxford*

Received 29 February 1960

THE occurrence of martensitic transformations in sodium and lithium is now well established. It is only recently, however, that any correlation has been found between the transformation and the physical properties of these metals. Barrett,[1–3] using mainly low temperature X-ray techniques, has shown that when lithium is cooled it starts to transform at 72° K from the body-centred cubic phase to a hexagonal phase with faulty stacking, and that sodium has a similar transformation starting at 36° K. Specific heat and electrical resistivity experiments, reviewed by Dugdale,[4] show changes in these properties which agree closely with the X-ray data obtained by Barrett. Some difficulties have arisen regarding the amount of the transformed phase at a particular temperature. For example, in sodium the X-ray measurements indicated that only 7 per cent of the body-centred cubic high temperature phase had transformed to close packed hexagonal martensite at 4·2° K, whereas the specific heat results of Martin[5] suggest that about 50 per cent transformation has occurred. Electrical resistivity measurements[6] are very sensitive to the transformation and can be used to determine the effects of temperature cycling, plastic deformation, etc., on the transformation; they suggest that about 25 per cent transformation takes place.

The most direct way to detect the martensitic transformation and determine the amount of transformed phase is to take advantage of the shear characteristics of the transformation. The change of crystal structure results from a shear mechanism and produces a change of shape which is revealed on a flat surface by the tilting of the transformed regions. The tilts are microscopically homogeneous and when polished specimens are examined the tilts are readily detected. However, martensitic transformations, with one or two exceptions, are not thermally activated and they take place over a range of temperatures. They are also reversible in non-ferrous metals and alloys, so that to observe the transformation the metal has to be examined at the temperature at which the new phase is stable. High and low temperature microscope stages have been devised to follow the transformations. The main difficulties in observing low temperature transformations are avoiding condensation on the specimens and bringing the microscope objective sufficiently close to the specimen. For transformations between 293 and 90° K, as in 60:40 copper–zinc alloys, Hull and Garwood,[7, 8] using a modification of a low temperature stage designed by Greninger and Mooradian,[9] overcame these difficulties by surrounding the specimen and objective with a flexible rubber sleeve and maintaining an extremely dry atmosphere in the enclosed space. The specimen was cooled by clamping it to the end of a copper rod immersed in either solid carbon dioxide and acetone mixture or liquid oxygen. For observing transformations in sodium and lithium, much greater attention is required in cooling the specimen and in avoiding condensation, and in addition it is difficult to prepare smooth oxide-free surfaces on these metals.

In this paper we shall describe the low temperature apparatus that has been developed and the metallography of the martensitic transformations in sodium and lithium. Preliminary notes on the results for sodium and on the experimental method have already been published.[10–12]

The apparatus and the experimental method

The main problems to be overcome in designing the experimental arrangement are (1) the specimen must be in a vacuum, (2) its surface must be fairly close (within a few millimetres) to the microscope objective, and (3) the surface of the specimen, once prepared, must remain uncontaminated. The apparatus which was used is shown in Figure 1. It is a small portable cryostat which will fit on to the stand of a Cooke, Troughton, and Simms bench microscope. The lower innermost copper container A holds about 120 cm^3 of liquid helium and is surrounded by a copper radiation shield B. This screws on to the base of the upper container C which contains liquid air. A 4·7 mm annealed copper rod D, which is in thermal contact with the liquid helium passes through a hole in C to within about 5 mm of the outer casing. A hole into which the specimen holder may be screwed is tapped into the top of this rod. The outer brass jacket E is fitted with a valve and quick release coupling F so that it may be evacuated, sealed, and then removed from the pumping line. The lower part of E is screwed on to the top plate where it is sealed with an 'O'-ring. The specimen is viewed through a Pyrex glass window K, 0·3 mm thick, which is set into the top plate of E, just above D. This window rests on a well greased 'O'-ring and when the apparatus is evacuated this acts as a satisfactory seal. The helium container is supported by its thin walled stainless steel filling tube G. This tube is only attached to the top of the liquid air container

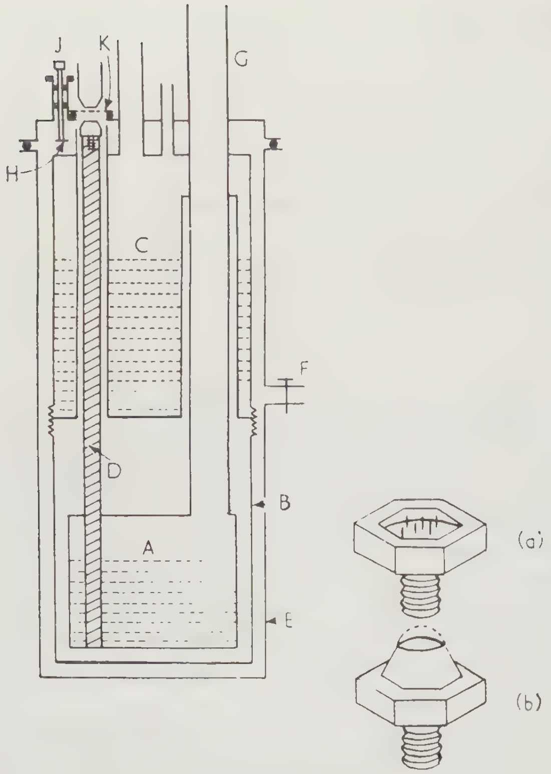

Figure 1. Diagram of low temperature cryostat used for the metallographic examination of metals at liquid helium temperature. (a) shows the holder in which the pellet of metal is held and (b) illustrates the method of sectioning the cone-shaped specimen

and not to the bottom, so as to reduce the heat influx. When the helium container was well polished, one filling of helium would last about $3\frac{1}{2}$ hr.

The specimen was held in a small copper cup shown in the inset to Figure 1. The lower part of the base was turned down and a thread was cut on to it. The outside of the cup was hexagonal so that the holder could be screwed into the copper rod D with a box spanner. Six vertical tinned copper wires were soldered into holes in the base of the cup. They were about 2 mm long and they assisted in making good mechanical and thermal contact between the cup and the specimen.

The holder, shown in Figure 1(a), was loaded as quickly as possible with a small pellet of metal from which all traces of grease and oil had been removed. This pellet was pressed into the holder until it was about 3 mm higher than the walls and it was then trimmed so that a cone of metal projected above the top of the cup, as is shown in Figure 1(b). It was then screwed into the apparatus and, after the thermocouple had been attached (see below), the glass window was fitted. The apparatus was then evacuated.

The specimen surface was prepared by cutting off the tip of the cone, so that the metal was about 2 mm thick, with a sharp highly polished blade H which could be rotated in a horizontal plane from outside the apparatus by means of the rod J. The vacuum seal for this rod was made with two 'O'-rings. It was found that no matter how long the apparatus was pumped at room temperature there was always sufficient water vapour left to cloud the specimen surface a few minutes after it had been cut. To stop this, the liquid air container was filled. This condensed the water vapour, but the specimen only cooled a few degrees below room temperature. After being cut the specimen itself was cooled by filling container A with liquid air. This liquid air was emptied by inverting the apparatus and then A was filled with liquid helium. When the apparatus was inverted, C, of course, was also emptied and it had to be refilled with liquid air.

To produce sodium with a fine grain size it is necessary to prepare the surface at a low temperature. The specimen was cooled to 90° K with liquid oxygen in the helium container and the surface was cut. It was then warmed up for 5 min at 170° K (above the recrystallization temperature) with pre-cooled acetone in the helium container and was then re-cooled to 90° K and the experiment was continued in the usual manner.

The specimen temperature was measured with a copper–constantan thermocouple. The leads for this were set in Araldite in a groove cut in rod D. They ran to the bottom of this rod and then up to the top of the apparatus again in the space between the rod and the liquid air container, where they were thermally anchored to C. They were taken out of the top plate through an Apiezon wax seal. The cold junction was pressed into the body of the specimen and the warm junction was immersed in a bath of liquid oxygen which was kept stirred. Copper–constantan thermocouples are not very sensitive at liquid helium temperatures (they have a sensitivity of about 4 μV/deg.K), but this was considered satisfactory because the specimen temperature needed to be known only to about a degree. The specimen temperature was usually about 6° K when A was filled with liquid helium.

When the transformation temperatures were being determined the specimen was first cooled with liquid air and then it was cooled slowly with small quantities of liquid hydrogen. With a little practice a slow rate of cooling could be achieved and the transformation temperature could be determined to within about a degree.

The specimen was illuminated vertically in the usual way, with mercury light and a green filter. This did not seem to alter the specimen temperature to any extent. A 16 mm objective was used. The glass window tended to cloud over after a time but this was easily cleared with a hot air blower.

The lithium used was 99·7 per cent pure, the sodium and potassium were high purity vacuum distilled metals with purities of 99·998 and 99·999 per cent, respectively.

Experimental observations

The specimen surface after cutting was smooth and flat but was covered with fine scratch marks. For those cuts which were made near room temperature it is expected that any damage produced by the cutting process would immediately anneal out. Grain boundary migration was observed after the specimen was cut and this confirmed

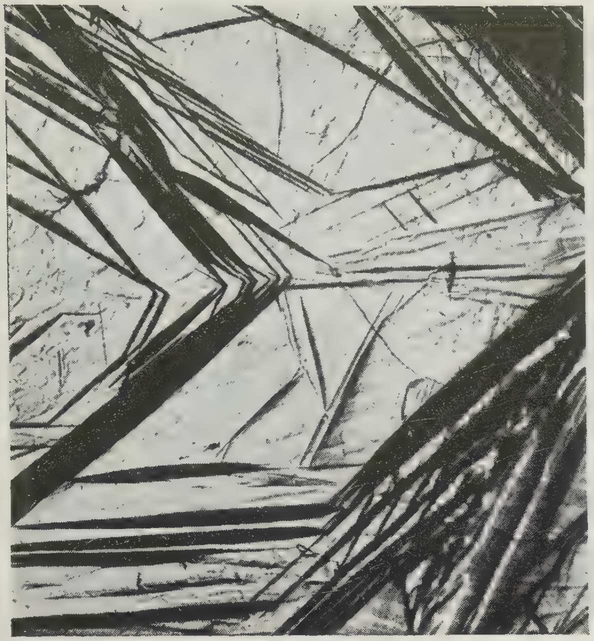

Figure 2. Surface relief effects produced on sodium cooled to 6°K. The black markings are plates of the new martensitic phase (× 200)

that the surface was strain-free. Since the specimens prepared at 90°K were afterwards warmed above the recrystallization temperature, they too should be strain-free. The surfaces remained clean and free from oxide after a number of cycles of cooling and heating. The diameters of the grains in lithium were about 0·15 mm and in sodium they were 1 mm and 0·1 mm when the surfaces were prepared at room temperature and 90°K, respectively.

When specimens of sodium are cooled the first evidence of transformation is the appearance of fine lines which grow rapidly in length and thicken slowly. The lines or plates form a series of zigzag networks, Figures 2 and 3, formed by the intersection of parallel bands at an acute angle. In any one zigzag group there are plates with four different orientations, alternate parallel plates producing tilts with opposite senses. As cooling proceeds more lines appear parallel to the original ones which continue to thicken. The growth is erratic, some plates forming almost instantaneously whilst others grow slowly. Many of the broad bands are formed by two bands merging together. When the specimens are heated the plates disappear in the same way in which they formed. The plates leave scars on the surface as observed by Barrett.[3] Figure 4 shows the same specimen as in Figure 3 at 90°K when the reversal to the high temperature phase is complete.

The growth of martensite in lithium is similar to sodium. Figures 5 and 6 show two stages in the transformation. In agreement with Barrett, no transformation was detected in potassium when it was cooled to 6°K.

In four specimens of sodium prepared at room temperature the start of transformation was 31°, 31°, 32°, and 31°K. Just below this, a large amount of martensite was produced and at 20°K about 40–50 per cent transformation had occurred. The actual amount of transformation varied considerably in different parts of the specimen. There was a negligible amount of transformation on further cooling to 6°K. On the reverse cycle transformation back to the high temperature phase was practically complete (within 3 per cent) at 65°K.

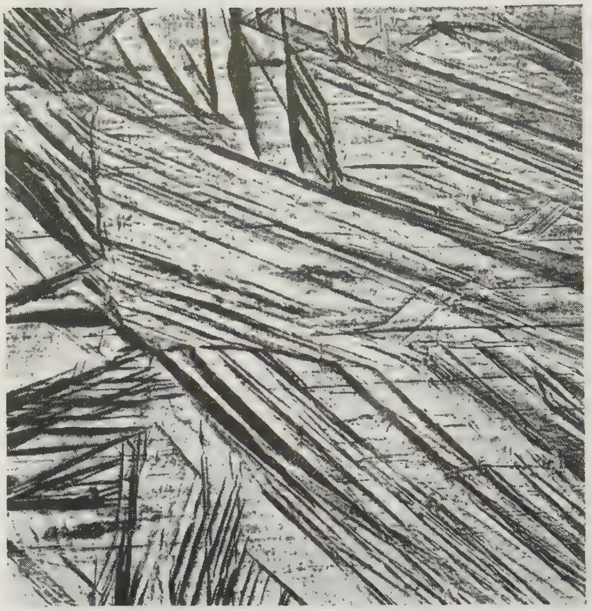

Figure 3. Zigzag groups of martensitic plates (× 100) on sodium at 20°K

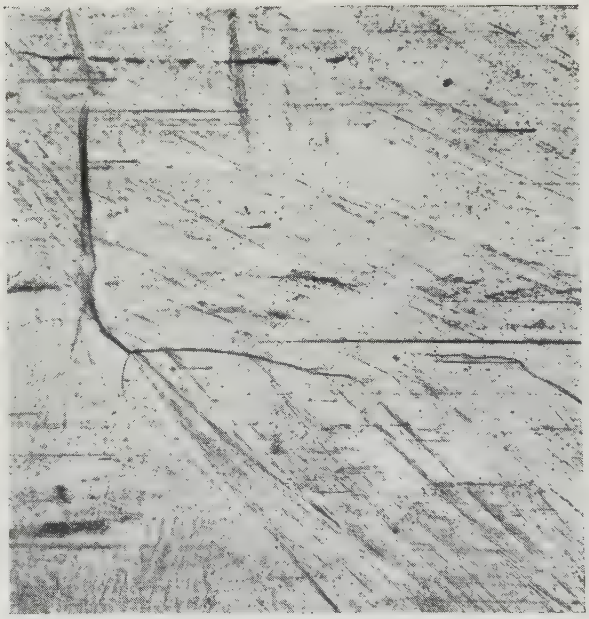

Figure 4. The same field as Figure 3 after the specimen was heated to 90°K. The martensitic plates leave scars on the surface. Note also the fine scratch marks produced by cutting the specimen (× 100)

When the specimens were re-cooled without heating above 90°K, the transformation started at the same temperature as for freshly prepared specimens to within 2°, but

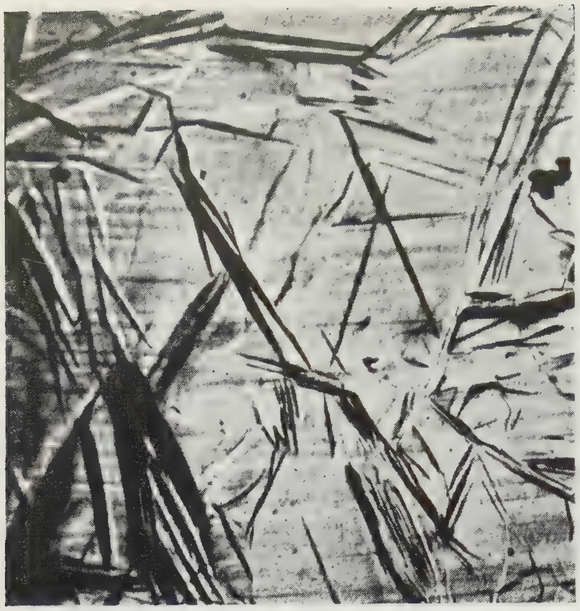

Figure 5. Martensitic plates formed in lithium just after transformation has started, approximately 70°K (× 100)

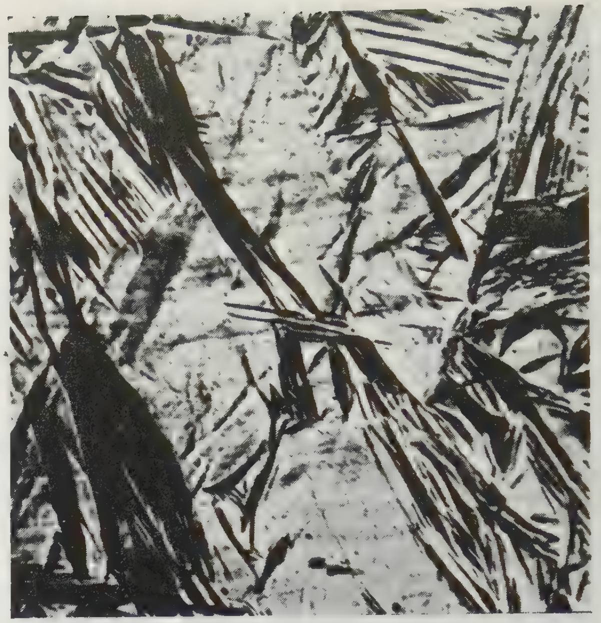

Figure 6. The same field as Figure 5 after the specimen was cooled to 20°K. Transformation is almost complete (× 100)

the amount of transformation was reduced. Figure 7 shows the same region at 20°K after three successive cooling cycles. In general, the martensite plates form in the same places after each cycle, but in some cases the plates formed in different positions.

For the sodium specimens prepared at 90°K the transformation started at approximately the same temperature, but at 20°K only a few per cent of the metal had transformed and no further transformation could be detected on cooling to 6°.K The transformation in three different lithium specimens started at 74°, 76°, and 78°K. At 20°K transformation was complete and no changes were observed on further cooling to 6°K. Approximately 90 per cent transformation had occurred.

Discussion

Observations have shown that at 20° and 6°K in large grained specimens about 50 per cent of the body-centred cubic sodium has transformed to martensite. This agrees well with that estimated by Dugdale[4] from the specific heat results of Martin.[5] The results for fine grained specimens, where only a small amount of transformation occurred, are in agreement with the results of Barrett from X-ray analysis. His specimens were also prepared at low temperatures and they were fine grained. The transformation temperatures of both sodium and lithium confirm the observations of previous workers. It is particularly interesting to compare the results for sodium with the electrical resistivity measurements of Gugan and Dugdale.[6] Their results indicate that transformation starts at 33°K and that the majority of the transformation occurs between 30° and 20°K. There is only a small change below 20°K. On the heating cycle the reverse transformation starts at 48°K and is complete at 70°K. These results agree closely with the present work and it follows that electrical resistivity measurements can be used to study the progress of the transformation with some precision although it is difficult to use them to obtain an absolute value of the amount of the new phase formed.

Whilst all the observations have been made on the surface of the specimens it is believed that this is representative of the specimen as a whole. In other martensite transformations in which the martensite phase is stable at room temperature, the amount of transformation detected by surface examination agrees closely with that found when the specimen is sectioned. Our observations are also supported by their agreement with the amount of transformation deduced from the measurements of the specific heat of sodium by Martin.[5]

It has been shown previously[11] that the martensitic transformations in sodium and lithium have a marked effect on the stress–strain curves of these metals. At 20° and 4·2°K lithium has a serrated stress–strain curve which probably results from a second transformation from a hexagonal close packed to face-centred cubic structure induced by strain at these temperatures. No evidence for this second transformation was detected in unstrained lithium at 6°K although it does not follow that transformation has not occurred. There is a marked hardening in sodium between 20° and 4·2°K although in unstrained specimens no further transformation is observed. However, it is expected that strain-induced transformation will occur more readily at the lower temperatures and this will result in greater hardening.

In the past many experiments have been made on the alkali metals and in particular on sodium because these are the ones to which it is most easy to apply theoretical predictions. The present results, together with those of the

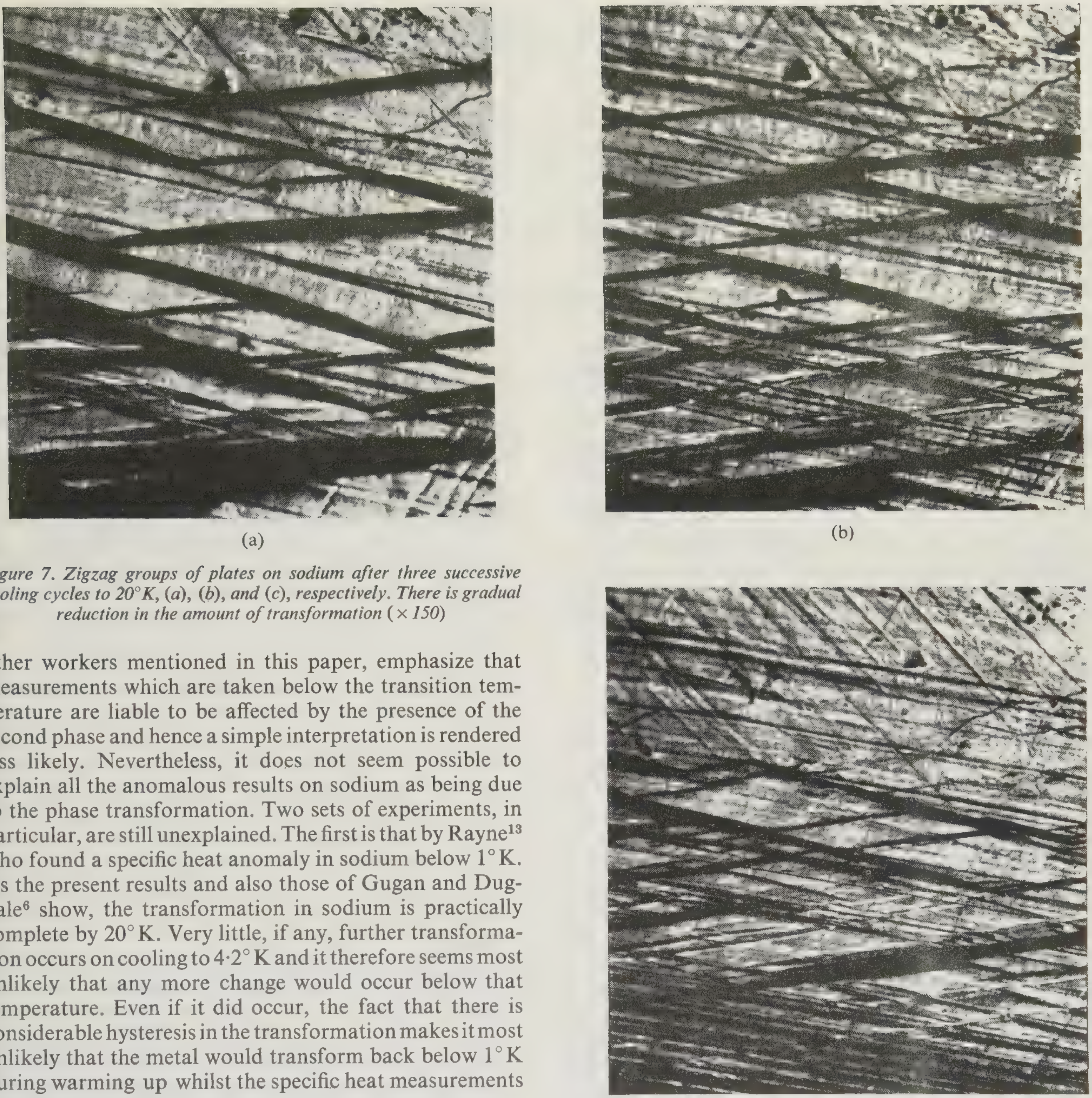

(a)

(b)

(c)

Figure 7. Zigzag groups of plates on sodium after three successive cooling cycles to 20°K, (a), (b), and (c), respectively. There is gradual reduction in the amount of transformation (× 150)

other workers mentioned in this paper, emphasize that measurements which are taken below the transition temperature are liable to be affected by the presence of the second phase and hence a simple interpretation is rendered less likely. Nevertheless, it does not seem possible to explain all the anomalous results on sodium as being due to the phase transformation. Two sets of experiments, in particular, are still unexplained. The first is that by Rayne[13] who found a specific heat anomaly in sodium below 1°K. As the present results and also those of Gugan and Dugdale[6] show, the transformation in sodium is practically complete by 20°K. Very little, if any, further transformation occurs on cooling to 4·2°K and it therefore seems most unlikely that any more change would occur below that temperature. Even if it did occur, the fact that there is considerable hysteresis in the transformation makes it most unlikely that the metal would transform back below 1°K during warming up whilst the specific heat measurements were being taken.

The second set of experiments which are still unexplained are those by MacDonald, White, and Woods,[14] and Woods[15] on the electrical resistivity of sodium. These workers showed that in the region between 5° and 10°K the 'ideal' electrical resistivity (i.e. that part of the resistivity which is produced by the scattering of the electrons by the lattice vibrations) is proportional to T^6 instead of to T^5 as is predicted by the elementary theory of electron scattering. It does not seem possible in any straightforward way to ascribe this deviation to an effect of the transformation. As has already been noted, in this temperature range the transformation has been practically completed. One can consider the metal as being composed of regions of two different resistivities each of the form $R_0 + AT^5$, where R_0 is the constant residual resistivity which is present at the lowest temperatures. Since R_0 and A are not very different for each phase it does not seem possible to combine the resistivities in any way such that the temperature dependent part would be proportional to a power of T greater than five. If some transformation was still occurring, then, since the new phase has a value of A which is less than that for the old phase,[4] the resistivity of the combined phases might decrease more rapidly than T^5 over a limited temperature range. On balance, however, it seems unlikely that these results, or the specific heat work of Rayne[13] can be explained in any simple way as being directly due to the transformation.

If experiments on sodium are required in which the existence of the transformation might lead to complications, the experiments show that it is possible to inhibit the formation of the new phase to a certain extent by controlling the grain size. Thus the use of the metal in the form of very fine particles may depress the transformation appreciably. The temperature for the start of martensitic transformation may also be depressed by previous plastic deformation above the transformation temperature, but this method is unlikely to be suitable.

We should like to thank Mr. G. W. Horsley of A.E.R.E., Harwell, for supplying the lithium, sodium, and potassium, and we are grateful to Prof. C. S. Barrett, Dr. Z. S. Basinski, and Dr. J. S. Dugdale for valuable discussions. This work was carried out at the Clarendon Laboratory, and formed part of a joint programme of research between the Laboratory and the Metallurgy Division of A.E.R.E., Harwell. D.H. is now at Department of Physics, University of Liverpool.

REFERENCES

1. Barrett, C. S. *Phys. Rev.* **72,** 245 (1948)
2. Barrett, C. S. *J. Inst. Metals* **84,** 43 (1955)
3. Barrett, C. S. *Acta cryst. Camb.* **9,** 671 (1956)
4. Dugdale, J. S. *Report on the Martensitic Transformations in Sodium and Lithium* (N.R.C., Ottawa, 1958)
5. Martin, D. L. *Phys. Rev. Letters* **1,** 4 (1958)
6. Gugan, D., and Dugdale, J. S. *Canad. J. Phys.* **36,** 1248 (1958); *Proc. roy. Soc.* **A254,** 184 (1960)
7. Hull, D., and Garwood, R. D. *J. sci. Instrum.* **32,** 232 (1955)
8. Hull, D., and Garwood, R. D. Symposium on the Mechanism of Phase Transformations in Metals (Institute of Metals, 1956)
9. Greninger, A. B., and Mooradian, V. G. *Trans. Amer. Inst. min. (metall.) Engrs* **128,** 337 (1938)
10. Hull, D., and Rosenberg, H. M. *Phys. Rev. Letters* **2,** 205 (1959)
11. Hull, D., and Rosenberg, H. M. *Phil. Mag.* **4,** 303 (1959)
12. Hull, D., and Rosenberg, H. M. *J. photogr. Sci.* **7,** 173 (1959)
13. Rayne, J. *Phys. Rev.* **95,** 1428 (1954)
14. Macdonald, D. K. C., White, G. K., and Woods, S. B. *Proc. roy. Soc.* **A235,** 358 (1956)
15. Woods, S. B. *Canad. J. Phys.* **34,** 223 (1956)

A Cryostat for Studying Transuranic Substances

G. T. Meaden *Clarendon Laboratory, Oxford*
J. A. Lee *Atomic Energy Research Establishment, Harwell*

Received 1 March 1960

THE need for conducting low temperature research on the transuranic elements has long been felt by plutonium metallurgists. These elements are extremely radioactive and can only be investigated in a laboratory where all the necessary and complex facilities are available. So it was through the joint co-operation of the plutonium section of the Atomic Energy Research Establishment, Harwell, and the Clarendon Laboratory, Oxford, that a suitable cryostat came to be designed and built at A.E.R.E.

The design, construction, and operation of this cryostat are described below. Results obtained from its use will be published in due course.

Problems involved

As is well known, toxic hazards arise in working with the transuranic elements. In the case of plutonium the hazard lies not so much in the strength of its alpha-emission (the alpha-particle range in air is only 3·7 cm), but rather in its readiness to oxidize quickly into a non-adherent oxide consisting of exceedingly fine particles. This leads to a rapid build-up of alpha-active dust in the surrounding atmosphere and, as the total body burden is set at the very low level of 0·6 μg, operations have to be conducted inside a glove-box.

The usual procedure then is to handle plutonium in a glove-box possessing an inert gas atmosphere. In this way it is ensured that active specimens and any equipment that may have been in contact with them do not contaminate the open laboratory.

Another consequence of the alpha-emission of plutonium is its very high self-heating. The value given by Stout and Jones[1] for the rate of energy production by plutonium-239 is $1{\cdot}923 \pm 0{\cdot}019$ mW/g. This results in a rod of plutonium, 2 mm in diameter, being about 0·5° K warmer than its surroundings if these are solely gaseous, or about 2° K warmer if the sample is in a vacuum. Thus the question of temperature measurement, especially at lower temperatures, is raised.

This problem does not arise in the case of neptunium where the self-heating is negligibly small. The toxic hazards, however, still remain.

Methods

There are two distinct methods by which low temperature experiments can be performed on active substances, viz., (1) by sealing specimens in small capsules and then making use of a conventional cryostat, or (2) by constructing a special cryostat for use with a glove-box.

The first method immediately imposes severe limitations on the variety of possible experiments. For while it is not unsuitable for experiments involving, for example, susceptibility measurements where ballistic mutual inductance techniques can be employed, it is not easily adaptable to those experiments where it is necessary to have leads attached to the specimens. Nevertheless, some experiments of this type have been performed successfully on both neptunium and plutonium rods. The manner in which these specimens were sealed will now be described briefly.

Each container was cylindrical in shape and made of brass. The overall length was 8 cm, the diameter 12 mm, and the wall thickness 1 mm (Figure 1). A platinum–glass seal made from a 1 cm length of 6 mm diameter platinum tubing had four platinum wires passing through it. These wires were enclosed for most of their lengths in glass capillaries which gave them increased strength and eliminated the possibility of a short circuit with the container. After spot-welding the wires on to a specimen, the container was filled with helium gas. The seal was then soft-soldered into its neck. The exteriors of the capsule and seal having been previously coated with shellac, contamination was later

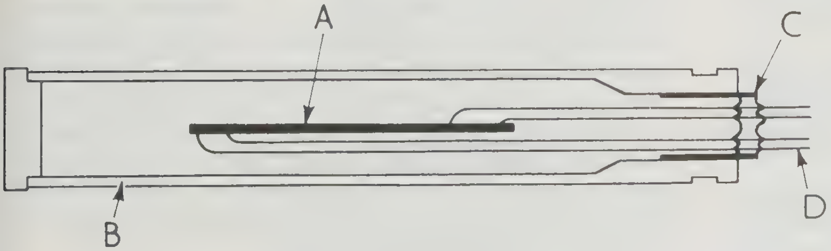

Figure 1. Method of sealing an active specimen in a capsule (glass capillaries not indicated)

A: Sample
B: Brass cylinder
C: Platinum tube
D: Platinum wires

removed merely by dissolving away the shellac with acetone.

The capsules made in this way were found to be perfectly safe and reliable, and most of them made over half a dozen descents to liquid helium temperatures. Thus, three specimens, canned by this method, could be taken to the Clarendon Laboratory and electrical resistivity measurements made in a cryostat where temperatures of 0·75° K were obtainable.[2]

The major drawback to working with active specimens in this manner is soon found if one of the spot-welded contacts becomes loose. The repair of the weld is then a lengthy job occupying several hours since it can only be carried out in a glove-box.

Also, in the case of plutonium, there is some uncertainty concerning its precise temperature due to its high self-heating. This matters most at the lower end of the temperature scale and for this reason thick platinum wires were used. Even then, however, the temperature difference between the specimen and the helium bath was possibly as large as 0·05° K.

In the cryogenic glove-box described below this problem of temperature measurement at helium temperatures does not arise.

The cryogenic glove-box

On account of the general difficulties and restrictions always encountered when using a glove-box, it was evidently desirable that the operational side of the cryostat should be kept as simple as possible. Accordingly, it was decided to limit our investigations in the first instance to the measurement of properties such as electrical resistance and Hall effect, where adiabatic conditions are not essential—as they are, for example, in calorimetric or thermal conductivity experiments. The advantage of this is that continuous readings can easily be taken on such quantities while the system is slowly warming or cooling.

The cryostat was designed principally for operation in the helium temperature range, though it can be used to cover continuously in warming the entire range up to room temperature.

The question of temperature measurement in the helium range was solved by arranging for the active specimens to be immersed in liquid helium itself. The temperature of the specimen, carbon resistor, and liquid helium may then be taken as being essentially the same. (The Kapitza boundary heat resistance between a 1 g plutonium rod supplying 2 mW of energy and liquid helium II gives $\Delta T < 0{\cdot}01$° K, even at 1·4° K.) Thus temperatures are measured by the helium vapour pressure scale with a carbon resistor as a secondary thermometer.

In addition, the cryostat had to be of such a shape as to allow magnetic experiments to be performed, and to be constructed in such a way that specimen introduction and removal would be relatively straightforward.

The glove-box is basically a normal one of the free-standing type as widely used at A.E.R.E. That is to say, it is argon-filled, perspex fronted and roofed, with two neoprene gloves on the front panel and a posting-in port at one side (see Figure 2). General descriptions of this type of box and its operation can be found in the literature.[3, 4]

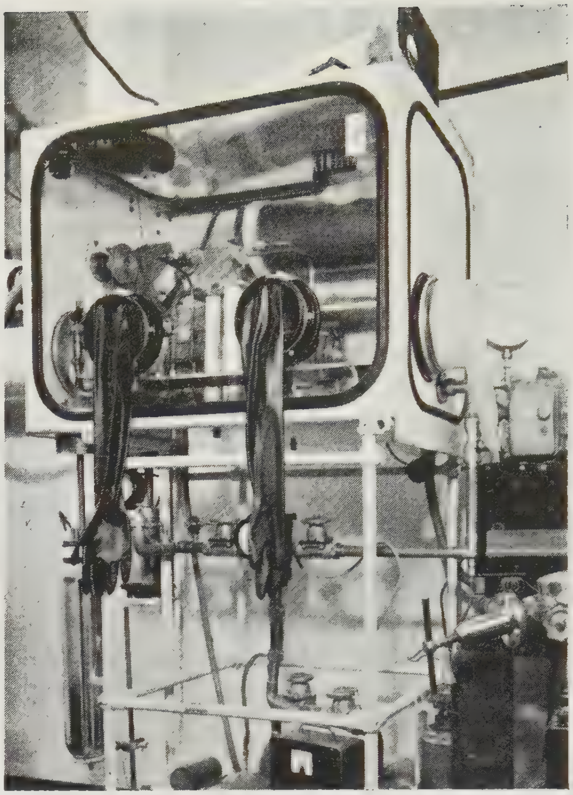

Figure 2. The cryogenic glove-box

The main central tube of the cryostat, which is almost 1 m in length and 15 mm in diameter, is essentially an extension of the glove-box vertically downwards from its floor (see Figure 3). The cryogenic services being all outside this tube, modification or repair of the cryostat can be carried out without disturbance of the glove-box. In the event of any major modification to the 'active' part of the cryostat being necessary, however, it is possible to remove the whole cryostat by standard PVC bag techniques and to take it to a laboratory fume cupboard.

The upper half of this cryostat tube is made of brass but the lower half is of 15 mm German silver tubing with copper forming the bottom 13 cm. It is within this copper part that the specimens are suspended and the helium condensed. The top of the long tube leads to a vacuum system, the helium gas supply, and oil and mercury manometers (Figure 4). These manometers and the entire vacuum system including a 60 l./min DR1 direct drive Metrovac rotary pump are actually inside the box. Also within the box is an 18 l. helium storage vessel which is filled to a pressure of nearly 2 atm before a run from a helium cylinder outside.

Around the middle of the long central tube and inside the inner Dewar is a brass container that can be filled with liquid nitrogen. This serves to reduce heat leaks down the 15 mm German silver tube and also acts as a radiation shield for the liquid in the Dewar.

The liquid helium used in this laboratory is obtained in 10 l. Dupree-Swift transport Dewars from the National Physical Laboratory. From one of these Dewars liquid helium is siphoned into the inner Monax Dewar of the cryostat. Here, it can be pumped by an external vacuum system, consisting of two 340 l./min rotary pumps running in parallel. The outer Dewar of the cryostat is for liquid nitrogen.

A small gas thermometer is also included to give a continuous indication of the temperature within the inner Dewar.

The specimen is mounted in a special holder along with a carbon resistor and several thermocouples. This holder is attached to the lower end of a long 1 mm diameter German silver tube which passes right down the centre of the cryostat (see Figure 3(b)). Thin metal disks with small holes in them are fixed to the tube at roughly 10 cm intervals, and they serve the dual purpose of guides for the leads and radiation shields for the liquid helium in the cryostat. There are at present in the apparatus eight insulated 40 gauge constantan wires and three copper–constantan thermocouple pairs, and all of these leave the cryostat at its top through a black-wax seal. This whole assembly of specimen holder, German silver tubing, and leads, including the black-wax seal, is lifted into the cryostat by the use of a pulley situated in a tower in the roof of the glove-box.

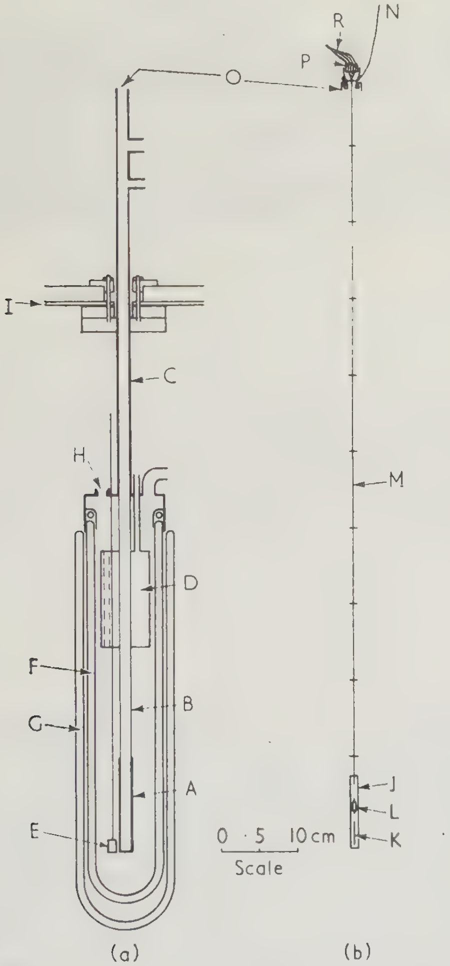

A: Main tube, copper
B: Main tube, german silver
C: Main tube, brass
D: Liquid nitrogen container
E: Gas thermometer
F: Inner (helium) Dewar
G: Outer (nitrogen) Dewar
H: Hole for siphon
I: Shell of glove-box
J: Specimen holder
K: Specimen
L: Carbon resistor
M: 1 mm german silver tube
N: Nylon cord to pulley
O: 'O'-ring seal
P: Black-wax seal
R: Leads

Figure 3. Approximate scale drawing of the cryostat

Copper–constantan thermocouples on the specimen are used for temperature measurement down to 20° K, and below this a carbon resistor is used.

General procedure

With the specimen already pre-cooled to 77° K in a helium atmosphere, liquid helium is siphoned into the inner Dewar. Pumping on this liquid helium is then commenced and helium is condensed into the copper extension of the main tube of the cryostat by passing in gas at a small over-pressure. Usually, 20 to 25 cm^3 are liquefied in this way. The temperature of this internal liquid helium is then controlled by pumping on the liquid in the helium Dewar. Since the Dewar can hold 1·5 l., temperatures below 4·2° K can easily be maintained for 6 hr or more. Manual control of a 1 in. Saunders valve and a needle valve enables any temperature to be maintained within limits of ±0·005° K

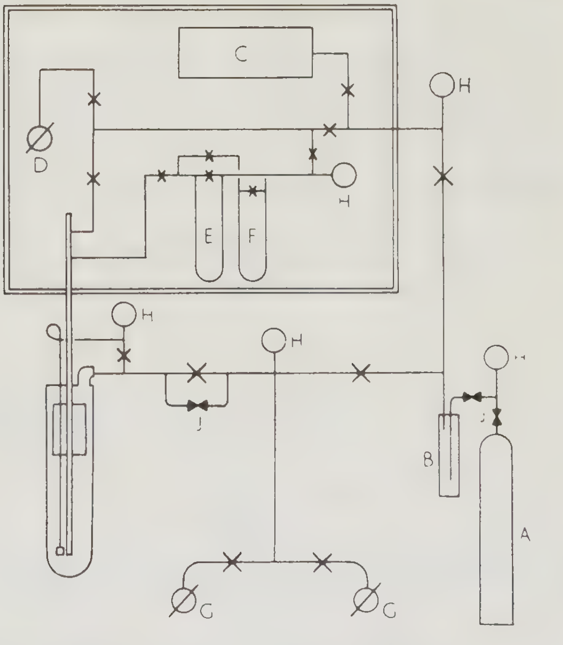

A: Helium cylinder
B: Charcoal cleaner
C: Helium storage vessel
D: DR1 rotary pump
E: Mercury manometers
F: Oil manometer
G: N.G.N. rotary pumps
H: Vacuum and pressure gauges
J: Needle valves

Figure 4. Simplified flow diagram, illustrating the distribution of apparatus inside and outside the glove-box

for whatever length of time is desired, though 30 min is the longest that has so far been attempted. As a rule, sufficient helium is obtained from a 10 l. Dupree-Swift Dewar for about three runs spread over a week.

Once the liquid helium level has fallen below the bottom of the copper part of the cryostat, careful control of the pumping speed coupled with the heat leak down the cryostat allows a controlled slow rise in the temperature of the specimen to be achieved. In fact, as long as some liquid helium remains this rate of warming can be made as slow as is required. A rise from 4° to 20° K in 2 hr, for instance, is readily obtained. With care, steady temperatures between 4° and about 12° can be held in rather unstable equilibrium for several minutes. When, finally, the last of the liquid helium has evaporated, the helium Dewar is evacuated and the outer Dewar of liquid nitrogen removed. Under these conditions the warming to room temperature from 4° K takes 7–10 hr. Faster rates are obtained when necessary by electrical heating in the helium Dewar.

Another method of ensuring an initial slow temperature rise from 4° has also been employed. A lead cylinder 18 cm in length and 1,800 g in weight is suspended concentrically around the cryostat tube. Liquid hydrogen must now be used as an intermediate cooling stage. About 0·5 l. of liquid hydrogen is evaporated in cooling the lead from 77° to 20° K and then about 0·5 l. of liquid helium in bringing the temperature to 4° K. Now, after the final evaporation of helium, the large thermal capacity of the lead ensures that the rate of warming is slow and uniform. 20° K is then reached in 1 hr and 77° K in 3 hr.

We wish to thank Dr. K. Mendelssohn of the Clarendon Laboratory, Oxford, and Dr. M. B. Waldron, A.E.R.E., Harwell, for valuable advice and criticism. One of us (G. T. Meaden) is indebted to A.E.R.E. for a research grant and for the facilities afforded to him there.

REFERENCES

1. Stout, J. W., and Jones, W. M. *Phys. Rev.* **71,** 582 (1947)
2. Lee, J. A., Meaden, G. T., and Mendelssohn, K. *Proc. phys. Soc. Lond.* **74,** 671 (1959)
3. Lord, W. B. H., and Waldron, M. B. *J. Inst. Metals* **86,** 385 (1957–58)
4. Walton, G. N. (Ed.) *Glove-Boxes and Shielded Cells for Handling Radioactive Materials* (Butterworths, London, 1958)

On the Properties of the Vapour Pressure Curve

E. H. Brown *National Bureau of Standards, Boulder, Colorado*

Received 3 March 1960

Both the sublimation and vaporization curves of pure substances have been studied extensively and a wealth of data and numerous empirical equations have been obtained. Using mathematical methods, this paper re-derives some known properties of the entire condensation curve from zero temperature to the critical point in a simpler manner and obtains new properties for the first time.

For convenience, we will use variables $p, v = 1/\rho, T$, $Z = p/\rho T$, which are reduced by their critical values; when needed, unreduced variables will be indicated by the same letters primed. A first assumption, which we will call the *axiom of the perfect gas*, asserts that

$$\lim_{p \to 0} Z'(p,T) = 1, \quad T > 0$$

and

$$Z'(0,T) = 1, \quad T > 0$$

and is in accordance with all reliable experimental results. (In reduced variables, the value and limit, i.e. 1, must be replaced by $Z^0 = 1/Z_c' =$ constant, where the superscript 0 and subscript c indicate zero pressure and the critical point, respectively.) An immediate consequence of this axiom and the definition of Z is that

$$\lim_{p \to 0} \rho(p,T) = 0, \quad T > 0$$

and

$$\rho(0,T) = 0, \quad T > 0$$

Clearly, the above limits must hold on any arbitrary curve terminating on the T axis and lying entirely in the vapour.

Indicating the difference between the vapour and condensed phase densities by $\Delta\rho$, a first-order phase transition curve ϕ is defined by the requirement that $\Delta\rho \neq 0$ at every point $[p_\phi(T), T]$ of the curve except a terminal point lying in the *interior* of the p, T domain (that is, *the* critical point). The second terminal point of such a curve ϕ clearly cannot lie on the boundary $T = 0$, $p > 0$, since a vapour cannot exist under such conditions. Since $\rho = 0$ everywhere on the boundary $p = 0, T > 0$, the requirement $\Delta\rho \neq 0$ then implies that the second terminal point of ϕ must be at $P = (p = 0, T = 0)$ regardless of the nature of the condensed phase.

Let $\bar\psi_0$ be a curve $p_{\bar\psi,0}(T)$ lying entirely in the vapour, which is infinitely differentiable (that is, for which

$$p^{(n)}_{\bar\psi,0}(T) = \left(\frac{\mathrm{d}^n p}{\mathrm{d}T^n}\right)_{\bar\psi,0}$$

exists at all points of $\bar\psi_0$ for every finite n), which terminates at the point $\bar P = (p = 0, T = T_0), T_0 > 0$, and which, at least initially, is otherwise arbitrary. If this entire curve is translated parallel to the T axis to form a curve ψ_0 terminating at $P = (p = 0, T = 0)$, the new curve will not necessarily lie entirely in the vapour. In particular, since

$$\lim_{p \to 0} \frac{p}{T} = \lim_{p \to 0} Z\rho = Z^0 \lim_{p \to 0} \rho = 0$$

on any curve lying entirely in the vapour and since $\lim\limits_{T \to 0} p^{(1)}_{\psi,0}(T)$ exists by the assumption of infinite differentiability, evaluation of

$$\left(\lim_{T \to 0} \frac{p}{T}\right)_\psi = \left(\lim_{p \to 0} \frac{p}{T}\right)_\psi$$

implies that for ψ to be in the vapour we must have $p^{(1)}_{\psi,0}(0) = 0$. Using this as a necessary condition, we can form a new curve $\bar\psi_1$ which again lies entirely in the vapour, is infinitely differentiable, terminates at $\bar P$, and which is otherwise arbitrary except for the additional requirement $p^{(1)}_{\bar\psi,1}(0) = 0$.

On the new curve $\bar\psi_1$ defined above, we must then have

$$\left(\frac{\mathrm{d}Z\rho}{\mathrm{d}T}\right)^0_{\bar\psi,1} = \lim_{T \to T_0} \left[\left(\frac{\partial Z\rho}{\partial T}\right)_{p,\bar\psi,1} + \left(\frac{\partial Z\rho}{\partial p}\right)_{T,\bar\psi,1} p^{(1)}_{\bar\psi,1}(T)\right]$$

$$= \left(0 + \frac{1}{T_0} . 0\right) = 0$$

Translating $\bar\psi_1$ parallel to the T axis to form a curve ψ_1 terminating at P, the limit

$$\left(\frac{\mathrm{d}Z\rho}{\mathrm{d}T}\right)^0_{\psi,1} = 0$$

must remain valid due to one-sided continuity in the vapour phase and the fact that

$$p^{(n)}_\psi(T) = p^{(n)}_{\bar\psi}(T + T_0) \frac{\mathrm{d}}{\mathrm{d}T}(T + T_0) = p^{(n)}_{\bar\psi}(T + T_0), n \geqslant 0$$

This implies that

$$Z^0 \lim_{T \to 0} \frac{\rho}{T} = \lim_{T \to 0} \frac{Z\rho}{T} = \lim_{T \to 0} \left(\frac{\mathrm{d}Z\rho}{\mathrm{d}T}\right)^0_{\psi,1} = 0$$

and, thus

$$\left(\lim_{T\to 0}\frac{p}{T^2}\right)_{\psi,1} = \lim_{T\to 0}\frac{p^{(1)}_{\psi,1}(T)}{2T} = \tfrac{1}{2}p^{(2)}_{\psi,1} = 0$$

We can now form a new curve $\bar{\psi}_2$ which satisfies all the conditions on $\bar{\psi}_1$ and the additional requirement $p^{(2)}_{\bar{\psi},2}(0)=0$, but is otherwise arbitrary. Repeating the previous process, that is, determining that

$$\left(\frac{\mathrm{d}^2 Z\rho}{\mathrm{d}T^2}\right)^0_{\bar{\psi},2} = \lim_{T\to T_0}\left(\frac{\mathrm{d}^2 Z\rho}{\mathrm{d}T^2}\right)_{\bar{\psi},2} = \lim_{T\to T_0}\left\{\frac{\mathrm{d}}{\mathrm{d}T}\left[\left(\frac{\partial Z\rho}{\partial T}\right)_p + p^{(1)}\left(\frac{\partial Z\rho}{\partial p}\right)_T\right]\right\}_{\bar{\psi},2}$$

$$= \lim_{T\to T_0}\left[\left(\frac{\partial^2 Z\rho}{\partial T^2}\right)_p + 2p^{(1)}_{\bar{\psi},2}\frac{\partial^2 Z\rho}{\partial p\,\partial T} + p^{(2)}_{\bar{\psi},2}\left(\frac{\partial Z\rho}{\partial p}\right)_T + p^{(1)2}_{\bar{\psi},2}\left(\frac{\partial^2 Z\rho}{\partial p^2}\right)_T\right] = 0$$

and applying this result, we find that

$$\left(\frac{\mathrm{d}^2 Z\rho}{\mathrm{d}T^2}\right)^0_{\psi,2} = 0$$

$$\left(\lim_{T\to 0}\frac{Z\rho}{T^2}\right)_{\psi,2} = Z^0\left(\lim_{T\to 0}\frac{\rho}{T^2}\right)_{\psi,2} = 0$$

$$\left(\lim_{T\to 0}\frac{p}{T^3}\right)_{\psi,2} = 0$$

and

$$p^{(3)}_{\psi,2}(0) = 0$$

By induction, we can thus show that for any infinitely differentiable curve ψ lying entirely in the vapour and terminating at P

$$\left(\lim_{T\to 0}\frac{p}{T^n}\right)_{\psi} = 0$$

$$\left(\lim_{T\to 0}\frac{\rho}{T^n}\right)_{\psi} = 0$$

$$\left(\lim_{T\to 0}\frac{\mathrm{d}^n Z\rho}{\mathrm{d}T^n}\right)_{\psi} = 0$$

and

$$\lim_{T\to 0} p^{(n)}_{\psi}(T) = 0$$

for every finite n, and thus the additional result

$$\lim_{n\to\infty}\left[\lim_{T\to 0} p^{(n)}_{\psi}(T)\right]_{\psi} = 0$$

(We shall soon see that the two limits in the last result *cannot* be interchanged.) Essentially, the above proof consists of a continuing process in which knowledge of the fact that $\left[\lim_{T\to T_0}(Z\rho/T^n)\right]_{\bar{\psi}} = 0$ implies that $p^{(n+1)}_{\psi}(0) = 0$; and since

$$p^{(n+1)}_{\psi}(0) = p^{(n+1)}_{\psi}(T_0)$$

then

$$\left(\lim_{T\to T_0}\frac{Z\rho}{T^{n+1}}\right)_{\bar{\psi}} = 0$$

With the exception of the *necessary* conditions at the point P which are derived above, ψ can then be chosen arbitrarily in the vapour in the neighbourhood of $T=0$. Therefore, if ϕ is infinitely differentiable, curves ψ in the vapour can be chosen such that all of the derivatives $p^{(n)}_{\psi}(T)$ can be made arbitrarily close to the values $p^{(n)}_{\phi}(T)$ of the vapour condensation curve, and the limits

$$p^{(n)}_{\phi}(0) = \left[\lim_{T\to 0} p^{(n)}_{\phi}(T)\right]_{\phi} = 0 \qquad \text{for every } n \geqslant 0$$

and

$$\lim_{n\to\infty}\left[\lim_{T\to 0} p^{(n)}_{\phi}(T)\right]_{\phi} = 0$$

must also be valid. In addition, we must *define* the values at $T=0$ by their limit *on the right* on ϕ, $p^{(n)}_{\phi}(0)=0$, for every $n \geqslant 0$. For a simple thermodynamic system, this definition involves no loss of generality since the temperature cannot be negative.

This same result could have been obtained from the recent demonstration of Glass and Klein,[1] who in the process of discussing the applicability of the Third Law of Thermodynamics to the sublimation curve, show that, while the number density in the gas vanishes exponentially for $T\to 0$, the entropy per particle diverges only as $1/T$. Their proof depends on the assumption that the condensed phase is a crystal: by equating the chemical potential of the saturated crystal and the saturated vapour they show that the vapour cannot be degenerate, and that the number density of the vapour vanishes as $T^{3/2}\exp(-\chi/kT)$, where χ is positive and equal to the difference between the energy of the lowest state of a free atom in the gas and the energy of the lowest state of the atom bound in the crystal.

In our case, we have shown that ρ vanishes more rapidly than any power of T and thus also that ρ must vanish exponentially as $T\to 0$. The fact that the vapour pressure curve for helium II has apparently the same mathematical properties in the vicinity of $T=0$ as ordinary sublimation curves indicates, as we have demonstrated above, that this limiting behaviour is of much more general validity and does not depend on any assumption of classical laws or on the fact that the condensed phase is a solid.

In passing, we note that the conclusion of Glass and Klein, that the Third Law remains valid and applicable even in the case of sublimation, *could* be true only for a system of fixed total volume. Since thermodynamic laws are as frequently applied to systems of fixed total mass, the question of the applicability (though *not* the validity) of this Law still exists. This question, however, is answered if we consider an actual vaporization or sublimation process at $T=0$. Such a sublimation process can be achieved by placing a system of either fixed total mass or fixed total volume (which is *defined* to be initially completely condensed at $p=0$, $T=0$) in an infinite heat bath whose temperature $T=\epsilon>0$ is arbitrarily small. The final state will be one of a vapour at $T=0$ and $p=0$.

If we wish now to re-condense the system from the final state achieved above, we cannot do so by increasing the pressure to some $p=\epsilon>0$ which is arbitrarily small (since the limit $(\mathrm{d}T/\mathrm{d}p)_\phi=+\infty$ implies that even a vanishingly small increase in pressure could result in a *finite* increase in the temperature of the system; as soon as the system leaves the point P, the inaccessibility form of the Third Law implies that the system cannot be returned to P). Similarly, we cannot re-condense the system by placing it in a 'heat' bath with a temperature $T=-\epsilon<0$ since the Second Law of Thermodynamics requires the temperature of a simple thermodynamic system to be *positive*. Thus, even though sublimation or vaporization at 0° K may be considered as of 'reversible type', they are *not* reversible *in fact*, since no reverse processes are conceptually possible. Since the Third Law applies only to *reversible processes*, we can assert that the Third Law of Thermodynamics is not applicable to the sublimation (or vaporization) at 0° K of *any* system. This statement remains true even for a system of fixed total volume for which the *results* ($\Delta S\to 0$, where S is the *total* entropy of the system) are identical.

We now introduce an ad hoc assumption which, although its plausibility is indicated by known results of supercooling near the triple point, must be considered a second axiom: that *the section of ϕ between the triple point and the critical point is identical with the section of the curve which would exist for equilibrium between the vapour and a phase maintained liquid (though unstable) to zero temperature, and that the section of ϕ between zero and the triple point is identical with the section of the curve for equilibrium between the vapour and a phase maintained solid (or liquid II for helium) at least to the triple point.* Thus we can consider the vapour condensation curve $p_\phi(T)$ to be composed of sections of two intersecting curves, $p_1(T)$ and $p_2(T)$, both terminating at P and both possessing the same general mathematical properties, including the same zero limits and values for all their derivatives at P. Clearly, only one of these curves can terminate at a critical point since a condensed phase possessing order or symmetry in either co-ordinate or momentum space cannot vary in a continuous manner to the random vapour phase.[2]

Considering either of the above curves and, for convenience, omitting the subscript, we now introduce as a *third axiom* the completely mathematical assumption that *$p^{(n)}(T)$ exists*, for every $n\geqslant 0$, and for every T in the closed interval $0\leqslant T\leqslant 1$. This axiom is equivalent to the statement that $p(T)$ is *infinitely differentiable* in $[0,1]$, which is a necessary, but not sufficient, condition for $p(T)$ to be *analytic* (in the real sense, that is, possessing a convergent Taylor series). Since each $p^{(n)}(T)$ has a derivative, it must be continuous and bounded; and, since each $p^{(n)}(T)$ is the indefinite integral of its derivative, it must be absolutely continuous and, thus, of bounded total variation. From a *fourth axiom*, $p\geqslant 0$, which is required by the conditions for stable mechanical equilibrium, we can immediately conclude that a number δ_1 exists such that, for $0<T\leqslant\delta_1$, $p^{(1)}(T)>0$, since $p(T)$ can become positive only by initially having a positive derivative (we disregard the trivial case where $p(T)$ is identically zero for all T). Applying this result and each succeeding result for $n=2, 3, \ldots$, leads to the *existence* of a set of intervals $(0,\delta_n]$ such that $p^{(n)}(T)>0$ for $0<T\leqslant\delta_n$, for every n; that is, there is *no* value of n for which $p^{(n)}(T)$ is everywhere negative on $(0, 1]$.

If $p^{(n)}(T)$ were analytic, we could expand it in a Taylor series about $T=0$. Thus, in the expression

$$p^{(n)}(T) = \sum_{m=0}^{M}\frac{1}{m!}p^{(n+m)}(0)\,T^m+R_M(T)$$

the partial sums Σ_M would converge to the value $p^{(n)}(T)$ and the remainder R_M would approach zero with increasing M. However, the partial sums are always zero for every M and, thus, converge only to zero, while the remainder does *not* approach zero with M, for arbitrary $T>0$, and must be always equal to $p^{(n)}(T)$. Therefore, $T=0$ cannot be an analytic point of $p^{(n)}(T)$ for any $n\geqslant 0$ or, equivalently, no convergent power series $\Sigma a_k T^k$ for $p(T)$ can exist everywhere in $[0, 1]$.

Considering $p(T)$ as expanded in a *finite* Taylor series with remainder about the point $T=0$, then, since the finite sum always vanishes, we can write[3]

$$\begin{aligned} p(T) &= T^{m+1}\int_0^1\frac{(1-x)^m}{m!}\,p^{(m+1)}(xT)\,\mathrm{d}x \\ &= \int_0^T\frac{(T-x)^m}{m!}\,p^{(m+1)}(x)\,\mathrm{d}x \end{aligned}$$

Using the Schwarz inequality,

$$\begin{aligned} |p(T)|^2 &\leqslant \int_0^T\left|\frac{(T-x)^m}{m!}\right|^2\mathrm{d}x\,.\int_0^T|p^{(m+1)}(x)|^2\,\mathrm{d}x \\ &\leqslant \frac{T^{2m+1}}{m!^2(2m+1)}\int_0^T|p^{(m+1)}(x)|^2\,\mathrm{d}x \end{aligned}$$

or,

$$\int_0^T|p^{(m+1)}(x)|^2\,\mathrm{d}x \geqslant \frac{2m+1}{(T^m/m!)^2}\cdot\frac{p^2(T)}{T},\quad 0<T\leqslant 1$$

Thus, the integral increases without bound with m, which implies that $|p^{(m)}(x)|$, itself, is unbounded with m on a subset which is not of measure zero in every interval $(0, T]$.

If $p(T)$ is assumed *non*-analytic at every point T_0 in $[0,1]$, then by similar reasoning from the Schwarz inequality,

$$\int_{T_0}^T|p^{(m+1)}(x)|^2\,\mathrm{d}x \geqslant \frac{2m+1}{[(T-T_0)^m/m!]^2}\cdot\frac{|p(T)-\Sigma_m|^2}{T-T_0}$$

where $$\Sigma_m = \sum_{k=0}^{m}\frac{1}{k!}p^{(k)}(T_0)\,(T-T_0)^k$$

The integral, of course, must become zero as $T \to T_0$ since it is absolutely continuous. However, since by assumption Σ_m does not converge to $p(T)$, for $T \neq T_0$ the integral must become unbounded with m which, again, implies that $|p^{(m)}(x)|$ increases without bound with m on a subset which is not of measure zero in every non-vanishing sub-interval of $[0, 1]$.

If, however, $p(T)$ *is* assumed analytic at points $T_0 \neq 0$, in the interior of the interval of convergence, its Taylor series will converge absolutely and, thus, unconditionally. Therefore, the terms of the series can be rearranged to obtain a power series

$$\sum_{k=0}^{\infty} a_k T^k$$

where the constants are given by

$$a_k = \frac{1}{k!} \sum_{h=0}^{\infty} \frac{(-1)^h}{h!} p^{(k+h)}(T_0) T_0^h$$

and are independent of T. As noted above, this power series cannot be convergent to $p(T)$, at least in the neighbourhood of $T = 0$; that is, the Cauchy criterion

$$\lim_{m,n \to \infty} \left| \sum_{k=0}^{n} a_k T^k - \sum_{k=0}^{m} a_k T^k \right| = 0$$

cannot be satisfied as $T \to 0$.

In particular, choosing $m = n - 1$ in this criterion, we must have

$$\lim_{n \to \infty} |a_n T^n| \geqslant \epsilon$$

where ϵ is any arbitrarily assigned number such that $\epsilon > 0$; then

$$\lim_{T \to 0} \lim_{n \to \infty} |a_n T^n| \geqslant \epsilon$$

which implies that

$$\lim_{n \to \infty} |a_n| \to \infty$$

From the series expansion of a_n we then can only conclude that $|p^{(k)}(T_0)|$ is unbounded with k for *every* T_0 in $(0, 1]$.

Up to this point we have been considering $p^{(n)}(T)$ only for $0 \leqslant T \leqslant 1$. If infinite differentiability is maintained over the entire interval $[0, \infty)$, however, a function $f(T)$ is uniquely defined on this semi-infinite interval such that $p^{(n)}(T) = f^{(n)}(T)$ in $[0, 1]$. Then the above discussion applies equally well to the $f^{(n)}(T)$, that is, the magnitude of these functions must increase without bound at any point of $[1, \infty]$. For any $T < \infty$, $f^{(n)}(T)$ is bounded. If we make the additional assumption that for some m the $\lim_{T \to \infty} f^{(m)}(T) < \infty$ then $f^{(m+1)}(T)$ must either become negative for some finite T or approach zero as $T \to \infty$.

Designating by $T_{(m+1)}$ the smallest zero of $f^{(m+1)}(T)$, clearly $f^{(m+2)}(T)$ must have a zero $T_{(m+2)}$ for which $T_{(m+2)} < T_{(m+1)}$ and, in general, zeros such that $T_{(n+1)} < T_{(n)}$ must exist for all $n > m$. Since the $T_{(n)}$ form a monotonic decreasing sequence bounded below by $T = 0$ they must approach a limit point $T_{(\infty)}$. If $T_\infty > 0$, then $\lim_{n \to \infty} |f^{(n)}(T_\infty)|$ would *not* be unbounded in n; thus, this limit point must be $T_\infty = 0$. Consequently, in any non-vanishing sub-interval of $[0, 1]$ an m large enough can be found such that $p^{(m)}(T)$ assumes *negative* values on the sub-interval.

Let us define N to be the largest integer such that, for $n \geqslant N$, $p^{(n)}(T) > 0$ for all T in $(0, 1]$. The determination of N is clearly of considerable importance for the shape of the vapour pressure curve. Preliminary investigations, however, indicate that N varies with the particular substance and may possibly be as low as two for helium-3, three for helium-4, and four for hydrogen (H_2). It should be noted that only experimental data of very high accuracy are useful in determining higher-order derivatives; thus, results of future investigations must depend strongly on basic theoretical considerations.

REFERENCES

1. Glass, S. J., and Klein, M. J. *Physica* **25**, 277 (1959)
2. Landau and Lifschitz. *Statistical Physics*, p. 260 (Addison-Wesley, Cambridge, Mass., 1958)
3. Graves, L. M. *The Theory of Functions of Real Variables*, p. 95 (McGraw-Hill, New York, 1946)

On the Specific Heat of Liquid Helium in Brenig's Theory

W. E. Parry and D. ter Haar *Clarendon Laboratory, Oxford*

Received 17 March 1960

Liquid helium possesses many qualities which make it a fascinating subject for scientific research. Its low boiling point makes it the most widely used means for reaching very low temperatures, but its behaviour when it is liquid is itself of intrinsic interest. Feynman's work[1, 2] has been the basis of recent theories about the behaviour of liquid helium near the absolute zero and, at present, there seems to be general agreement that the superfluid behaviour of liquid helium at extremely low temperatures ($< 1°$ K) and the T^3 behaviour of its specific heat below 0·6° K can be readily explained from the fact that helium atoms are bosons, which leads to the appearance of sound waves (phonons) as the only low energy excitations. There is, however, another property of liquid helium which has engaged physicists for a long time, namely, the so-called lambda transition at 2·2° K, that is, the transition from liquid helium I, which behaves like an ordinary liquid, to liquid helium II, which shows superfluidity. Feynman[3] used his space–time approach[4] to discuss the partition function of a system of interacting bosons, but it seems questionable[5] whether the conclusion reached on the basis of introducing a number of simplifications can be applied to liquid helium. It is, therefore, of some interest to consider the problem of the specific heat curve of a system of interacting bosons. It is well known that a system of non-interacting bosons will show a so-called third-order transition, that is, a transition where the specific heat c_v is continuous, but where its temperature derivative $\mathrm{d}c_v/\mathrm{d}T$ has a discontinuity. The specific heat of liquid helium shows a different behaviour: at the lambda point it has a discontinuity without, however, becoming infinite. In a recent paper, Brenig[6] derived an approximate expression for the energy spectrum of a system of helium atoms which he claimed would lead to a second-order transition. His claim was based (private communication) on the fact that his energy spectrum would lead to an increase in the specific heat above that of a perfect boson gas at low temperatures, due to an energy gap in the quasi-particle spectrum (see equation (3) below), while also leading to a decrease at temperatures above the lambda point which is essentially due to the restriction on the number of quasi-particle degrees of freedom. It is the purpose of the present paper to discuss briefly Brenig's energy spectrum and to give the results of evaluating the specific heat using an energy spectrum of the Brenig type which fully bears out Brenig's claims.

The energy spectrum

Since it is known from Feynman's work that low energy excitations in liquid helium are sound waves, one may assume that for small absolute magnitudes of the wave vector $\mathbf{k}$ of the excitations, the energy $\epsilon(k)$ as a function of $\mathbf{k}$ will be given by the formula

$$\epsilon(k) = \hbar ks; \qquad k < k_0 \qquad \ldots (1)$$

where $\hbar$ is Dirac's constant, $k = |\mathbf{k}|$, and s is a constant equal to the velocity of sound. The number of degrees of freedom corresponding to the energy spectrum (1) is given by the formula[6]

$$N_{\mathrm{ph}} = \gamma^3 N_0/3, \qquad \gamma = k_0/k_{\mathrm{D}} \qquad \ldots (2)$$

where N_0 is the number of particles in the system and k_{D} the Debye wave number. Noting that phonons are longitudinal waves, Brenig assumed $\gamma = 1$ which corresponds to the case where all longitudinal degrees of freedom are taken up by the phonons.

To find the energy spectrum for $k > k_0$, Brenig used a slight variation of Tomonaga's method[7] of separating collective co-ordinates from (quasi-)particle co-ordinates. Introducing N_{part} $(= 3N_0 - N_{\mathrm{ph}})$ quasi-particle co-ordinates one can evaluate the rest of the energy spectrum approximately. The result is

$$\epsilon(k) = \hbar^2 k^2/2m, \qquad k > k_0 \qquad \ldots (3)$$

where m is an effective mass for which we shall write

$$m = \lambda m_{\mathrm{He}} \qquad \ldots (4)$$

where m_{He} is the mass of a helium atom. The factor λ depends on the cut-off wave number k_0. Assuming $k_0 = k_{\mathrm{D}}$ and making simplifying assumptions about the expression for the energy, Brenig found $\lambda = 3/2$. It is, however, very questionable whether the assumptions made by Brenig, especially the neglecting of the interaction between helium atoms, is justified, and we therefore decided to treat both λ and γ as adjustable parameters and to evaluate the specific heat for a series of λ and γ values. The calculations had to be done numerically and we therefore restricted ourselves to the following values: $\gamma = 0{\cdot}5$, $\lambda = 1{\cdot}5$, 2·0, 2·5; $\gamma = 0{\cdot}6$, $\lambda = 2{\cdot}2$; $\gamma = 0{\cdot}75$, $\lambda = 2{\cdot}5$; $\gamma = 1$, $\lambda = 1{\cdot}5$, 2·0, 2·5. The values $\gamma = 1$, $\lambda = 1{\cdot}5$ correspond to Brenig's values, the values $\gamma = 1$, $\lambda = 2{\cdot}5$ represent the Landau energy spectrum[8] most closely, while $\gamma = 0{\cdot}75$, $\lambda = 2{\cdot}5$

gives a transition temperature in closest agreement with the experimental one (see below). The energy spectrum used by us starts with a straight line through the origin, as does the Landau spectrum. It does not, however, show a maximum followed by a minimum, but a discontinuity at $k = k_0$. The value of $\epsilon(\mathrm{k})$ just before k_0 is higher than the Landau value, while just after k_0 the minimum value from which the parabola (3) starts is well below the Landau minimum.

The specific heat

We shall use the theory of the grand canonical ensembles[9] (we shall use the notation of this reference, except that we shall use β instead of μ for $1/\kappa T$, and we shall refer to it as ESM) to evaluate the specific heat. Using a Brenig-like spectrum we are dealing with a system of independent (quasi-)particles, and its thermodynamic behaviour is determined, once we know the grand potential q which is given by the equation (ESM (7.603))

$$q = -\Sigma_s \ln[1-\exp(\nu-\beta\epsilon_s)] \qquad \ldots (5)$$

where $\beta = 1/\kappa T$ (κ is Boltzmann's constant, T is absolute temperature), $\beta\nu$ is the thermal potential, ϵ_s are the single particle energy levels, and the summation is over all energy levels. We shall neglect the contribution to the specific heat made by the phonons, as this contribution even at the transition temperature only amounts to a few per cent; moreover, it is a contribution which is continuous for all T and can easily be taken into account. Changing over from a sum to an integral in equation (5) and using the normal expression for the density of states (ESM (4.504)), we get from (5)

$$q = -\ln(1-\exp\nu)+(V/v_0)\,g(\nu,\beta) \qquad \ldots (6)$$

where V is the volume of the system,

$$g(\nu,\beta) = -2\pi^{-1/2}\int_{\beta\epsilon_0}^{\infty} z^{1/2}\ln[1-\exp(\nu-z)]\,\mathrm{d}z$$

$$\epsilon_0 = \epsilon(k_0) \qquad \ldots (7)$$

and

$$v_0 = (\beta h^2/2\pi m)^{3/2} \qquad \ldots (8)$$

The quantity ν is determined by the equation (ESM (7.604))

$$N = \partial q/\partial\nu = [\exp(-\nu)-1]^{-1}+(V/v_0)(\partial g/\partial\nu) \ldots (9)$$

and the energy E is given by the equation (ESM (7.416))

$$\frac{E}{V} = -V^{-1}\frac{\partial q}{\partial\beta}$$

$$= (\tfrac{3}{2}v_0\beta)\,g(\nu,\beta)-\left(\frac{2\epsilon_0}{\pi^{1/2}v_0}\right)(\beta\epsilon_0)^{1/2}\ln[1-\exp(\nu-\beta\epsilon_0)] \qquad \ldots (10)$$

The difference between the present equations and those applying to the perfect boson gas lies in the lower limit $\beta\epsilon_0$ of the integral in equation (7). In the case of the perfect boson gas $\epsilon_0 = 0$.

It can be shown that the integral in equation (7) can be expanded in a power series in ν as long as ν is small. After a tedious, but straightforward calculation, one finds for c_v at low temperatures the expression

$$c_v = \left(\frac{\kappa}{\pi^{1/2}v_0}\right)\{5K_0+2(\beta\epsilon_0)^{5/2}[\exp(\beta\epsilon_0)-1]^{-1}\} \ldots (11)$$

with

$$K_0 = \sum_{r=1}^{\infty} r^{-5/2}\,\Gamma(\tfrac{5}{2}, r\beta\epsilon_0) \qquad \ldots (12)$$

where $\Gamma(5/2, r\beta\epsilon_0)$ is the incomplete gamma function.

At temperatures above the transition point one can expand in powers of $\exp\nu$. The result is

$$c_v = \left(\frac{2\kappa}{\pi^{1/2}v_0}\right)\sum_{n=1}^{\infty}\exp(n\nu)\,A_n$$

$$A_n = \exp(-n\beta\epsilon_0)(\beta\epsilon_0)^{5/2}+[(\tfrac{3}{2}n^{5/2})\,\Gamma(\tfrac{3}{2}, n\beta\epsilon_0)+$$

$$+n^{-1}\exp(-n\beta\epsilon_0)(\beta\epsilon_0)^{3/2}]\left[nT\left(\frac{\partial\nu}{\partial T}\right)+\tfrac{5}{2}\right] \ldots (13)$$

where ν follows from equation (9) in which the first term can now be neglected.

To find the transition temperature we note first of all that for $T < T_c$ and practically up to T_c, ν is small so that we may for those temperatures rewrite equation (9) in the form

$$N \simeq -\nu^{-1}+\left(\frac{V}{v_0}\right)\left(\frac{\partial g}{\partial\nu}\right) \qquad \ldots (14)$$

or

$$\nu^{-1} \simeq -N(1-\alpha T^{3/2}) \qquad \ldots (15)$$

where

$$\alpha = \left(\frac{2\pi V}{N}\right)\left(\frac{\partial g}{\partial\nu}\right)_{\nu=0}\left(\frac{2\kappa m}{h^2}\right)^{3/2} \qquad \ldots (16)$$

Trouble arises when ν^{-1} threatens to vanish and to a fair approximation we can thus find T_c from equation (15) and put

$$T_c \simeq \alpha^{-2/3} \qquad \ldots (17)$$

There occurs a jump in the specific heat Δc_v which can be evaluated from equations (11) and (13) putting in both $T = T_c$. The result is

$$\Delta c_v = -nT_c\left(\frac{\partial\nu}{\partial T}\right)_c\left\{\tfrac{3}{2}\sum_{r=1}^{\infty} r^{-5/2}\,\Gamma(\tfrac{3}{2}, r\beta\epsilon_0)-\right.$$

$$\left.-\tfrac{5}{2}(\beta\epsilon_0)^{3/2}\ln[1-\exp(-\beta\epsilon_0)]\right\} \qquad \ldots (18)$$

As long as $\partial\nu/\partial T$ does not vanish at $T = T_c$, there will be a discontinuity in the specific heat. Differentiating equation (9) with respect to T one finds that, indeed, $\partial\nu/\partial T \neq 0$ as long as $\epsilon_0 \neq 0$, but that as $\epsilon_0 \to 0$, $(\partial\nu/\partial T)_c \to 0$ leading to a third-order transition for the perfect boson gas.

It is of interest to note that expression (13) duly goes over into the classical value of $\frac{3}{2}\kappa$ per particle when $\beta \to 0$. The decrease in c_v from $T = T_c$ to $T \to \infty$ is gradual. Below

T_c, the specific heat is given by equation (11). It increases strongly with temperature. The specific heats were evaluated numerically, those from equation (11) by using a desk machine and those from equation (13) by using the Ferranti Mercury computer of the Oxford University Computing Laboratory. In the Table we have given the values of T_c, of c_v just below the transition, and of Δc_v for the eight pairs of λ and γ values given in the previous section.

γ	λ	T_c (°K)	$c_V . 10^{-5}$ *(ergs)*	$\Delta c_V . 10^{-5}$ *(ergs)*
0·5	1·5	3·20	98	41
0·5	2·0	2·40	104	48
0·5	2·5	1·92	108	53
0·6	2·2	2·34	131	73
0·75	2·5	2·26	141	82
1·0	1·5	4·19	128	61
1·0	2·0	3·14	142	81
1·0	2·5	2·51	143	79

Acknowledgements. We express our gratitude to the Department of Scientific and Industrial Research for a maintenance grant to one of us (W.E.P.) and to Dr. L. Fox and the staff of the Oxford University Computing Laboratory for making computing facilities available to us.

REFERENCES

1. FEYNMAN, R. P. *Phys. Rev.* **91,** 1301 (1953)
2. FEYNMAN, R. P. *Phys. Rev.* **94,** 262 (1954)
3. FEYNMAN, R. P. *Phys. Rev.* **91,** 1291 (1953)
4. FEYNMAN, R. P. *Rev. mod. Phys.* **20,** 267 (1948)
5. TER HAAR, D. *Phys. Rev.* **95,** 895 (1954)
6. BRENIG, W. *Z. Phys.* **144,** 488 (1956); *see also* TER HAAR, D. *Introduction to the Physics of Many-body Systems* Chap. 10 (Interscience, New York, 1958)
7. TOMONAGA, S. *Progr. theor. Phys.* **13,** 467 (1955)
8. LANDAU, L. D. *J. Phys. U.S.S.R.* **11,** 91 (1947)
9. TER HAAR, D. *Elements of Statistical Mechanics* Chap. 7 (Rinehart, New York, 1954)

A Cryogenic Device for Irradiation in Liquid Nitrogen

L. Bochirol, J. Doulat, and L. Weil *Centre d'Etudes Nucléaires, Grenoble*

Received 18 March 1960

Numerous devices for irradiation in liquid nitrogen in atomic piles have already been described in the literature. They employ, in general, commercial nitrogen, or, if they use very pure nitrogen, they have a nitrogen circulation arrangement to enable the nitrogen to condense outside the pile.

The device we are going to describe here is cheaper to make and very reliable in operation. We shall first recapitulate the difficulties presented by the use of nitrogen in atomic piles, and some of the devices which have already been employed to overcome these difficulties. We shall then list the results obtained with the cold loop designed by us.

The problem of using liquid nitrogen in atomic piles

Commercial liquid nitrogen always contains appreciable quantities of oxygen, of the order of 0·5–1 per cent. This oxygen is converted into ozone, or into oxygen–nitrogen compounds, and numerous explosions have already been reported.[1] The problem of the formation of unstable compounds is particularly grave with pool-type piles, owing to the very high gamma ray:neutron ratio in these piles (about 10 times as high as in the case of a graphite pile). This is certainly the reason for the explosions which were observed in the course of the first tests carried out on the pool pile at the Grenoble Atomic Research Centre, when a cold loop containing commercial nitrogen was used. Figure 1 shows as an example a view of the internal wall of the Dewar vessel (the gauge of the aluminium was 0·5 mm), after destruction during heating of the loop. We also observed formation of an increasing proportion of ozone, which could be condensed in a trap inserted in the circuit of the vaporized nitrogen issuing from the loop. A rather large quantity of alumina was also formed after the explosion, indicating a reaction of the ozone with the aluminium of the Dewar vessel.

Known solutions

It will be observed first of all that a certain number of cold loops have operated with commercial nitrogen in graphite piles without trouble,[2,3] owing to the low gamma flux in these piles.

Also, McReynolds and associates,[4] at Brookhaven, and Lucasson,[5] at Saclay in the EL2 pile, carried out periodical total evaporation of the bath, with increase of the temperature above the boiling point of oxygen. This method prevents concentration of oxygen, but the irradiation temperature is variable, and can be controlled only with difficulty.

Coltman and associates[6] preferred the method of using helium as an intermediate fluid, so that the liquid nitrogen remained in a heat exchanger outside the reactor, although this method somewhat limits the cooling effect, and there is some lack of certainty as regards the temperature of the samples obtained when using a gas as an intermediary fluid.

On the other hand, Sartain and Yockey[7] described a device employing high purity nitrogen circulating under pressure in a closed circuit. The nitrogen, remaining liquid, is cooled by ordinary liquid nitrogen, which is also placed in a heat exchanger outside the reactor, and the pure nitrogen is circulated by a pump. This device is obviously safe whatever the gamma radiation of the pile, but it is expensive to make and the consumption of liquid nitrogen is very high, amounting to 16 l./hr.

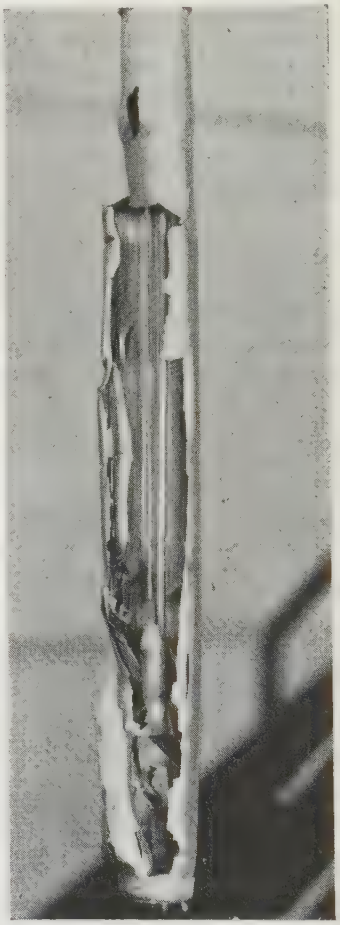

Figure 1. The broken inner wall of the first loop after an explosion

Principles of the proposed solution

We also employed two nitrogen circuits, as in the system suggested by Sartain and Yockey, but *instead of circulating the pure nitrogen outside the pile, we combined in one unit the very pure nitrogen system*, in which the substances are irradiated, *and the condenser*, which was cooled with commercial nitrogen. The two liquids, the pure and the

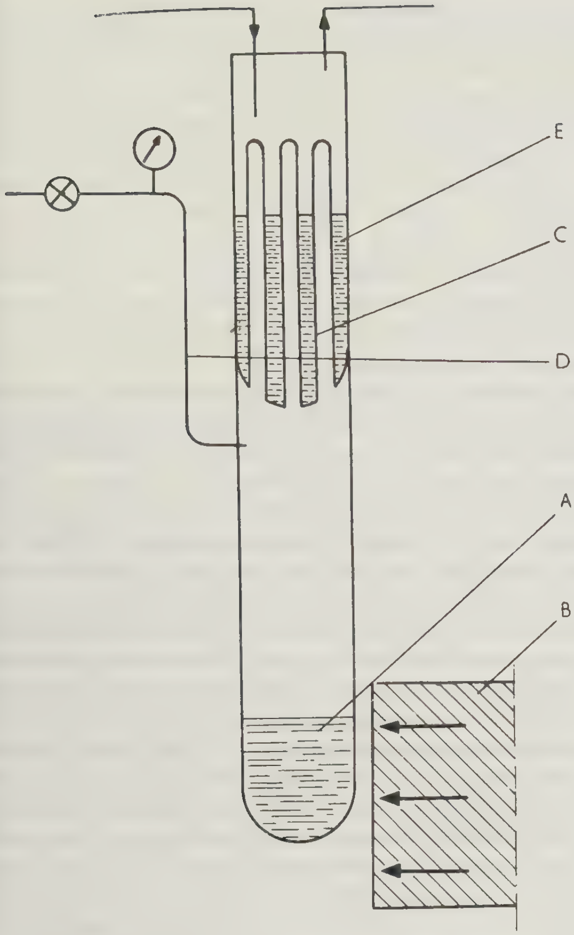

Figure 2. The general arrangement of the apparatus

commercial nitrogen, are separated from each other by a distance of about 1 m, which is large enough to ensure that the pure nitrogen is placed in the area of intensive radiation near the centre of the pile, while the commercial nitrogen is subjected only to a very limited amount of radiation. This latter circuit is also protected by lead screens.

The general scheme of the apparatus is shown in Figure 2. The samples to be irradiated are immersed in the bath of pure liquid nitrogen A, and subjected to radiation from core B. The nitrogen evaporated by the release of energy of radiation in the walls, the fluid, and the samples is liquefied on the surface of the condenser C, cooled by a bath of ordinary liquid nitrogen, and the condensate drops back into the bath A under the action of gravity.

The apparatus is filled with pure nitrogen, after the evacuation of the zone A, while the condenser is cooled. The pure nitrogen admitted under a slight over-pressure through the pipe D is finally liquefied in the condenser. With the aid of a dosing apparatus a quantity of gas designed to obtain in A a given quantity of liquid is introduced, after which the zone is closed, and remains closed.

The pressure in this zone is established under these conditions at a value which depends partly on the dissipated power and on the condenser temperature (i.e. the pressure in the zone E), and partly on the size of the useful area of the condenser. This area is again governed by the level of the commercial nitrogen. The pressure variation in the zone A is therefore governed by the level of the commercial nitrogen in the condenser, all other conditions remaining equal, and it can be utilized for operating the automatic control of the level of the commercial liquid nitrogen, i.e. the control of the supply of fresh nitrogen from an external storage vessel.

Some details of the design of the loop with two circuits

Figure 3 is a diagrammatic drawing of the equipment built according to this system. It is 7 m long, and is immersed in the water of the pool, reaching the edge of the core 3. The two baths 1 and 4 are isolated from each other by an annular space in which a pump acting through the pipe 8 maintains a vacuum of 10^{-4} mm Hg. This pipe spirals in the water to prevent noxious biological effects.

In order to enable the samples to be placed in the liquid and to be removed without reheating, the apparatus is made in two parts, which are made fluid-tight by a gasket 10. The internal part comprises the heat exchanger 4, the injection pipe for the liquid nitrogen 6, the evacuation pipe 7, and the pipe 5 through which the zone 1 can be filled and its pressure be measured. Through this pipe 5 pass also the electric connections for any measurements which may have to be carried out in the pile. The free space 11 is filled with a powdered thermal insulating material, perlite (main constituents: silica 76 per cent, alumina 16 per cent) whose thermal conductivity is reduced by a primary pump acting through the orifice 9.

In order to take out the samples, a calculated addition of pure nitrogen is injected so as to fill the vessel 13 containing the samples. The movable part of the apparatus is then quickly taken out, with the vessel 13 suspended from it, which is then immersed in a Dewar vessel filled with liquid nitrogen.

The lower part of the heat exchanger is about 70 cm above the top of the core, and would be subject to a flux equal to about 1 per cent of the flux present in the neighbourhood of the core. The lead screens 12 placed there as an additional safety measure reduce this flux by a further factor of 500. The flux in the ordinary nitrogen can therefore be estimated as 10^3 r/hr.

Some results

The apparatus has functioned in the core of the pile (output 1 MW, 10^{13} thermal neutrons/cm^2 sec, $2{\cdot}5 \times 10^{12}$ fast neutrons/cm^2 sec, gamma flux 5×10^7r/hr) for several continuous periods of 1 week, and for many shorter periods, without any incident, either during operation or reheating. No trace of corrosion was detected in the equipment. The samples were recovered in the cold condition.

It is naturally essential to take all possible precautions to prevent the condensation of atmospheric air on the bath 1, either by making sure that the vessel with pure nitrogen is and remains perfectly gas-tight, or by simply maintaining in this vessel a slight over-pressure with

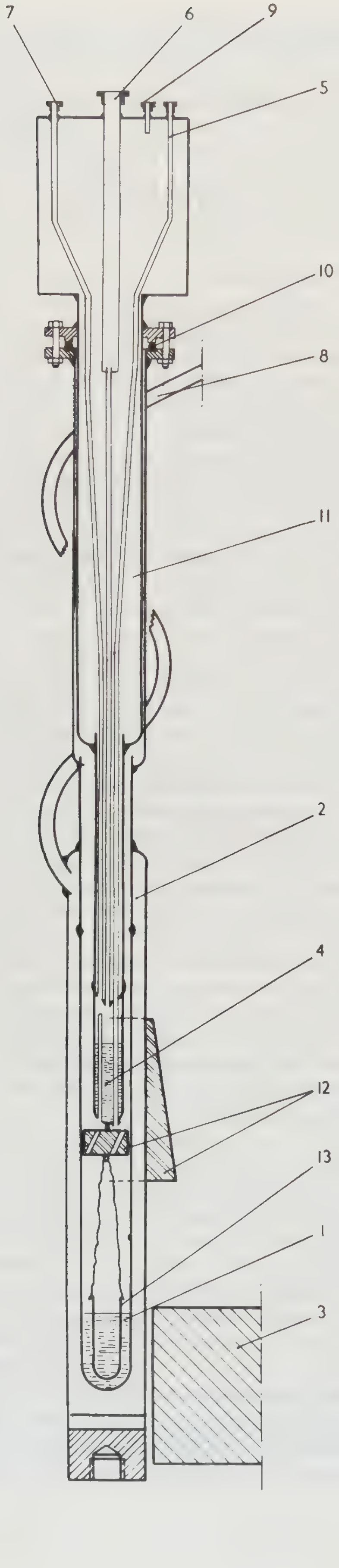

respect to the atmosphere (i.e. by avoiding any reduction of the pressure above the commercial nitrogen bath).

Since ordinary nitrogen boils in zone 6 under atmospheric pressure, the over-pressure above the bath of pure liquid nitrogen remains at about 80 mm Hg, at an output of 70 W (dissipated in the bath of liquid nitrogen, with a capacity of 200 cm^3, and in the samples and walls) using a condenser of maximum heat exchanging surface of 1,600 cm^2.

Under these conditions the consumption of nitrogen is approximately 80 l./day. By way of comparison we can mention here that Thompson and associates[2] and Bortels[3] registered nitrogen consumptions of 17–30 l./day in their direct-feed device with a gamma flux about 10 times lower than ours, while Sartain and Yockey[7] noted a consumption of 380 l./day in a gamma flux which is probably three times that of ours.

When located in a place where the gamma flux is the same as that of Thompson and associates, our loop requires about 25 l. of nitrogen per day, i.e. the same consumption as theirs. On the other hand, a new configuration of the core recently enabled us to make an experiment with a gamma flux twice and a fast neutron flux three times greater than the previous values reported above. We were thus very near to Sartain and Yockey's conditions, and the consumption did not exceed 100 l./day. A part of this consumption is due to losses in the supply duct. A modification of this duct is under consideration which is likely to yield an even more substantial gain with respect to the methods using an external circuit.

Conclusions

The device described above has the low consumption of liquid nitrogen and the perfect safety which we expected. It can be used wherever the coolant for low temperature irradiation needs protection from irradiation. It can also be used for the liquid-state irradiation of rare isotopes which would be gaseous at room temperature and which have to be confined in a reduced space.

REFERENCES

1. Cottrell, W. H. 'Ozone Explosions in Irradiated Cryogenic Apparatus and Implications upon N. S. Savannah Gaseous Waste Disposal System.' Unclassified CF-58-7-97
2. Thompson, M. W., and Jefferson-Loveday, D. W. 'A Cryostat for Reactor Irradiations in Liquid Nitrogen.' *J. sci. Instrum.* **35,** 397 (1958)
3. Bortels, B. 'Cryostat for Reactor Irradiation in Liquid Nitrogen.' *J. sci. Instrum.* **36,** 511 (1959)
4. McReynolds, Augustyniak, McKeown, and Rosenblatt. *Phys. Rev.* **98,** 418 (1955)
5. Lucasson. 'Dispositif d'irradiation à basse température dans une pile atomique.' *C. R. Acad. Sci., Paris* 678 (1957)
6. Coltman, R. R., Blewitt, Th., and Noggle, T. S. 'Techniques and Equipment Utilized in Low Temperature Reactor Irradiation.' *Rev. sci. Instrum.* **28,** 375 (1957)
7. Sartain, C. C., and Yockey, H. P. 'Cryostat for Reactor Irradiation.' *Rev. sci. Instrum.* **19,** 218 (1958)

Figure 3 (left). Diagrammatic section through the apparatus

The Effect of Radiation Damage on the Thermal Conductivity of Superconductors

K. D. Chaudhuri, K. Mendelssohn *Clarendon Laboratory, Oxford*
M. W. Thompson *Atomic Energy Research Establishment, Harwell*

Received 28 March 1960

The recent measurements of thermal conductivity of superconductors by Montgomery[1] and Rowell[2] have shown the value of thermal conduction measurements in the superconductive and normal states for the investigation of metal imperfections. Montgomery has shown that conduction in the normal state, which is due to electrons, is much reduced by the presence of point defects such as impurities, but largely uninfluenced by large-scale lattice defects such as dislocations. The opposite is true for the phonon conduction in the superconductive phase where large-scale defects contribute most to the resistivity. Montgomery's work has been extended by Rowell whose investigations have been concerned with the effect of controlled strain in lead and niobium. Rowell's experiment represents the first attempt at relating quantitatively the phonon conduction in superconductors to the number of dislocations. This work has now been extended to an investigation of the effect of radiation damage caused by pile neutrons.

Experimental procedure

The specimens were monocrystal rods of niobium or vanadium, roughly 50 mm × 4 mm diameter, which had been prepared by the 'floating zone' technique in an electron bombardment furnace.[3]

The apparatus for measuring thermal conductivity was the conventional cryostat having heat sink, thermal anchor, and radiation shield. The specimen, whose upper end was attached to the heat sink, carried two 33 Ω $\frac{1}{4}$ W LAB resistors and, at its lower end, a heater. By applying a magnetic field to the specimen the normal state could be restored.

The heat conductivity of the specimens was first measured in both superconductive and normal states. They were then irradiated in a hollow fuel element of the BEPO reactor at Harwell to a dose of 10^{18} fast neutrons cm^{-2}. The temperature of the specimens was within 5° of 30°C throughout the irradiation. After allowing a few weeks for radioactivity to decay, the specimens were returned to the laboratory and the conductivity measurements repeated.

Experimental results

In Figures 1 and 2 the thermal conductivities are compared before and after irradiation for niobium and for vanadium, respectively. In both cases there is an increase in superconductive thermal resistivity W_s which is inversely proportional to T^2, but only in the case of niobium is there a detectable increase of normal state resistivity W_n. The absolute magnitude of the change in W_n for niobium is 0·4 cm. deg. watt^{-1}, whereas the limit of detection in the case of vanadium is about 0·5 cm. deg. watt^{-1}, due to the relatively large value of W_n in vanadium. It is, therefore, uncertain whether or not vanadium and niobium behave as comparably in the normal state as they do in the superconductive state.

Discussion

Klemens[4] has predicted the scattering of lattice waves by static imperfections from second-order perturbation theory. An imperfection can be expected to perturb the

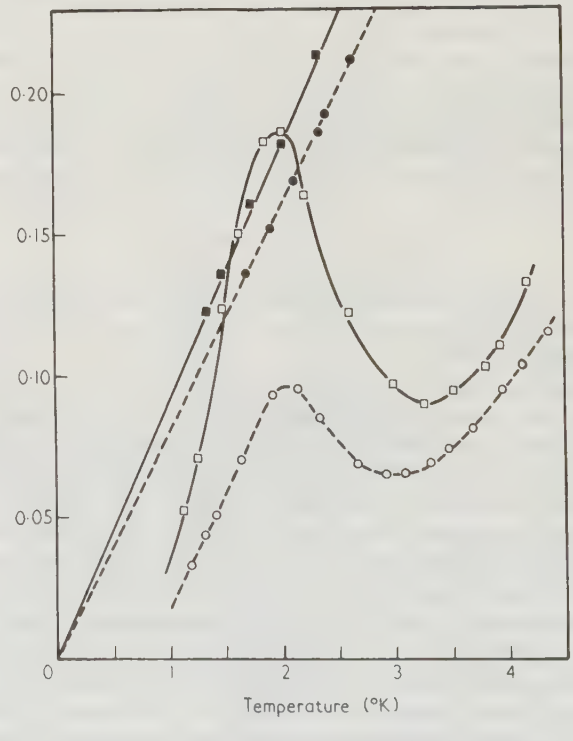

□ K_s before irradiation ○ K_s after irradiation
■ K_n before irradiation ● K_n after irradiation

Figure 1. Niobium single crystal

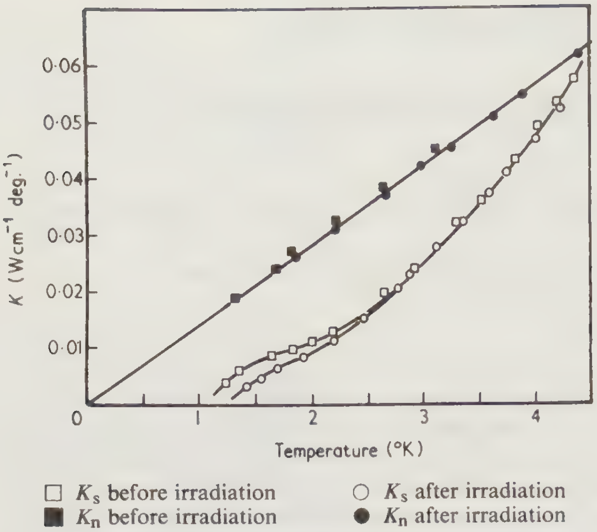

Figure 2. Vanadium single crystal

lattice potential on account of (1) the difference between the masses of the defect and the atoms on the parent lattice, (2) the difference between the elastic properties of the normal and defective atomic linkages, and (3) an elastic strain field which alters the elastic constants of the linkages as a result of deviations from Hooke's law. The thermal resistance due to the terms (1) and (2) has been shown by Klemens to be proportional to T and is quite insignificant at low temperatures. The thermal resistance due to (3) has been shown to be inversely proportional to T^2 and is therefore quite appreciable at low temperatures. Klemens has actually likened a dislocation to a line of point defects with a highly disordered core of radius a, surrounded by a strain field which falls off as $1/a$. He then deduces the scattering cross-section of such a model for phonons and gives the result for the increase in thermal resistance as

$$W_s T^2 = 16h^2 v D b^2/70k^3$$

where D is the dislocation density, v is the velocity of sound, b the Burgers vector, and h and k have their usual significance.

Current theories of radiation damage in b.c.c. metals (see, for example, Thompson[5]) suggest that radiation produces interstitial atoms and vacant lattice sites in equal numbers, the neutron cross-section for producing a single interstitial–vacancy pair being roughly 10^{-22} cm^2. The atomic concentration of interstitials or vacancies produced in our specimens should, therefore, be of the order 10^{-4}. Interstitials are thought to become mobile at temperatures as low as 20° K whereas vacancies are believed to migrate, in experimentally observable times, at a temperature roughly 20 per cent of the absolute melting point. Recent work by Smallman and Westmacott[6] using the electron microscope indicates that when such point defects migrate, a proportion condense into plates which collapse to form small dislocation loops. A further proportion condense on to the existing dislocation network causing jogs to appear on previously straight lines.

In both vanadium and niobium the irradiation temperature is such that interstitial migration will have occurred during irradiation. In the case of niobium the irradiation temperature is well below the expected temperature of vacancy migration; for vanadium this is not so, vacancy migration may have occurred during irradiation.

The observed increase in W_s may be explained by postulating an increase in dislocation density brought about by the condensation of interstitials either to form small loops or on to the existing network to form jogs. The increase in W_n may be explained as being due to vacancies produced directly by irradiation.

Let us now examine the magnitude of the quantities involved. A concentration C of interstitials, condensing in the ways described above, would produce an increase in dislocation density of order Cda^2/r, where d is the atomic density, a the lattice parameter, and r is either the radius of a circular loop or the jog length on a jogged dislocation. Assuming C to be of the order 10^{-5} (i.e. 10 per cent condensation) and r of the order 100 Å, the expected increase in D is of the order 10^9 lines cm^{-2}. Using Klemens' formula to calculate the increase in dislocation density from the observed change in W_s we obtain 3×10^9 lines cm^{-2} in the case of niobium and 10^{10} lines cm^{-2} for vanadium. Bearing in mind that the values of C and r are only rough estimates and that Klemens' formula cannot be expected to give exact quantitative results, this agreement seems surprisingly good.

Theoretical and experimental estimates of the electrical resistivity induced in copper by 1 per cent of vacancies lead to a value of about 1 $\mu\Omega$cm. Let us therefore assume the reasonable figure of 0·05 $\mu\Omega$cm for the change in electrical resistivity of niobium brought about by a vacancy concentration of 10^{-4}. Then using the Wiedmann–Franz law to translate this into a normal state thermal resistivity, a change of 1 cm. deg. watt^{-1} is expected for 10^{-4} vacancies. This is very close to the 0·6 cm. deg. watt^{-1} found in the case of niobium.

The postulated mechanisms offer a reasonable explanation of the observed effects. We therefore conclude that neutron irradiation at 30°C increases the dislocation density by introducing loops and jogs, and introduces point defects which are probably vacancies.

We are grateful to Dr. A. R. Powell, F.R.S., and Mr. A. Calverley for making and supplying the specimens. K. C. is now at Physics Dept., University of Delhi.

REFERENCES

1. Montgomery, H. *Proc. roy. Soc.* **A244,** 85 (1958)
2. Rowell, P. M. *Thesis*, Oxford; *Proc. roy. Soc.* **A254,** 542 (1960)
3. Calverley, A., Davies, M., and Lever, R. F. *J. sci. Instrum.* **34,** 142 (1957)
4. Klemens, P. G. *Proc. phys. Soc. Lond.* **A68,** 1113 (1955); *Solid State Physics* Vol. 8 (1958)
5. Thompson, M. W., *Phil. Mag.* To be published (1960)
6. Smallman, R. E., and Westmacott, K. H. *J. appl. Phys.* **30,** 603 (1959)

Cryostats for Optical Investigations

P. Pesteil and R. Philip

Laboratoire de Physique P.C.B., Faculté de Sciences de Marseille, France

Received 25 May 1960

We describe here some cryostats for optical investigations. These instruments have been utilized in our laboratory for several years, and have been found to be quite satisfactory. They are cheap to make and easy to use, and they are therefore convenient for research workers who are not used to low temperature techniques. We feel that the description of these instruments will help to persuade a greater number of physical chemists to carry out optical investigations in the neighbourhood of absolute zero.

We shall briefly summarize the properties expected of a cryostat of this type:

(1) The consumption of liquid hydrogen or helium must be as small as possible;
(2) Visible, ultra-violet, or infra-red light must pass through the apparatus, and the windows must not frost over in any circumstances;
(3) So that it may be portable, the apparatus should be as small as possible;
(4) It should be arranged so that it can easily be dismantled in order to facilitate the cleaning of the transparent parts.
(5) It must be possible to insert samples, withdraw them, or change their position, without any difficulty while the apparatus is in use, i.e. while they are immersed in the coolant.

The three cryostats described below have these properties, and the type to be used should be selected according to whether the sample is immersed in liquid coolant, in a gaseous atmosphere, or remains in a vacuum.

We shall now give a brief list of examples of the application of these instruments.

For the spectrographic examination of the visible or ultra-violet absorption or luminescence of a sample with the aid of a slide-type spectrograph, the sample can be immersed in liquid hydrogen or helium. Bubbles do not interfere with the work because the receiver integrates the luminous flux received during a comparatively long period. Experience has also shown that the effect of the bubbles on the polarization of the light is negligible.

A photoelectric receiver, on the other hand, can be used only if the sample is placed in a vacuum or in a gaseous atmosphere; a liquid bath cannot be used because the bubbles interfere with the response of the receiver.

In the case of infra-red absorption, the glass or quartz windows must be replaced by salt disks (sodium chloride, potassium bromide, or the like). The sample should also be placed in a vacuum to avoid the necessity of joints between glass and salt or metal and salt which are difficult to make.

The dark current of a photomultiplier can be reduced by cooling the apparatus. The cell would be placed in a gaseous atmosphere and the cryostat is designed in such a way that the beam of light falling on to the photocathode does not pass through any liquid.

The cryostats described by us here are suitable for the purposes briefly listed above.

Cryostat No. 1

In this cryostat (Figure 1), the three outer tubes are made of metal (nickel silver or stainless steel). They are intended to protect the liquid hydrogen or helium contained in the central tube. The annulus formed by two

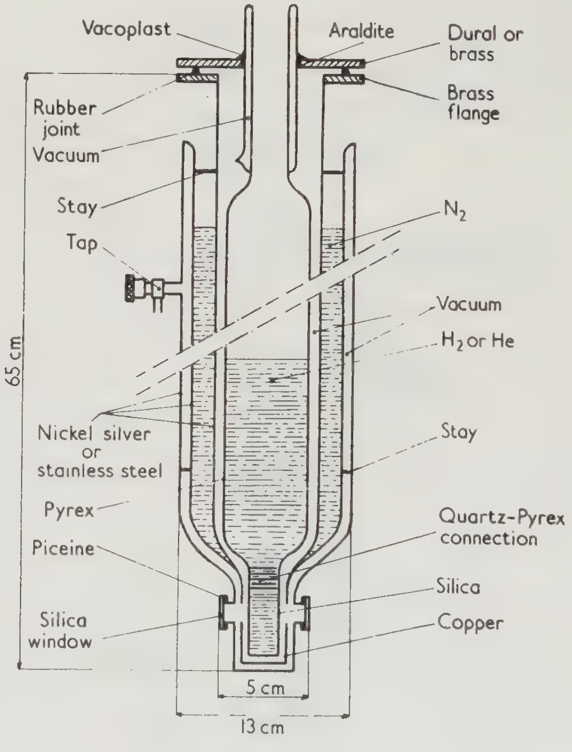

Figure 1. Cryostat No. 1

of these tubes contains liquid nitrogen. The lower part of the vessel is extended by a copper tube, provided with windows, which protects the lower part of the central tube from heat influx.

The central tube, which is made of glass, is stuck with Araldite No. 101 to a Dural flange, the tightness of the joint is ensured by a layer of Vacoplast. The cooling of the glue and of the Vacoplast is prevented by two tubes, the space between these tubes being well evacuated.

For measurements in ultra-violet light the lower part of the central tube must be made of silica. It is fixed to the glass tube through a quartz–Pyrex connection. The outer metal tube has windows on which Pyrex or silica disks are stuck with Picein.

The apparatus is first evacuated through a tap. A rotary oil pump is suitable for reaching a vacuum of about 5×10^{-3} mm Hg, and this is adequate as the coolant subsequently improves the vacuum.

The sample is introduced from the top, either suspended from a very fine wire or fixed to a rod having a hook at its end. The rod is removed before the liquid is siphoned into the vessel. In the latter case the orientation of the sample can be rectified by means of a small magnetron magnet acting on a steel bar fixed to the sample.

Characteristic features of this apparatus are as follows:

Coolant capacity: 1 l.
Coolant consumption: 1 l. of hydrogen per 24 hr, or 2 l. of helium per 24 hr.
Nitrogen capacity (for the protecting jacket): 1 l.
Nitrogen consumption: 4 l. per 24 hr
Initial vacuum: 5×10^{-3} mm Hg

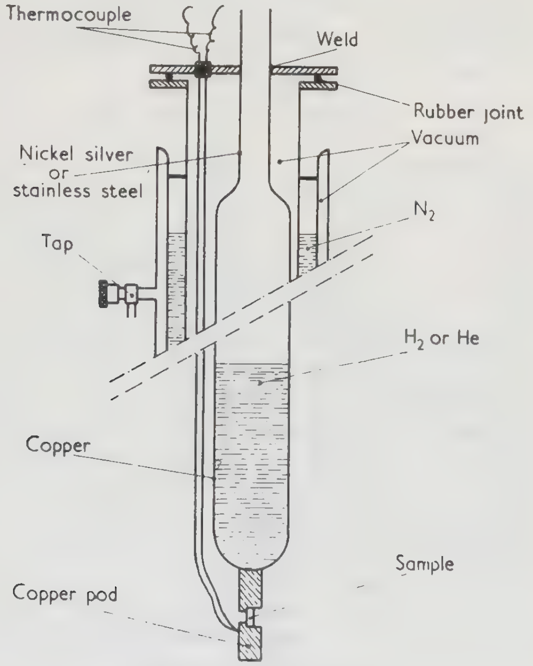

Figure 2. Cryostat No 2

Cryostat No. 2

This cryostat (Figure 2) is a variant of the preceding apparatus. It should be used if the sample must be kept in a vacuum; for instance, when the absorption of infra-red rays is to be investigated. The outer part of the apparatus, not shown in Figure 2, is identical with that shown in Figure 1. The glass tube is replaced by a metal container with a hollow copper bar brazed to its lower end. This bar contains the sample, with the external apertures directly over the sample. The apertures are covered with potassium bromide for the investigation of infra-red absorption and are fixed with Picein, like the glass.

The temperature of the sample will naturally be higher than that of the coolant, but the two temperatures converge with increase in the diameter of the copper bar. A thermocouple passing through the upper flange enables the temperature to be measured.

Cryostat No. 3

This cryostat (Figure 3) is used if the sample must be kept in a gaseous atmosphere. Its outer part is quite similar to the corresponding part in the other two cryostats, but it should be noted that the vessel containing nitrogen has one or several transverse tubes opposite the windows to allow the passage of the light-beam. The central part, made of glass, consists of two cylindrical tubes of circular cross-section, one tube eccentric with respect to the other. The space between these two tubes contains the coolant and the central tube contains the sample or the photoelectric cell. The atmosphere in this central tube is hydrogen or helium, kept at atmospheric pressure by means of a rubber bladder, which compensates for the lowering of the pressure due to the reduction of the temperature. The two container walls are connected together by one or several tubes, according to the number of windows required.

As the beam of light does not pass through the coolant liquid the light is not disturbed by bubbles. For measurements in ultra-violet light, quartz–Pyrex connections are used at the points marked in Figure 3.

Characteristic features of this device are as follows:

Coolant capacity: 1·5 l.
Coolant consumption: 1·5 l. of hydrogen per 12 hr
Nitrogen capacity (for the protecting jacket): 1·5 l.
Nitrogen consumption: 3 l. per 12 hr
Initial vacuum: 5×10^{-3} mm Hg

(This cryostat has not been utilized at the temperature of liquid helium, because any gas becomes liquid below 4° K. However, investigations at 4° K can be carried out if helium pressures of less than atmospheric are acceptable.)

Examples of uses of equipment

Cryostat No. 1 can be used for the examination of absorption spectra and of luminescence, by arranging

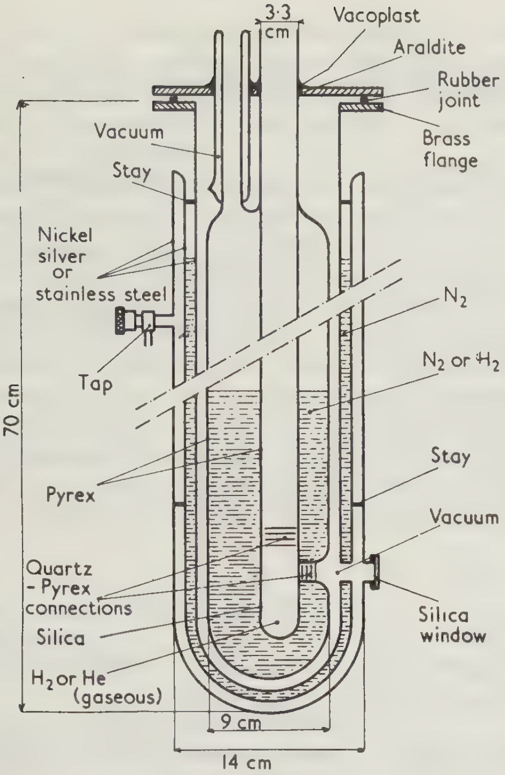

Figure 3. Cryostat No. 3

three windows in the same horizontal plane. It has been used by one of the authors for the examination of aromatic crystals.[1]

Cryostat No. 3 has been used in photometric work, where cells with electronic photomultipliers are quite often used as receivers. When a voltage is applied to these cells they have, like all instruments of this kind, a certain dark current. The existence of this current interferes with the proportionality between the response and the applied illumination. Again, in those comparative investigations where the dark current has to be measured in order to subtract it from the total current supplied by the cell, this parasitic current must remain stable during a complete measurement. The best means of stabilizing this current, and of reducing its interference, is obviously to remove it completely.

The dark current is mainly due to the conductivity of the walls and the thermionic emission of the cathode. It is known that these two effects fall exponentially with the temperature. For this reason we cooled a photomultiplier with the aid of this apparatus, using first liquid nitrogen and later liquid hydrogen.

We employed a type RCA No. 1P 28 photomultiplier. The breech part surrounding the transparent tube was removed in order to prevent any dangerous mechanical stresses during cooling or re-heating.

The stabilized supply voltage was 600 or 1,000 V, and the dark current was measured with the aid of a Lemouzy PA 14 pico-ammeter. The results are shown in Table 1.

Table 1

Conditions	*Dark current*	
	at 600 V	*at 1,000 V*
Room temperature	$0{\cdot}9 \times 10^{-9}$ A	$1{\cdot}8 \times 10^{-9}$ A
Liquid nitrogen temperature	$4{\cdot}0 \times 10^{-14}$ A	$27{\cdot}0 \times 10^{-14}$ A
Liquid hydrogen temperature	down to 10^{-14} A	down to 10^{-14} A

The measuring equipment was not sensitive to currents of less than 10^{-14} A, so that we could not determine the dark currents at the temperature of liquid hydrogen, but it can be seen that liquid nitrogen has already produced quite satisfactory results.

REFERENCE

1. Pesteil, P., et al. *C. R. Acad. Sci., Paris.* Various papers 1951–60

Letters to the Editors

The Electrical Resistivity of Plutonium, Neptunium, and Some Plutonium Alloys

In this letter, electrical resistivity measurements on samples of plutonium, neptunium, and three δ-stabilized plutonium–aluminium alloys are reported. The specimens were rods about 2 mm in diameter and 3–4 cm in length, and the temperature range covered was from 1·5° K to nearly 300° K. The cryostat used in this investigation has been described elsewhere.[1] Standard potentiometric techniques were employed for the measurement of resistance, and connections to the specimens made by spot-welding.

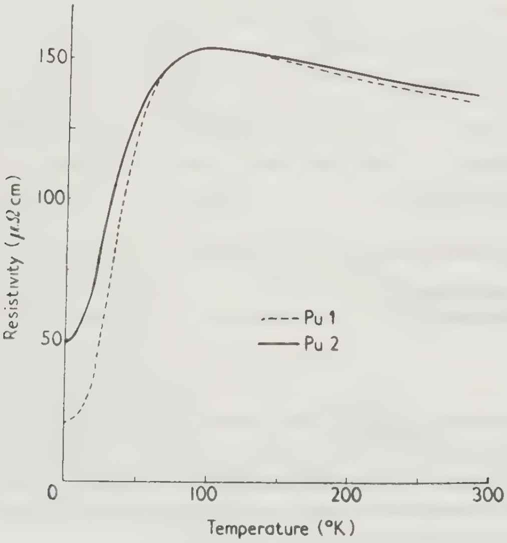

Figure 1. Resistivity vs temperature for two specimens of plutonium in the α-phase. Experimental points were too numerous to be drawn on the graph. The scatter was such that all the points lay within the thicknesses of the lines

Resistivity–temperature data for two plutonium samples are given in Figure 1. One specimen, Pu 1, had a density of 19·625 g/cm³, which compares well with the theoretical value of 19·82. The density of the other specimen, however, was much lower at 19·195 g/cm³. The purities of the two samples as indicated by spectrographic analysis were 99·96–99·97 per cent. Ferromagnetic impurity content was very low, amounting only to 57 and 60 parts per million in specimens 1 and 2, respectively.

Both samples had high and widely differing residual resistances (ρ_0) though their ice-point readings were almost the same. The respective values of ρ_0 for Pu 1 and Pu 2 were 13·9 and 32·6 per cent of their ice-point readings. A $\rho = \rho_0 + BT^n$ relationship was obeyed at low temperatures. For Pu 1, n equalled 2·3 below about 33° K. For Pu 2, n was 2·0 below 26° K.

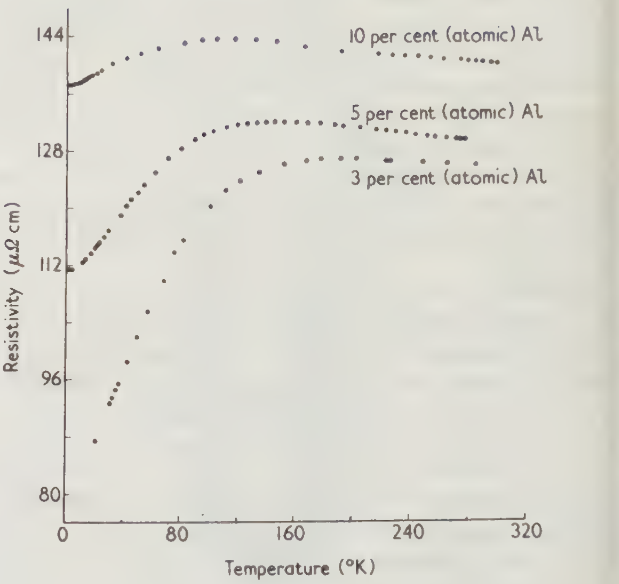

Figure 2. Resistivity versus temperature for three metastable δ-plutonium alloys

The resistive behaviour throughout bears a remarkable resemblance to that of α-manganese[2] where a T^2 law also holds below 20° K. It is highly probable that in manganese the anomalous temperature dependence of resistance below 100° K is due to antiferromagnetic ordering.[3] Neutron diffraction experiments are therefore being carried out on plutonium in order to find directly whether plutonium also is antiferromagnetic.

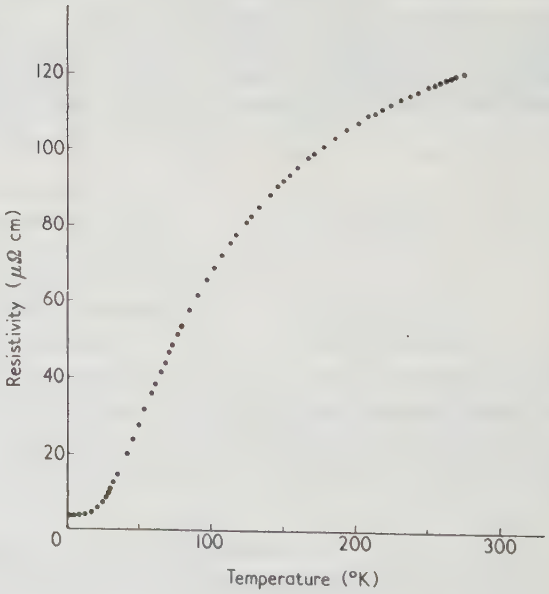

Figure 3. Resistivity versus temperature for α-neptunium

In Figure 2 are shown our measurements on three δ-stabilized plutonium–aluminium alloys. The similarity with the α-plutonium curves suggests that the same feature is responsible for the anomalous resistive behaviour in both phases.

Figure 3 shows the variation of the electrical resistivity of α-neptunium with temperature down to 1·4° K. Below 31° K, ρ was found to be proportional to $T^{3\cdot 1}$. Overall purity of this specimen was only about 99 per cent (wt), the major impurities being 0·34 per cent (wt) calcium and 0·22 per cent (wt) uranium. Nevertheless, the residual resistivity of 3·55 μΩ cm (2·7 per cent of the ice-point value) was very small in comparison with those of the plutonium samples. If plutonium is indeed antiferromagnetic, the high values of ρ_0 may possibly be due to incomplete ordering of the spins caused by the presence of specific impurities in solid solution.

J. A. Lee
Atomic Energy Research Establishment,
Harwell, Berks.
G. T. Meaden
K. Mendelssohn
Clarendon Laboratory,
Oxford.

(*3 May 1960*)

REFERENCES

1. Meaden, G. T., and Lee, J. A. *Cryogenics* **1**, 33 (1960)
2. White, G. K., and Woods, S. B. *Canad. J. Phys.* **35**, 346 (1957)
3. Coles, B. R., *Advanc. Phys.* **7**, 40 (1958)

Fine Structure of the Luminescence Spectra of Organic Molecules in Crystalline Solutions

It has been known for some years that luminescence and absorption spectra of aromatic molecules in solution in paraffin hydrocarbons at low temperature are composed of lines which can be extremely fine if the solvent is suitably chosen.[1, 2] The electron transition is decomposed into a large number of thick lines whose intensity generally varies with concentration[3] and with temperature.[4]

Up to the present time, it has been admitted that each component of the transition corresponded to a given orientation of the molecule in solution in the solvent system; for want of a better, we ourselves accepted this hypothesis put forward by Bowen.[5] It seemed improbable, however, that a very large number of different 'sites' (up to 8 components) could be possible in the solvent system. This difficulty led us to seek another explanation for the separation of the electronic transition into several components.

One of us carefully examined the spectra obtained with a fairly high dispersion prism spectrograph (u.v. 120; S.G.O.), and was able to perceive numerous weak lines which were extremely fine and regularly spaced at from 4 to 10 cm^{-1} according to the case. The thick lines themselves often seemed to be made up of several fine lines.

The idea of an interference phenomenon on the walls of the vessel containing the solution first occurred to us, but we were able to dismiss this possibility for the following reasons:

(1) Two vessels of differing thickness gave identical spectra;
(2) The fine lines appeared neither on the continuous bottom nor in the neighbourhood of the mercury lines of the excitor lamp;
(3) These lines are not to be seen in the case of exciton spectra of pure crystals obtained in the same conditions.

Our measurements were made on the S–S and T–S spectra of the following molecules in solution in *n*-pentane at 20° K and at 4° K: benzene, deuterobenzene, naphthalene, deuteronaphthalene, acenaphthene, deuteroacenaphthene, fluorene, phenanthrene, anthracene. All these molecules are plane.

We observed a striking analogy between the structure of our spectra and that of the rotator. The theory of the free rotator is known; Dennison[6, 7] and Nielsen[7, 8] have investigated the case of plane molecules. They have shown that the ratio B/A of the moments of inertia in relation to two axes contained in the plane determines the style of the rotation spectrum. In the case of fluorescence and absorption spectra the dipolar moment certainly vibrates in the plane of the molecule; the aspect of the spectra should therefore be analogous to that of Dennison's 'A' and 'B' bands. Type 'C' bands can only be met with in the case of phosphorescence spectra. It is therefore seen that the aspect of the bands should give indications about the orientation of the dipole in relation to the axes of the ellipsoid of inertia of the molecule.

Since the molecules studied were very heavy, their moments of inertia are large and the separation which one would expect from the free rotation theory less than 1 cm^{-1}; the spectra of these molecules in the gaseous state do not, moreover, show any structure. Again, it is difficult to admit that a molecule taking the place of a single molecule of solvent can rotate freely at low temperature (it is known that the molecules of a molecular crystal do not generally rotate but actually oscillate about their position of equilibrium).

The fine structure of luminescence spectra can therefore only be explained if the existence of holes, of defects in the system, occupied by the molecules in solution be admitted. The theory of the restricted rotator placed in the periodic field of neighbouring solvent molecules[9, 10] enables the wide separation of the lines to be explained. It is in fact known that the movement of the rotator leads to a Mathieu equation and that the levels have a separation *n* times greater than that of the free rotation (where *n* is the angular period of the field surrounding the solute molecule).

This hypothesis, which explains the aspect of luminescence spectra in a plausible way, should give information about the polarization of the transition considered (fine structure) and about the dimensions of the holes (value of number *n* related to period of field in which the solute molecule is plunged). One of us (A.C.) will shortly give, in a more comprehensive article, the complete results which were obtained, and which are only briefly touched upon here.

A. Ciais
P. Pesteil

Laboratoire de Physique P.C.B.,
Faculté des Sciences de Marseille,
France.

(*26 May 1960*)

REFERENCES

1. Shpol'skii, E. V., and Klimova, L. A. *Bull. Acad. Sci., U.R.S.S.* **20,** 471 (1956); Shpol'skii, E. V., and Il'ina, A. A. *C. R. Acad. Sci., U.R.S.S.* **87,** 945 (1952); Bolotnikova, T. N. *Bull. Acad Sci., U.R.S.S.* **23,** 29 (1959); Bolotnikova, T. N. *Opt. i Spektrosk.* **7,** 217 (1959)
2. Ciais, A., and Pesteil, L. *C. R. Acad. Sci., Paris* **248,** 1308 (1959); Pesteil, L. *C. R. Acad. Sci., Paris* **250,** 497 (1960); Rousset, A. *C. R. Acad. Sci., Paris.* In press
3. Ciais, A., and Pesteil, L. *C. R. Acad. Sci., Paris* **248,** 2321 (1959)
4. Shop'skii, E. V. *Opt. i Spektrosk.* **7,** 852 (1959)
5. Bowen, E. J., and Brocklehurst, B. *J. chem. Soc.* 4320 (1955)
6. Dennison, D. M. *Rev. mod. Phys.* **3,** 280 (1931)
7. Herzberg, G. *Infrared and Raman Spectra* p. 472 (Van Nostrand, Princeton, N.J., 1956)
8. Nielsen, H. H. *Phys. Rev.* **38,** 1432 (1931)
9. Eyring, H., Walter, J., and Kimball G. E. *Quantum Chemistry* p. 358 (Wiley, New York, 1954)
10. Wilson, E. B. *Chem. Rev.* **27,** 31 (1940)

EDITORIAL NOTES

The editors have been informed that helium-3 gas is now available at the price of 15 cents (U.S.) per millilitre. Further information will be supplied by the Atomic Energy Commission's Mound Laboratory, Miamisburg, Ohio.

Material for a full bibliography of papers on low temperature research up to the present is being made available to the editors by the kindness of Arthur D. Little, Inc. The editors have decided to publish this bibliography as a special supplementary issue of CRYOGENICS.

Among review articles scheduled for future issues are:
- 'New Methods of Producing Cold' by H. O. McMahon.
- 'Irradiation at Low Temperatures' by L. Weil.

Papers to be published include:
- 'A Cryostat for Electrical Measurements on Semiconductors' by B. V. Rollin, J. R. Mills, and J. P. Russell.
- 'Density of Liquid Oxygen as a Function of Pressure and Temperature' by A. van Itterbeek and O. Verbeke.
- 'Cooling by Adiabatic Magnetization of Superconductors' by M. Yaqub.
- 'A Low Temperature Plant for the Production of Heavy Water' by J. Hänny.
- 'Enthalpy Diagrams' by M. Ruhemann.
- 'Pressure Effects on Superconductors' by A. C. Gross and J. L. Olson.

Book Reviews

Problems of Low Temperature Physics and Thermodynamics. (*Pergamon Press*) 345 pages. 70*s*.

This report of a conference in Delft in 1958 raises some interesting questions. Are conferences worth while? Should their proceedings be published? Is there such a thing as low temperature physics? Now that low temperature techniques have become so widespread they are being applied to an ever wider range of physical problems, and to some extent it is only the community of techniques which binds the subject of low temperature physics together. Indeed this particular conference had its main stress on techniques—and what a variety it offered—bubble chambers, superconducting computing elements, helium-3 cryostats, radiation damage, and nuclear resonance to mention only a selection. Perhaps it is just the variety of this mixed bag which provides the main justification for conferences of this kind. For although the applications lie in fields as far apart as nuclear physics and the theory of metals, the practitioner in one may often pick up useful tips from the other which he would perhaps miss in his ordinary routine. Again, it is only on occasions like this that physicists and engineers rub shoulders, and such conferences can well catalyse new ideas arising out of the unusual contacts they provide.

The value of a published report is more questionable. Usually a year or more elapses between the conference and the publication and by then, or soon after, anything really important should either have been published in the regular scientific journals or else best be forgotten. Certainly such a volume provides a historical record—though the poor quality of the paper of this particular record does not make it a very worthy one in spite of the high price—and occasionally an illuminating remark in discussion can be found of a kind not appearing in the formal presentation of a paper in a scientific journal. It is true, too, that the report is a useful record of who is doing what at the time, and so provides a kind of bibliography not easily to be found in the abstract journals. But evidently such advantages are ephemeral and though the reviewer has a sentimental attachment to historical records and likes to see on his shelves a collection of volumes such as this, it is rare indeed that he has occasion to consult a conference report more than two years old. One escape from this dilemma is to arrange very speedy publication—if necessary in duplicated rather than printed form and consisting of intelligent summaries of the proceedings rather than detailed presentations. An excellent example was the report of the Oxford low temperature physics conference in 1951, the proceedings of which were circulated within a few months of the conference so that they still had a useful life of a year or so before transmutation into a merely sentimental memento.

To return to the conference itself, perhaps the most interesting trend in the development of low temperature technique has been the steady improvement in the engineering of low temperature experiments—particularly in what used to be regarded as the difficult range of temperatures below 1°K. The development of techniques based on liquid helium-3 and adiabatic demagnetization used both separately and in combination is making experiments in this region more and more of a commonplace, and we may look forward to some interesting scientific dividends during the next few years.

D. Shoenberg

Evaporation and Droplet Growth in Gaseous Media. *N. A. Fuks. Translated from the Russian by J. M. Pratt.* (*Pergamon Press*) 72 pages. 30*s*.

This is essentially a critical literature survey of theoretical and experimental work concerned with the kinetics of evaporation and growth of droplets of pure liquids. It covers in detail the study of such phenomena as the formation of cloud droplets, the evaporation of fuel in the internal combustion engine, the drying of viscous solutions by atomization, the cooling of hot gases by water spray, fogs and atmospheric pollution, atomic explosion clouds, the condensation of vapour on gaseous ions, etc.

This book will be primarily of interest to specialists, but would also be useful as an introduction to anyone considering research on the above phenomena.

Despite the attempt to keep the price of this book down to a reasonable figure by the use of photolithography, it is still very expensive for its size.

B. R. Brown

Bibliography

The following list of papers and letters concerning low temperature physics and engineering has been compiled from a wide range of periodicals and covers the period January–May 1960. A list of recent publications will be a regular feature of CRYOGENICS.

Abrahams, S. C. 'Liquid-Helium Goniometer-Mounted Cryostat for a Single Crystal Automatic Neutron Diffractometer.' *Rev. sci. Instrum.* **31,** 174 (1960)

Adelson, H. E., Bostik, H. A., Moyer, B. J., and Waddel, C. N. 'Use of the Four-inch Liquid Hydrogen Bubble Chamber.' *Rev. sci. Instrum.* **31,** 1 (1960)

Allen, J. F. 'Film Transfer in He-II.' *Nature, Lond.* **185,** 831 (1960)

Ancenot, C., and Couture, L. 'Etude Optique à Basse Température des Aluns de Chrome et de Potassium Magnetiquement Dilués.' *J. Phys. Radium* **21,** 47 (1960)

Andronikashvili, E. L., and Tsakadze, D. S. 'Experimental Investigation of the Harmonic Oscillations of a Disk in Rotating Helium-II.' *J. exp. theor. Phys.* **37,** 562 (1960), *Soviet Phys. JETP* **37,** 397 (1960)

Anon. 'La Mesure des Températures Extrêmes.' *Atomes* No. 164, 77 (1960)

Anon. 'Les Eléments Electroniques à Supra Conductibilité.' *Atomes* No. 166, 163 (1960)

Anon. 'Low-temperature Distillation of Hydrogen Isotopes.' *J. Refrig.* **3,** 8 (1960)

Anon. 'Precision Thermometry for Low Temperatures.' *Instrum. Pract.* **14,** 532 (1960)

Babenko, V. P., Broude, V. L., Medveden, V. S., and Prikhot'ko, A. F. 'Methods and Apparatus for Low-temperature Optical and Spectral Investigations.' *Pribory i Tekhnika Eksperimenta* **1,** 115 (1959), *Instruments and Experimental Techniques* **1,** 119 (1960)

Bancie-Grillot, M., Gross, E. F., Grillot, E., and Razbirine, B. S. 'Influence de la Température sur les Deux Séries de Bandes du Spectre de la Fluorescence Verte à Basse Température du Sulfure de Cadmium Pur.' *C. R. Acad. Sci., Paris* **250,** 2868 (1960)

Becherer, R. 'La Résonance des Protons du Charbon Actif à Différentes Températures.' *C. R. Acad. Sci., Paris* **250,** 2883 (1960)

Bhagat, S. M. ' "Eddy" Viscosity in Liquid Helium II.' *Proc. phys. Soc. Lond.* **75,** 303 (1960)

Blanchard, R. L., and Sherburne, A. E. 'The Hydrogen Quartector—A New Phase Detector for Exotic Liquid–Gas Systems.' *Proc. Inst. Radio Engrs, N.Y.* **48,** 779 (1960)

Bockhoff, F. J., Petrella, R. V., and Pace, E. L. 'Thermodynamic Properties of Sulfuryl Fluoride from 12° K to its Boiling Point. Entropy from Molecular and Spectroscopic Data.' *J. chem. Phys.* **32,** 799 (1960)

Borelius, G. 'Thermodynamics of the λ-transition in Superconductors.' *Ark. Fys.* **16,** 337 (1960)

Borst, L. B. 'Low-temperature Neutron Moderation.' *Phys. Rev. Lett.* **4,** 131 (1960)

Brandt, N. B., Dubrovskaya, A. E., and Kytin, G. A. 'An Investigation of the Quantized Oscillations in the Magnetic Susceptibility of Bismuth at Extremely Low Temperatures.' *J. exp. theor. Phys.* **37,** 572 (1959), *Soviet Phys. JETP* **37,** 405 (1960)

Broida, H. P., and Nicholls, R. W. 'Phosphorescence of Nitrogen and Nitrogen–Argon Deposited Films at 4·2° K.' *J. chem. Phys.* **32,** 623 (1960)

Buchhold, T. A. 'Applications of Superconductivity.' *Sci. Amer.* **202,** No. 3, 74 (1960)

Cammerer, W. F. 'Measurement of Heat Conductivity of Insulation Materials at Low Temperatures.' *Kaltetechnik* **12,** 107 (1960)

Careri, G., Fasozi, U., and Gaeta, F. S. 'Experimental Behaviour of Ionic Structures in Liquid Helium-II.' *Nuovo Cim.* **15,** 774 (1960)

Carr, W. J., Jr. 'Explanation for the Low-temperature Behaviour of the Anisotropy of Iron.' *J. appl. Phys.* **31,** 69 (1960)

Chase, C. E. 'Evidence for the Quantization of Circulation in Liquid Helium-II.' *Phys. Rev. Lett.* **4,** 220 (1960)

Cini-Castagnoli, G., and Ricci, F. P. 'Diffusion of ^{37}A, Kr, HT in Liquid Argon Between 84 and 90° K.' *Nuovo Cim.* **15,** 795 (1960)

Cini-Castagnoli, G., and Ricci, F. P. 'Self-diffusion in Liquid Argon.' *J. chem. Phys.* **32,** 19 (1960)

Daunt, J. G. 'Liquid Helium-3.' *Science* **131,** 579 (1960)

Denton, W. H. 'Overall Economics of Plate-fin Heat Exchangers.' *Brit. chem. Engng* **5,** 40 (1960)

Denton, W. H., and Ward, D. E. 'Applications and Design of Plate-fin Heat Exchangers.' *Brit. chem. Engng* **5,** 18 (1960)

DeSorbo, W. 'Study of the Intermediate State in Superconductors using Cerium Phosphate Glass.' *Phys. Rev. Lett.* **4,** 406 (1960)

Dininny, R. E., and Pace, E. L. 'Thermodynamic Properties of Trifluoromethanethiol from 12° K to its Boiling Point. Entropy from Molecular and Spectroscopic Data.' *J. chem. Phys.* **32,** 805 (1960)

Dresselhaus, M. S., and Dresselhaus, G. 'High-frequency Studies on Superconducting Tin.' *Phys. Rev. Lett.* **4,** 401 (1960)

Dugdale, J. S., and Gugan, D. 'The Electrical Resistivity of the Two Phases of Sodium at Low Temperatures.' *Proc. roy. Soc.* **A254,** 184 (1960)

Edwards, M. H., and Woodbury, W. C. 'Condensation of Supersaturated He^4 Vapour in a Cloud Chamber.' *Canad. J. Phys.* **38**, 335 (1960)

Eselson, B. N., and Shvets, A. D. 'The Use of a Superconducting Ring for Registering the Phase Transition in Liquid Helium.' *J. exp. theor. Phys.* **37**, 323 (1959), *Soviet Phys. JETP* **10**, 228 (1960)

Ewing, G. E., Thompson, W. E., and Pimentel, G. C. 'Infrared Detection of the Formyl Radical HCO.' *J. chem. Phys.* **32**, 927 (1960)

Galkin, A. A., and Korolyuk, A. P. 'Oscillations in the Absorption Coefficient of Sound in Tin at Low Temperatures.' *J. exp. theor. Phys.* **37**, 310 (1959), *Soviet Phys. JETP* **10**, 219 (1960)

Gamtsemlidze, G. A. 'On the Critical Mode in Experiments with an Oscillating Disk in Helium II.' *J. exp. theor. Phys.* **37**, 950 (1959). *Soviet Phys. JETP* **37**, 678 (1960)

Ginzburg, N. I., and Shal'nikov, A. I. 'Destruction of Superconductivity in Thin Films by Field and Current.' *J. exp. theor. Phys.* **37**, 399 (1959), *Soviet Phys. JETP* **37**, 285 (1960)

Goldstein, L. 'Some Thermal Properties of Liquid Helium Three.' *Phys. Rev.* **117**, 375 (1960)

Goodman, B. B. 'L'existence Probable des Eléments Supraconducteurs de Température de Transition Extrêmement Basse.' *C. R. Acad. Sci., Paris* **250**, 683 (1960)

Gor'kov, L. P. 'The Critical Supercooling Field in Superconductivity Theory.' *J. exp. theor. Phys.* **37**, 833 (1959), *Soviet Phys. JETP* **37**, 593 (1960)

Grassman, P. 'Application of Very Low Temperature to Electrical Engineering.' *Kaltetech.* **12**, 38 (1960)

Grey, J. 'Calibration of Turbine Flowmeters for Cryogenic Operation.' *J. Amer. Rocket Soc.* **30**, 192 (1960)

Gush, H. P., Hare, W. F. J., Allin, E. J., and Welsh, H. L. 'The Infrared Fundamental Band of Liquid and Solid Hydrogen.' *Canad. J. Phys.* **38**, 176 (1960)

Hart, H. R., Jr., and Wheatley, J. C. 'Self-diffusion in Liquid He^3.' *Phys. Rev. Lett.* **4**, 3 (1960)

Haseda, T. 'Paramagnetic Susceptibility of $CoCl_2.6H_2$0 and its Deuterated Salts.' *Proc. phys. Soc. Japan* **15**, 483 (1960)

Hedgcock, F. T., Muir, W. B., and Wallingford, E. 'The Electrical Resistance of Dilute Magnesium and Aluminium Alloys at Low Temperatures.' *Canad. J. Phys.* **38**, 376 (1960)

Henry, W. E. 'Low Temperature Magnetic Remanence, Molecular Field, and Approach to Saturation of Holmium Metal.' *Phys. Rev.* **117**, 89 (1960)

Hentley, E. L., and Ford, R. A. 'A Low-temperature Cell for the Perkin–Elmer Spectracord 4000.' *Spectrochim. Acta* No. 12, 1125 (1959) ✓

QD1 S74

Hercules, D. M., and Rogers, L. B. 'Luminescence Spectra of Naphthols and Naphthalenediols: Low-temperature Phenomena.' *J. phys. Chem.* **64**, 397 (1960)

Hill, R. W., and Lounasmaa, O. V. 'The Thermodynamic Properties of Fluid Helium.' *Phil. Trans.* **A252**, 357 (1960)

Hsu, A. C. T., and McKinley, C. 'Purify Liquid Oxygen via Adsorption.' *Chem. Engng Progr.* **56**, No. 2, 80 (1960)

Huffman, D. R., and Norwood, M. H. 'Specific Heat and Elastic Constants of Calcium Fluoride at Low Temperatures.' *Phys. Rev.* **117**, 709 (1960)

Hughes, T. P. 'The Application of Refrigeration Lubrication Systems to Heat Pumps.' *J. Refrig.* **3**, 12 (1960)

Itskevich, E. S., and Strelkov, P. G. 'Heat Capacity of $CdCl_2$ and CdI_2 between 1·6 and 300° K. Enthalpy and Entropy of $CdCl_2$ and CdI_2 at 298·16° K.' *J. Phys. Chem., Moscow* **7**, 1575 (1959)

Jaggi, R., and Sommerhalder, R. 'Messung der Eindringtiefe an supraleitenden Hohlkorpern.' *Helv. phys. acta* **33**, 1 (1960)

Kogan, A. V., Reinov, N. M., Sokolov, I. A., and Stel'makh, M. F. 'A Device for Obtaining Very Low Temperatures and Orienting Nuclei.' *J. tech. Phys., Moscow* **29**, 1039 (1959), *Soviet Phys. Tech. Phys.* **4**, 946 (1960)

Kuper, C. G. 'Mechanism of Superfluid Flow.' *Nature, Lond.* **185**, 832 (1960)

Kurova, I. A., and Kalashnikov, S. G. 'Electrical Conductivity of Germanium at Low Temperatures.' *Soviet Phys. Solid State* **1**, 1353 (1960)

Lock, J. M. 'Cryotrons and Other Superconducting Computer Devices.' *Research, Lond.* **XIII**, 49 (1960)

Lowenthal, G. C., and Harper, A. F. A. 'Resistance–Temperature Relationship of Platinum at Low Temperatures and its Influence on Precision Thermometry.' *Brit. J. appl. Phys.* **11**, 295 (1960)

Lucas, W. R., and Riehl, W. A. 'An Instrument for Determination of Impact Sensitivity of Materials in Contact with Liquid Oxygen.' *Bull. Amer. Soc. Test. Mat.* No. 244, 29 (1960)

Lucasson, A. 'Irradiation à Basse Température de Metaux de Transition par des Neutrons.' *J. nucl. Energy* **11A**, 108 (1960)

Maiman, T. H. 'Maser Behaviour: Temperature and Concentration Effects.' *J. appl. Phys.* **31**, 222 (1960)

Martin, D. L. 'The Specific Heat of Sodium from 20 to 300° K: The Martensic Transformation.' *Proc. roy. Soc.* A254, 433 (1960); 'The Specific Heat of Lithium from 20 to 300° K: The Martensic Transformation.' *Proc. roy. Soc.* **A254**, 444 (1960)

Meissner, H. 'Superconductivity of Contacts with Interposed Barriers.' *Phys. Rev.* **117**, 672 (1960)

Mendelssohn, K., and Shiffman, C. A. 'The Thermal Resistance of Tin–Indium Alloys in the Intermediate State.' *Proc. roy. Soc.* **A255**, 199 (1960)

Nabauer, M., and Schmeissner, F. 'Untersuchungen mittels Neutronen bei tiefsten Temperaturen.' *Z. angew. Phys.* **12**, 133 (1960)

Nambu, Y. 'Quasi-particles and Gauge Invariance in the Theory of Superconductivity.' *Phys. Rev.* **117,** 648 (1960)

Pant, D. D., and Khandelwal, D. P. 'Fluorescence Spectra of Solutions of Uranyl Nitrate at Liquid Air Temperatures. Part 1: Rapidly Cooled Solutions.' *Proc. Ind. Acad. Sci.* **LI,** A, 60 (1960)

Powell, R. L., Bunch, M. D., and Gibson, E. F. 'Low-temperature Transport Properties of Commercial Metals and Alloys. III. Gold–Cobalt.' *J. appl. Phys.* **31,** 504 (1960)

Powell, R. L., Hall, W. J., and Roder, H. M. 'Low-temperature Transport Properties of Commercial Metals and Alloys. II. Aluminiums.' *J. appl. Phys.* **31,** 496 (1960)

Powell, R. W., and Challoner, A. R. 'Proposed Values for the Thermal Conductivities of Some Liquid Refrigerants.' *Mod. Refrig.* **63,** 42 (1960)

Reed, S. G., and Herzfeld, C. M. 'Theory of Flame Propagation in Solid Nitrogen at Low Temperatures.' *J. chem. Phys.* **32,** 1 (1960)

Reimann, R., and Beauvillain, R. 'La Résonance des Protons du Diphénylpicrylhydrazyl aux Très Basse Températures.' *C. R. Acad. Sci., Paris* **250,** 2880 (1960)

Rhoderick, E. H. 'Low Temperature Storage Elements.' *J. Brit. Instn Radio Engrs* **20,** 37 (1960)

Robertson, J. H. 'X-ray Diffraction by Single Crystals at Low Temperatures: A Cryostat for Use with Liquid Hydrogen.' *J. sci. Instrum.* **37,** 41 (1960)

Robinson, W. K., and Friedberg, S. A. 'Specific Heats of $NiCl_2.6H_2O$ and $CoCl_2.6H_2O$ Between 1·4° and 20° K.' *Phys. Rev.* **117,** 402 (1960)

Romer, R. H. 'Nuclear Spin Relaxation in Liquid He^3.II.' *Phys. Rev.* **117,** 1183 (1960)

Rowell, P. M. 'The Thermal Conductivity of Some Superconductors.' *Proc. roy. Soc.* **A254,** 542 (1960)

Sarachik, M. P., Garwin, R. L., and Erlbach, E. 'Observation of the Energy Gap by Low-temperature Penetration Depth Measurements in Lead.' *Phys. Rev. Lett.* **4,** 52 (1960)

Schuftan, P. M. 'Low-temperature Heat Exchangers.' *Brit. chem. Engng* **5,** 12 (1960)

Scott, R. B. 'Liquid Hydrogen for Chemical and Nuclear Rockets.' *Discovery* **XXI,** 74 (1960)

Smith, G. E., Galt, J. K., and Merritt, F. R. 'Electron Spin Resonance in Bismuth and Antimony.' *Phys. Rev. Lett.* **4,** 276 (1960)

Smith, G. W., and Housley, R. M. 'Nuclear Magnetic Resonance of Solid Hydrogen (67–86% Ortho) and Solid Deuterium (33 and 55% Para).' *Phys. Rev.* **117,** 732 (1960)

Smith, J. F., and Gjevre, J. A. 'Elastic Constants of Yttrium Single Crystals in the Temperature Range 4·2–400° K.' *J. appl. Phys.* **31,** 645 (1960)

Smith, R. C., and Wyard, S. J. 'Electron Spin Resonance in Hydrogen Peroxide–Water Solutions at 90° K Irradiated with Ultra-violet Light.' *Nature, Lond.* **186,** 223 (1960)

Sreedhar, A. K., and Daunt, J. G. 'Vapor Pressure of He^3–He^4 Solutions.' *Phys. Rev.* **117,** 891 (1960)

Stanton, R. M., Jennings, L. D., and Spedding, F. H. 'Heat Capacity of Terbium from 1·4 to 4·0° Kelvin' *J. chem. Phys.* **32,** 630 (1960)

Stewart, J. N. 'Phase Transitions and Compressions of Solid CH_4, CD_4, and O_2.' *J. Phys. Chem. Solids* **12,** 122 (1959)

Stokes, H. J. 'Apparatus for the Measurement of Young's Modulus between −200 and 700° C.' *J. sci. Instrum.* **37,** 117 (1960)

Thouless, D. J. 'Strong-coupling Limit in the Theory of Superconductivity.' *Phys. Rev.* **117,** 1256 (1960)

Vinograd-Finkel, F. R., Ginsburg, F. G., Fyodorova, L. A., and Kaukhcheshvili, E. L. 'The Application of Refrigeration for Prolonged Preservation of Blood.' *World Refrig. and Air-condit.* **11,** 65 (1960)

Ward, D. E. 'The Application of Regenerators and Heat Exchangers. *Brit. chem. Engng* **5,** 15 (1960)

Wentzel, G. 'Superfluidity and Superconductivity in Electron Gases.' *Phys. Rev. Lett.* **4,** 349 (1960)

White, D., and Lassettre, E. N. 'Theory of Ortho-para Hydrogen Separation by Adsorption at Low Temperatures, Isotope Separation.' *J. chem. Phys.* **32,** 72 (1960)

Yunker, W. H., and Halsey, G. D., Jr. 'The Solubility, Activity Coefficient and Heat of Solution of Solid Xenon in Liquid Argon.' *J. phys. Chem.* **64,** 484 (1960)

Zahn, C. T. 'Dewar System for Low Temperature Experiments.' *Rev. sci. Instrum.* **31,** 328 (1960)

Zharkov, V. N., and Silin, V. P. 'Theory of Weak Solutions of He^4 in Liquid He^3.' *J. exp. theor. Phys.* **37,** 143 (1959), *Soviet Phys. JETP* **10,** 102 (1960)

Zhuralev, N. N., et al. 'On the Superconductivity of the Compound BiPt.' *J. exp. theor. Phys.* **37,** 880 (1959), *Soviet Phys. JETP* **37,** 627 (1960)

Zinov'eva, K. N., and Peshkov, V. P. 'Phase Diagrams for Liquid He^3-He^4 Solutions.' *J. exp. theor. Phys.* **37,** 33 (1959), *Soviet Phys. JETP* **10,** 22 (1960)